OBJECT-BASED SPATIAL CLASSIFICATION OF FOREST VEGETATION WITH

IKONOS IMAGERY

by

Minho Kim

(Under the direction of Marguerite Madden)

ABSTRACT

Object-based image analysis (OBIA) is employed to classify forest types, including

deciduous, evergreen and mixed forests, in a U.S. National Park unit using very high spatial

resolution (VHR) IKONOS satellite imagery. This research investigates the effect of scale on

segmentation quality and object-based forest type classification. Average local variance and

spatial autocorrelation analyses are utilized to determine the quality of segmentation. This

research also examines the effect of grey-level co-occurrence matrix (GLCM) texture measures

on forest classification results.

The comparison of a manual interpretation revealed that three distinct levels of segmentation

quality were yielded depending on scale: over-, optimal- and under-segmentation. Over-

segmentation produced larger number and smaller size of image objects (or segments) than those

of manually interpreted forest stands. Under-segmentation generated the smaller number of

image objects with larger average size compared with manual interpretation. On the other hand,

optimal segmentation with a scale (i.e., scale parameter) of 18 generated similar image objects

much resembling manually interpreted forest stands in number and average size. Based on visual

assessment, image segments were similar to manually interpreted forest stands in terms of location, shape, number and average size.

Statistical analyses supported these results. A graph of average local variance against segmentation scale also indicated an optimal scale of 18. According to spatial autocorrelation analysis, this research found that over- and under-segmentations were related to positive autocorrelation, while optimal segmentations achieved lower, or even negative, Moran's I values.

This research discovered that optimal segmentations achieved higher accuracy of forest type classification than over- and under-segmentation. In particular, a scale of 19 produced the highest overall classification accuracies when using only spectral bands (79 % in overall accuracy and 0.65 in Kappa). The research found that the incorporation of individual texture measures did not improve OBIA forest classification at scale 19. Instead, the use of multiple texture measures enhanced OBIA forest type classification accuracies to 83 % in overall accuracy and 0.71 in Kappa by disentangling classification confusions.

OBIA with multiple GLCM texture measures are expected to be a useful approach to automatically classify forest types. In addition, OBIA will play a role in closely coupling remote sensing and GIS with its ability to create a GIS database to be utilized for further GIS analyses.

INDEX WORDS: Object-based image analysis, IKONOS, Segmentation quality, Spatial autocorrelation, Forest type classification, Grey-level co-occurrence matrix texture

OBJECT-BASED SPATIAL CLASSIFICATION OF FOREST VEGETATION WITH

IKONOS IMAGERY

by

Minho Kim

B.A., Seoul National University, Republic of Korea, 1997

M.A., Seoul National University, Republic of Korea, 2002

A Dissertation Submitted to the Graduate Faculty of The University of Georgia in Partial

Fulfillment of the Requirements for the Degree

DOCTOR OF PHILOSOPHY

ATHENS, GEORGIA

2009

OBJECT-BASED SPATIAL CLASSIFICATION OF FOREST VEGETATION WITH

IKONOS IMAGERY

by

Minho Kim

Major Professor: Marguerite Madden

Committee: Elgene O. Box

Thomas Jordan

Xiaobai Yao

Electronic Version Approved:

Maureen Grasso
Dean of the Graduate School
The University of Georgia
May 2009

ACKNOWLEDGEMENTS

TABLE OF CONTENTS

LIST OF TABLES

LIST OF FIGURES

CHAPTER 1

INTRODUCTION AND LITRATURE REVIEW

1.1 MANUAL INTERPRETATION AND IMAGE CLASSIFICATION

Aerial photographs have been employed for manual interpretation and mapping of natural

resources in the U.S. since the 1940s (Colwell, 1960; Heller, 1975; Lachowski *et al*., 2000). The

basic elements of image interpretation, such as size, shape, shadow, tone, color, texture, pattern,

associated relationships and context are typically used to produce detailed forest maps (Jensen,

2000). Human interpreters largely employ three fundamental interpretation elements of spectral,

textural and contextual information (Haralick *et al*., 1973; Haralick and Shanmugam, 1974). On

the other hand, automated image classification techniques were developed in the 1970s and

1980s with the advent of moderate-spatial-resolution (20 to 80 m) satellite imagery. For example,

the U.S. Landsat Multispectral Scanner (MSS), Thematic Mapper (TM) and Enhanced Thematic

Mapper Plus (ETM+) and the European Satellite Pour l'Observation de la Terre (SPOT) were

launched to be utilized for land-use and land-cover (LULC) classification including forest types

(Connors *et al.*, 1987; Nelson *et al*., 1987; Woodcock *et al.*, 1994; Kimes *et al.*, 1999; Oetter *et

al.*, 2000; Salovaara *et al.*, 2005)

   Until the 1990s, the major differences between air photos and satellite imagery for use in

forest classification were spatial resolution and manual vs. automated techniques to identify

forest classes. Aerial photographs, particularly large-scale color infrared (CIR) air photos, have

1

been interpreted manually for vegetation database development and forest resource management in state and federal conservation lands managed by agencies such as the National Park Service (NPS), the U.S. Forest Service and the U.S. Bureau Land Management (Welch *et al*., 2002). However, the cost of aerial photographs for broad-area forest mapping generally cost more than moderate-resolution satellite imagery (Read *et al*., 2003). In addition, manual interpretation is labor intensive, and several months to years may be needed to develop vegetation databases of National Park units ranging in size from hundreds of hectares to hundreds of square kilometers (Welch *et al*., 2002).

With the launch of the commercial satellite IKONOS in 1999 by Space Imaging, Inc. (now GeoEye, Inc.), very high resolution (VHR) 4-m multispectral and 1-m panchromatic image data became available for resource inventory and monitoring (GeoEye, 2008). The launch of the IKONOS satellite was quickly followed by DigitalGlobe's launch of the QuickBird satellite in 2001 and the acquisition of 2.44-m multispectral and 0.61-m panchromatic bands (DigitalGlobe, 2006). VHR satellite imagery, such as IKONOS and QuickBird, matches the spatial quality of aerial photographs and may be an alternative to air photos to characterize forest structure and dynamics with automatic image classification techniques. These VHR images offer a mapping potential for scales ranging from 1:5,000 to 1:10,000 (Puissant *et al*., 2005; Jacobsen, 2003). In particular, IKONOS data are now widely employed in forest mapping as an alternative to the aerial photographs (Franklin *et al*., 2001a; Asner and Warner, 2003; Read *et al*., 2003; Wulder *et al*., 2004; Metzler and Sader, 2005; Souza and Roberts, 2005).

Remotely sensed data have been interpreted automatically largely on the basis of pixel-based image classification, i.e., the statistical analysis of each pixel's spectral value (Blaschke and Strobl, 2001). The conventional pixel-based classification approaches, however, have

limitations to be considered when used with VHR imagery because these procedures ignore spectral reflectance characteristics of neighboring pixels (Fisher, 1997; Towonshend *et al*., 2000; Brandtberg and Warner, 2006). Although improvements have been made to pixel-based classification methodologies, such as fuzzy classifiers, step-wise and hybrid classifiers, without fully utilizing spatial and spectral information of surrounding pixels, the pixel- and spectral-based methods of traditional image classification were doomed to yield unsatisfactory results with VHR images (Blaschke, 2003; Maillard, 2003).

In addition, the advent of VHR data provides increased information on land cover details from local to national scales (Alpin *et al*., 1999), but these images require much more complex classification techniques (Carleer *et al*., 2005). This is attributed, in part, to decreased statistical separability between spectral classes (i.e., between-class variance) caused by increased internal spectral variability within homogeneous land cover units (i.e., within-class variance) (Woodcock and Strahler, 1987; Marceau *et al.*, 1990; Hay *et al*., 1996; Franklin *et al*., 2001b; Shiewe *et al*., 2001; Carleer *et al*., 2005; Yu *et al.*, 2006; Lu and Weng, 2007). The increased within-class variability decreases the classification accuracy drawn from the traditional per-pixel classification with VHR images (Shiewe *et al*., 2001). Since forest scenes usually show significant spectral variations in VHR imagery and between-class variance is an important factor affecting the classification accuracy of forest classes (Straher *et al.*, 1986; Marceau *et al*., 1994a), it is imperative to develop classification procedures which decrease within-class variance and increase between-class variability. In this sense, many attempts have been made to develop various image classification techniques, including object-based, textural and contextual image classifications, that reduce the limitations related to conventional pixel-based classification and VHR imagery (Guo e*t al.*, 2007; Lu and Weng, 2007).

1.2 RESEARCH OBJECTIVES

This study develops a methodology to obtain *a priori* information of optimal segmentation for OBIA forest type classification. A 4-m multispectral IKONOS image was used to classify forest types of a National Park unit of the southeastern U.S., i.e., Guilford Courthouse National Military Park, located in Greensboro, North Carolina. In particular, the study investigates the potential of using a graph of average local variance in VHR imagery and spatial autocorrelation analysis in estimating an optimal segmentation scale for delineating forest stands with a benchmark of manual interpretation. This research also explores how scale affects the quality of segmentation in terms of automatic forest stand delineation.

In addition, object-based image classification with the addition of object-specific texture is used to answer three questions in forest type mapping:

1) Does the quality of segmentation related to segmentation scale have a direct effect on forest type classification with IKONOS imagery?

2) Can the methods of local variance and spatial autocorrelation be utilized to determine optimal segmentation scale before object-based forest type classification?

3) Does the addition of object-specific texture, computed with grey-level co-occurrence matrix (GLCM), enhance object-based forest type classification.

In this study, a series of image segmentations and classifications is conducted to investigate these objectives with VHR imagery, i.e., IKONOS. It is anticipated that this research will contribute to concepts of object-based image processing in remote sensing and ultimately provide park management decision makers with useful information related to more accurate and automated techniques of forest classification for timely and critical monitoring of natural and cultural resources.

1.3 LITERATURE REVIEW

1.3.1 Vegetation/Forest mapping

The purposes of vegetation mapping are considered to communicate a complex set of information in a simplified and spatially referenced form and to provide spatially referenced numerical data for further analytical purposes (Millington and Alexander, 2000). To meet these purposes, ecologists and biogeographers have developed ground-based (or field survey) vegetation mapping methods with their expertise of sampling, taxonomy and classification. Field survey methods can produce much more detailed information of vegetation and obtain information about sub-surface conditions (e.g., soils and hydrology) that are difficult to be detected by remote sensing methods (Wyatt, 2000). In addition, floristic-level vegetation mapping is well suited to the ground-based methods (Gerard *et al.*, 1998). These methods, however, require intensive labor with high levels of knowledge about vegetation. It is not be practical to apply ground-based methods for extensive or inaccessible areas. On the contrary, remote sensing methods facilitate vegetation mapping in those areas and aid in updating existing vegetation databases with frequent revisits of the same area.

Natural resource managers have relied on the manual interpretation of aerial photographs since the 1940s and on automated classification of medium-resolution satellite image data since the 1970s (Colwell, 1960; Heller, 1975; Hoffer and Staff, 1975; Jensen, 1979; Lachowski *et al.*, 2000). Large-scale CIR aerial photographs have been interpreted manually to develop detailed forest databases and manage resources in state and federal conservation lands (Welch *et al*., 1995; Lund *et al.*, 1997; Welch *et al*., 1999). Manual interpretation to identify forest stands from aerial photographs is typically performed by human interpreters using basic image interpretation elements of tone, texture, shape, size, pattern, and associations (Avery, 1962; Teng *et al.*, 1997).

Although this technique provides a high level of detail, it is labor-intensive classification of forest types from digital imagery (Welch *et al*., 2002; Read *et al*., 2003).

VHR satellite imagery with spatial resolutions of similar magnitude to those of aerial photographs (1-4 m pixels) became available for resource inventory and monitoring with the successful launch of commercial imaging satellites in the late 1990s (Ehlers *et al.*, 2003; Ehlers, 2004). VHR imagery is an alternative to aerial photos for characterization of forest structure and dynamics using automatic image classification techniques. In recent years, for example, IKONOS imagery has been utilized frequently for forest/vegetation mapping using pixel-based image classification methods (Franklin *et al*., 2001a; Asner and Warner, 2003; Read *et al*., 2003; Wang *et al*., 2004a; Wulder *et al*., 2004; Metzler and Sader, 2005; Souza and Roberts, 2005).

1.3.2 Object-based image analysis

Object-based image analysis (OBIA) is a promising development within integrated geographic information system (GIS) and remote-sensing image analysis. It encompasses spectral information of surrounding pixels and incorporates information such as texture, shape, size, directionality, and spatial distribution of features in image classification (Blascke and Strobl, 2001; Kim *et al.*, in press). This approach was proposed in the late 1990s as a means of incorporating spatial and contextual information into the classification procedure to overcome the limitations of pixel-based classification. OBIA procedures are divided into two major steps: 1) image segmentation that generates image objects (or segments); and 2) image classification based on these image objects (Wang *et al.*, 2004a; Hay and Castilla, 2008; Kim *et al*., in press). Segmented images are less sensitive to the modifiable areal unit problem (MAUP) because geographic entities are represented by image objects rather than pixels, i.e. arbitrary spatial units

(Hay *et al.*, 2008; Hay and Castilla, 2008). MAUP is an interpretation error that might occur when original data are aggregated in geographic research (Openshaw, 1984). It is associated with the ecological fallacy, whose false assumption is the homogeneity of aggregated data.

Table 1.1 describes major differences between pixel- and object-based classification approaches. The basic difference is the unit to be utilized in image analysis and classification procedures. Conventional pixel-based approaches have largely depended on individual pixels, but OBIA employs image objects (or segments) that are defined as groups of pixels. The descriptive statistics of digital numbers, corresponding to pixels within each image segment, can be computed and utilized as the spectral information of individual image objects.

Table 1.1 Comparisons of pixel- and object-based classification approaches.

	Pixel-based approach	Object-based approach
Spectral information	Digital numbers of individual pixels	Representative values of image objects such as minimum, maximum, mean and standard deviation *etc.*
Spatial information	Texture	Texture, area, length, width, shape index and direction *etc.*
Contextual information		Relationship to neighbors, proximity and containment *etc.*

The grouping of pixels with homogeneous values provides a potential to overcome the high spectral variation of the same ground feature inherent in VHR imagery (Yu *et al.*, 2006). The spatial properties of each image object can also be defined and utilized to identify what ground

features the image objects represent in the real world. Moreover, OBIA makes it possible to

define contextual relationships between image objects, e.g. topological relationships of

adjacency, connectivity and containment, in image analyses. The spectral, spatial and contextual

characteristics of image segments are closely associated with basic image interpretation elements

that have been widely adopted by human interpreters. In this sense, OBIA is considered to be an

automatic remote sensing method with VHR imagery to emulate, to some extent, a human

interpreter's ability in classifying images (Blaschke and Strobl, 2001; Schiewe *et al.*, 2001; Benz

et al., 2004; Blascke, 2003; Meinel and Neubert, 2004; Yu *et al.*, 2006).

1.3.2.1 Image segmentation

The first step of OBIA processing is image segmentation to group pixels of relatively

homogeneous values into image objects (or segments). Segmentation techniques themselves are

not new and have been utilized in processing of remotely sensed data for forest/vegetation and

LULC classifications since the 1970s (Haralick *et al.*, 1973; Ryherd and Woodcock, 1996; Lobo,

1997; Katrikeyan *et al.*, 1998; Lobo *et al.*, 1998; Abkar *et al.*, 2000; Stuckens *et al.*, 2000;

Baskent *et al.*, 2001; Hay *et al.*, 2001; Dorren *et al.*, 2003; Sande *et al.*, 2003; Hall *et al.*, 2004;

Lalinerte *et al.*, 2004; Wang *et al.*, 2004a; Wang *et al.*, 2004b; Kim *et al.*, in press). Various

segmentation algorithms and their descriptions can be found in Haralick and Shapiro (1985), Pal

and Pal (1993), Ryherd and Woodcock (1996) and Cufi *et al.* (2002).

In recent years, some segmentation software packages have been developed and

distributed commercially or freely in remote-sensing and image-processing domains. Table 1.2

describes some available segmentation software packages based on Meinel and Neubert (2004)

and Neubert *et al.* (2006; 2008). As shown in the table, Definiens, Inc., München, Germany,

developed the first commercial segmentation software package, eCognition (version 2), in 2002 and the more recent packages Professional (versions 5 and 6) and Developer (versions 7 and 8). Definiens is considered to be one of the best segmentation software packages that well delineate landscape features in image segmentations (Meinel and Neubert, 2004). All the versions are mainly based on the *Multiresolution Segmentation* algorithm, which is a kind of region-growing techniques. This algorithm segments an image by generating seed pixels over the entire image area and grouping surrounding pixels around seed pixels with a specific criterion and input data. Additional segmentation algorithms are also implemented in Definiens software packages, including Chessboard, Quad Tree and Contrast Split segmentations.

The use of Definiens is very complex in terms of selecting parameters related to segmentation and classification, e.g., input data type, segmentation parameters, spectral, spatial and contextual attributes of individual image objects. For example, user-defined parameters must be entered in performing segmentation procedures by Multiresolution Segmentation algorithm: 1) a scale parameter (hereafter also called *segmentation scale or scale*); 2) the ratio of color and shape; and 3) the ratio of compactness and smoothness. Figure 1.1 illustrates the conceptual design of the segmentation algorithm in Definiens. As shown in the figure, the Multiresolution Segmentation produces image objects (or segments) so that individual pixels are grouped depending on several parameters.

Table 1.2. Summary of segmentation software packages.

	Developer	Algorithm	Application Field	Development year
eCognition	Definiens, Germany	Region growing	Remote sensing	2002
Data dissection tools	INCITE, Stirling University, U.K.	Superparamagnetic clustering	Image analysis and statistical physics	2002
CAESAR 3.1	N.A. Software, Ltd.	Simulated annealing	Remote sensing with RADAR data	1996
InfoPack 1.0	InfoSAR, Ltd.	Simulated annealing	Remote sensing with RADAR data	2003
Image segmentation - add-on module for ERDAS Imagine	Remote sensing applications center, U.S. Department of Agriculture Forest Service	Region growing	Remote sensing	2002
Minimum entropy approach	Institute of Compute Science, University of Bonn, Germany	Triangulation	Polygonization of noisy imagery	2002
Spring 4.0	National Institute for Space Research, Brazil	Region growing and watershed	Remote sensing	2003
HalconSEG	TU Munich and IOER Dresden	Hybrid (edge and region oriented)	Color images and mobile systems	2005
Imagine WS ERDAS Imagine extension	Commission for scientific visualization, Austrian Academy of Sciences	Hierarchical watershed	Remote sensing	2003

Table 1.2. Summary of segmentation software packages (continued).

	Developer	Algorithm	Application Field	Development year
PARBAT 0.32	Lucieer (2004)	Region growing	Remote sensing	2004
RHSEG 1.0	Goddard Space Flight Center, NASA	Hierarchical region growing	Remote sensing	2005
SEGEN	IBM Haifa research labs	Region growing	Color images	2006
SEGSAR 1.0	National Institute for Space Research, Brazil	Hybrid (edge/region oriented)	Remote sensing with RADAR data	2005
EDISON	Robust Image Understanding Lab, Rutgers University, U.S.	Mean shift	Color images	2003
EWS 1.0	Li and Xiao (2006)	Multi-channel watershed transformation	Remote sensing	2006
Definiens Developer 7.0	Definiens, Germany	Multiresolution segmentation	Remote sensing	2007
HalcoSEG 1.0	InfoSAR, Ltd.	Simulated annealing	Remote sensing with RADAR data	2006
RHSEG 1.3	Goddard Space Flight Center, NASA	Hierarchical region growing	Remote sensing	2007
SCRM	Castilla (2007)	Watershed and region growing	Remote sensing	2007
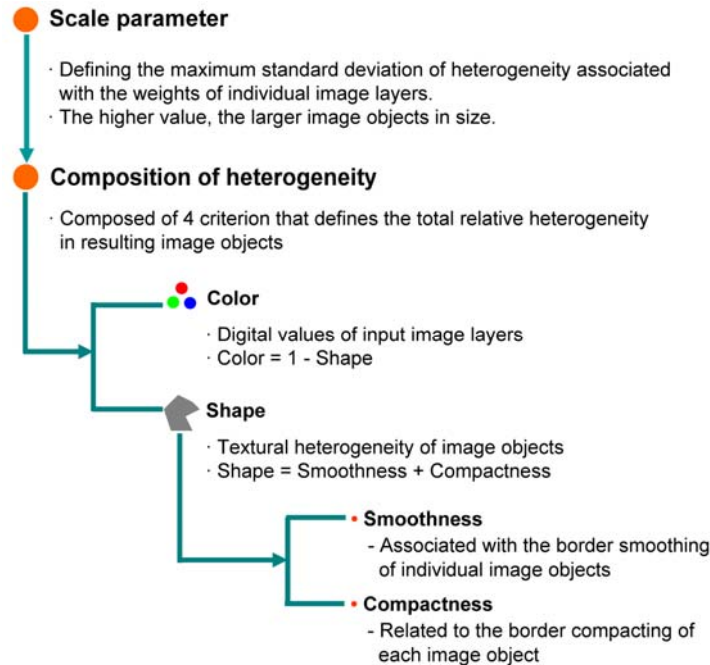
Figure 1.1. Conceptual framework of *Multiresolution Segmentation* in Definiens. The figure was adapted from Definiens Reference Book (2006).

The value of scale parameter denotes a maximum-allowable standard deviation to be utilized in a segmentation procedure. For instance, a value of 18 for the parameter means a standard deviation 18 that is computed from all pixels within a pair of adjacent image objects. The scale parameter is utilized to terminate segmentation procedures and determine the average size of image objects in a given segmentation (Definiens, 2004; Benz *et al.*, 2004). As shown in Figure 1.2, if the calculated value of heterogeneity exceeds a user-defined value of scale parameter, image objects 1 and 2 remains as separate segments, and iterative segmentation procedures are stopped. Otherwise, the two segments are merged into a single larger image object to be utilized in another segmentation procedure. In general, a larger value of scale parameter produces larger image segments in size (Benz *et al.*, 2004).
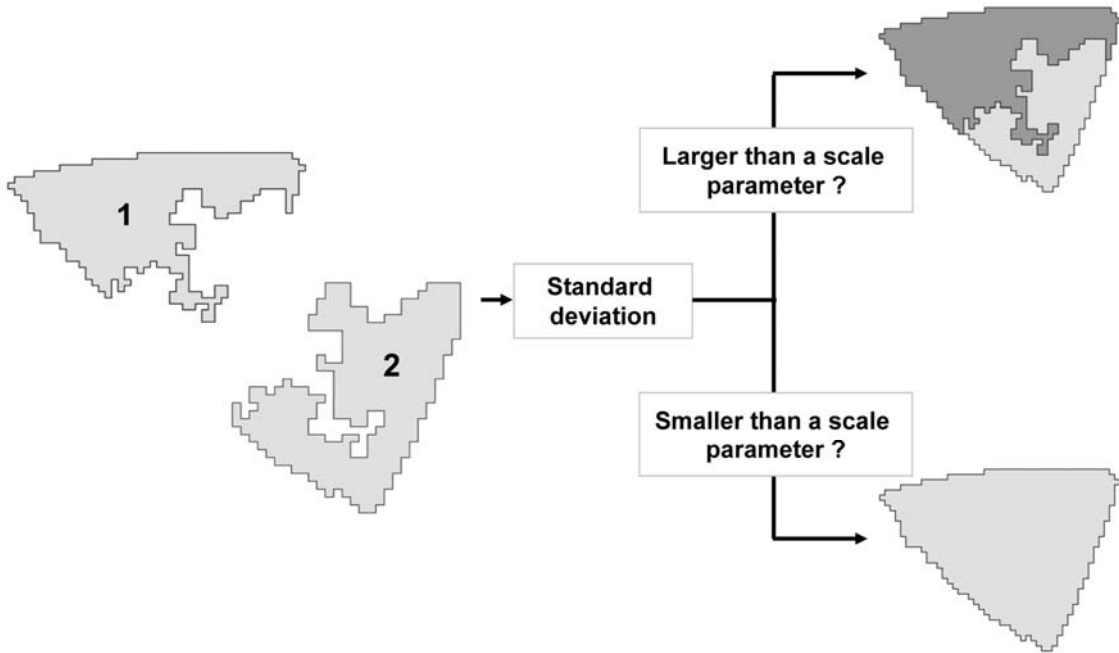
Figure 1.2. Scale parameter to be utilized in deciding merge of a pair of image objects.

The Multiresolution Segmentation algorithm optimizes segmentation procedures based on spectral and spatial heterogeneities, defined as

$$H = w \cdot h_{color} + (1-w) \cdot h_{shape} \cdots\cdots\cdots \text{Equation 1}$$

where H represents a heterogeneity value computed with a pair of image segments, h_{color} means spectral heterogeneity, and h_{shape} denotes spatial heterogeneity (Definiens, 2004). The ratio of color and shape indicates weights to be utilized in Equation 1. The total weight of color and shape is 1, and the values of the two weights are inversely proportional to each other. For example, if a weight value of 0.9 for color, then that of 0.1 is automatically set for shape. Larger

values of shape result in optimized segmentation for spatial heterogeneity, which means more regular shapes of image objects.

Spectral heterogeneity is the sum of the standard deviations with weight values of individual input image layer, defined as

$$h_{color} = \sum w \cdot \sigma \cdots\cdots\cdots \text{Equation 2}$$

where ω represent weight values of each input image layer and σ indicates the standard deviation of pixels within a pair of image objects. Spatial heterogeneity is calculated with the values of compactness and smoothness, defined as

$$h_{shape} = w \cdot h_{compactness} + (1 - w)h_{smoothness} \cdots\cdots\cdots \text{Equation 3}$$

where $h_{compactness}$ and $h_{smoothness}$ denote heterogeneities computed with the values of compactness and smoothness. Definiens (2004) describes provides algorithms to be utilized in computing heterogeneities of compactness and smoothness.

Figures 1.3 shows image objects that were derived from a CIR aerial photograph with 0.5-m spatial resolution by using Definiens Developer (version 7.0). A scale parameter of 40 was employed with the different values of colors, i.e., 0.9 (Figure 1.3a), 0.5 (Figure 1.3b) and 0.1 (Figure 1.3c). A default value of smoothness, i.e., 0.5, was adopted for these segmentations. As shown in Figure 1.3, the boundary shapes of individual image segments tend to be more regular with larger values of shape. The values of smoothness and compactness are associated with the

14

boundary shape of each image object. Image segments, derived from segmentation procedures, are then utilized in image classifications as basic units, instead of pixels.
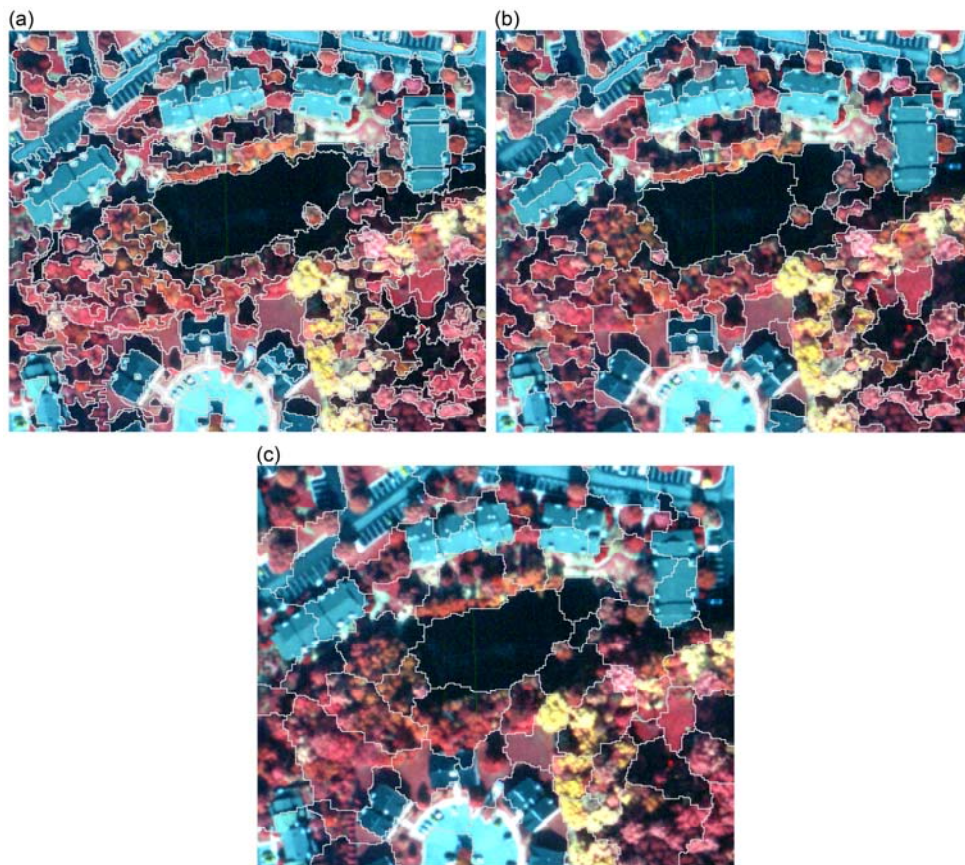
Figure 1.3. Image segmentations with a CIR aerial photograph using scale parameter 40 and smoothness of 0.5. The boundaries of individual image segments were delineated with solid lines in grey color and vary according to the ratio of colors and shape as 0.9 (a), 0.5 (b) and 0.1(c).

1.3.2.2 Segmentation quality

The OBIA approach appears to cast a promising light on overcoming the limitations of pixel-based approaches with VHR imagery, but there is an issue to be considered in association with segmentation quality. In relating image segments to ground features in the real world, OBIA results in distinct levels of segmentation quality associated with the number and the size of image objects: 1) *over- segmentation*, 2) *optimal segmentation* and 3) *under-segmentation* (Frauman and Wolff, 2005; Castilla and Hay, 2008; Kim *et al.*, 2008; Kim *et al.*, in press).

Over-segmentation is considered to result in objects that are too small relative to ground features of interest, since the contrast between some neighboring image segments is insufficient. Consequently, there would be an excessive number of image objects in an over-segmented result. Under-segmentation produces too few image objects, so some different ground features would be mixed and included in a single image object, thus affecting classification results. On the contrary, an optimal segmentation produces image segments that are similar to ground features of interest in size and number. Figure 1.4 illustrates the different levels of segmentation quality related to segmentation scale. The segmentations were yielded with selected scales using Definiens Developer (version 7). For building rooftops, smaller scale values tend to generate over-segmented results, as shown in Figures 1.4a and 1.4b, where individual rooftops are composed of several image segments. On the contrary, Figures 1.4c and 1.4d show optimal segmentations for building rooftops. With larger scale values of 130 and 160, these rooftops are mixed with adjacent ground features of grass and trees in under-segmentations, as in Figures 1.4e and 1.4f.

The quality of segmentation is known to have a direct effect on the accuracies of object-based classifications (Dorren *et al.*, 2003; Meinel and Neubert, 2004; Addink *et al.*, 2007; Kim *et al.*, in press). Segmentation scale has been reported to play an important role in yielding optimal

segmentation, so it is a critical and challenging issue in using object-based classification

approaches (Ryherd and Woodcock, 1996; Blaschke, 2003; Dorren *et al.*, 2003; Kim *et al.*, in

press). Ryherd and Woodcock (1996) demonstrate that segmentation controlled by minimum size,

functioning like a scale parameter, can increase overall accuracy with simulated forest imagery.

A threshold for minimum value was utilized to avoid the generation of large image objects in
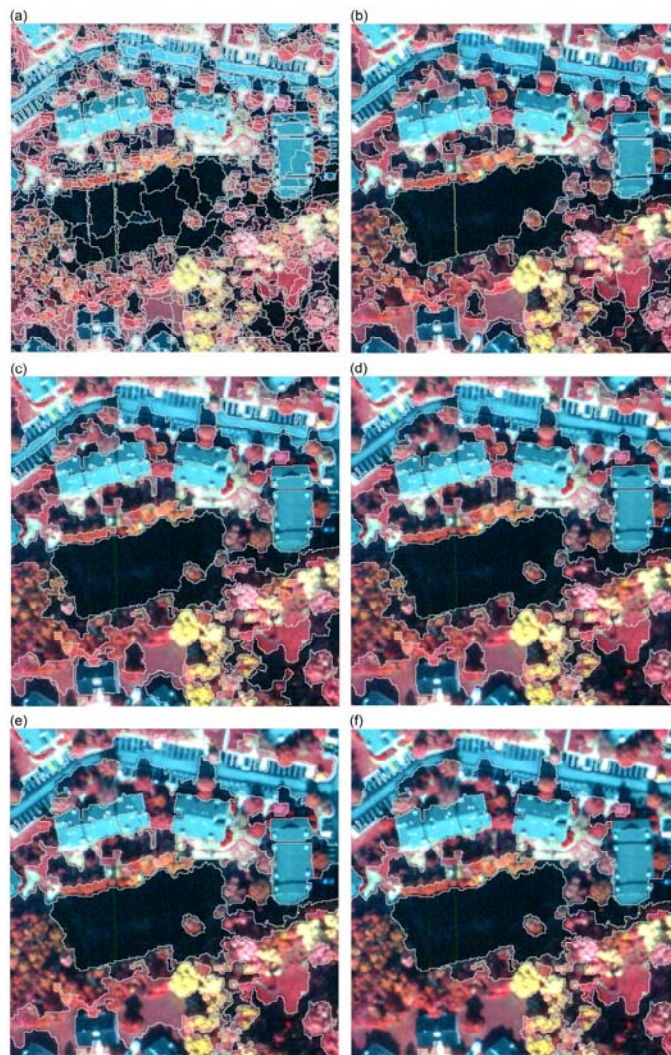
Figure 1.4. Segmentation quality associated with segmentation scales: (a) 10, (b) 40, (c) 70, (d)

100, (e) 130 and (f) 160.

17

their study. In addition, Dorren *et al.* (2003) acquired their best object-based forest type classification from a segmentation that produced average sizes of image objects similar to these forest types in the real world. For this reason, it is imperative to develop methodologies to determine an optimal segmentation associated with segmentation scale before proceeding to actual classification of image objects.

1.3.2.3 Estimation of optimal segmentation quality

Scale-related studies are mainly concerned with developing methods for determining the most appropriate scale (or resolution) and assessing their effects on automatic image classification (Cao and Lam, 1997). As for VHR imagery, the accuracy of classification is closely associated with the relative size of the ground features under investigation (Markham and Townshend, 1981).

Most studies concerning optimal scale have been based largely on pixel-based classification with two estimation methods: 1) graphs of local variance and 2) variogram analysis. The first method produces several levels of aggregated pixels to represent progressively coarser resolutions and to determine optimal spatial resolution for a particular remotely sensed image (Woodcock and Strahler, 1987; Marceau *et al*., 1994b; Coops and Culvenor, 2000; Raptis *et al*., 2003). The graphs of local variance, proposed by Woodcock and Strahler (1987), are used mainly for determining a single optimal spatial scale over an entire image. They computed variances within a 3-by-3 moving window for individual pixels and calculated average local variance on a whole scene. These average local variances are then graphed as a function of spatial resolution, i.e., the aggregated levels of pixels (or upscaling). On the other hand, in recent years, variograms have been widely employed for the same purpose, without upscaling

(Atkinson and Curran, 1997; Treitz and Howarth, 2000a; Wallace *et al.*, 2000; Atkinson and Aplin, 2004; Zawadzki *et al.*, 2005). In the analysis of variograms, point-centered sample data sets are utilized to find sill and range with the distance between a pair of sample points. In the object-based classification it seems difficult to determine which pixel within an image object should be selected to represent the image object for the variogram analysis. In addition, variogram-based analyses are rather complex compared with the method based on local variance.

In the OBIA approach there are no specific guidelines on this issue, and the selection procedure is highly dependent on trial-and-error methods that influence segmentation quality subjectively (Definiens, 2004; Meinuel and Neubert, 2004). However, a number of attempts were made to determine an optimal segmentation scale in recent years. Wang *et al.* (2004a) utilized Bhattacharya Distance (BD), a statistical separability index, to decide a segmentation scale that produced the best classification result of coastal mangrove species from IKONOS imagery. They selected training data representing several species of mangrove trees and image segmentation was applied to the training data instead of the whole scene, with scale parameters from 5 to 25. Several segmented images at each scale were classified, and they found the value of 25 to be optimal for mapping mangrove species. Kim and Madden (2006) examined the relationship between segmentation scale of general forest types (deciduous, evergreen and mixed forests) and classification based on average local variances (see Chapter 2). In addition, a computer programming approach, i.e., genetic algorithm, was adopted to determine optimal sets of segmentation parameters (Feitosa *et al.*, 2006).

In forest mapping there would be the potential to associate the spectral values of image objects to segmentation quality by employing spatial autocorrelation analysis. In over-segmentation, adjacent image segments would be similar in spectral values and spatially

autocorrelated. Under-segmentation would produce large image segments that show similar mixtures of spectral values, and this may result in relatively high autocorrelation. On the contrary, an optimal segmentation would be associated with the least autocorrelation between image segments. This research is presented in Chapter 2 of this dissertation.

1.3.3 Texture analysis

Texture, representing local spatial information, is a basic interpretation element which human interpreters employ in manual interpretation. Texture is a characteristic of physical surface properties of features such as smoothness or roughness has a tactile quality and is manifested by reflectance differences and the variance of color on a surface (Tuceryan and Jain, 1998). In general, images can be classified directly based on texture data or on texture data incorporated with spectral bands (Zhang, 1999). Texture is widely utilized in pixel-based classification for forest/vegetation (Franklin *et al*. 2000, 2001a, 2001b; Zhang *et al*., 2004), land use/land cover (Kiema, 2002; Herold *et al*., 2003; Coburn and Roberts, 2004; Lloyd *et al*., 2004; Puissant *et al*., 2005) and urban applications (Shaban and Dikshit, 2001; Zhang *et al*., 2003). The integration of texture in automated classification procedures is an increasingly important aspect of VHR imagery analysis (Coburn and Roberts, 2004). High-spatial-resolution imagery is considered to be highly textured in forest mapping (Wulder, 1998). Therefore, the analysis of texture has been widely used to introduce the spatial information of different ground features into image classification in order to improve classification results with VHR imagery (Zhang, 1999; Ferro and Warner, 2002; Puissant *et al*., 2005).

Texture can be acquired from remotely sensed images by structural, model-based, and statistical methods (Coburn and Roberts, 2004). Most of these methods have been developed in

pattern recognition and have not always been considered helpful in image analysis with remotely sensed data (Ryherd and Woodcock, 1996). In most cases, a statistical approach has been widely adopted for deriving texture from remote-sensing imagery. The grey-level co-occurrence matrix (GLCM), introduced by Haralick *et al.* (1973) and Haralick and Shanmugam (1974), is one of the most common methods used to calculate statistical texture measures (Franklin *et al*., 2001b; Chan *et al*., 2003; Coburn and Roberts, 2004). In recent years, GLCM texture has been frequently utilized to improve classification results in forest mapping studies (Franklin *et al*. 2000, 2001a; Maillard, 2003; Zhang *et al*., 2004).

A kernel (or moving window) is commonly utilized in image classification to define spatial information specified by a particular number of columns and rows surrounding a target pixel. Successful image classification with texture depends highly upon the kernel size selected, and so optimal kernel size is considered to be an important factor in deriving texture (Puissant *et al.*, 2005; Franklin *et al.*, 2001b). Puissant *et al*. (2005) point out that, if the window is too small, insufficient spatial information is extracted to characterize texture. On the contrary, if the window is too large, it can overlap two types of ground cover and thus introduce erroneous spatial information due to the edge effect of between-class texture (Ferro and Warner, 2002).

In OBIA, texture is computed for non-overlapping, irregularly-shaped "windows" that correspond to individual image objects (Benz *et al*., 2004). Such texture is called *object-specific texture* to distinguish it from texture computed with kernels, i.e. *kernel-based texture*. In using kernels, between-class texture is not distinguished from within-class texture, and this confusion usually degrades the overall performance of texture-based image classification (Ferro and Warner, 2002). That is, in kernel-based texture, both internal pixels and adjacent pixels outside a ground object are often included in the texture computation of a particular window (Figure 1.5a).

Between-class texture is potentially excluded, however, by computing texture based only on pixels from within the boundary of an image object, as long as the quality of the segmentation is reliable (Figure 1.5b). In addition, because image objects can potentially have various sizes, object-specific texture is not inherently limited to a single scale to the extent that fixed-kernel-size texture is.
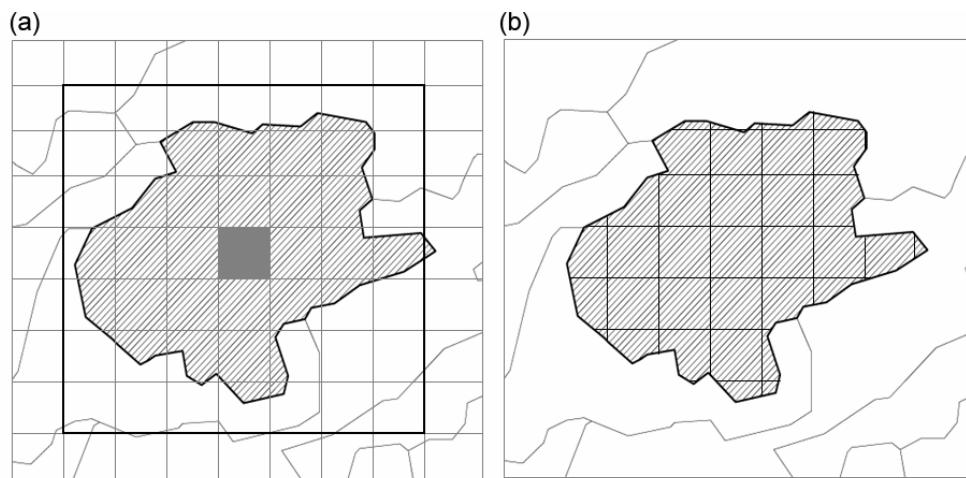
Figure 1.5. Kernel-based texture (a) and object-specific texture (b). A hatched ground object is a target for texture computation. In (a), adjacent pixels belonging to other ground features are included in calculating the texture of the hatched object.

Hay *et al.* (1996) utilized object-specific texture measures computed within individual triangulated areas, the vertices of which were derived from the centers of tree crowns. Although they did not adopt an image segmentation procedure, their calculation of texture is similar to that of the object-specific texture adopted in this study. They found that forest stand classification

using spectral bands alone had an accuracy of 65 %, which increased to 78 % with the inclusion of the texture information. In summary, it appears that object-specific texture has the potential to produce more accurate classifications than do classifications using traditional kernel-based texture.

1.4 STUDY AREA AND DATA

1.4.1 Study area

The study area is Guilford Courthouse National Military Park (GUCO), which was established in 1917 to preserve the vegetation and landscape that approximates battlefield conditions at the time of the American Revolution. The GUCO park was officially surrounded by the city limits of Greensboro, North Carolina, in 1984 (Figure 1.6) and thus lies in one of the most rapidly growing quarters of the city (Hiatt, 2003). This urban sprawl beleaguers managers of the park who aim to preserve the historical and vernacular landscape of GUCO. Left as the only green space within a matrix of commercial and residential development, the park is heavily used by visitors who use the paved trails within the park for recreational walking, running, biking, and dog walking. A current vegetation database is needed to assess heavy visitor use and surrounding land use changes that have potential impacts on the health of vegetation and animal populations within the park.

In 2004, the Center for Remote Sensing and Mapping Science (CRMS), Department of Geography at the University of Georgia, developed a vegetation geodatabase in conjunction with the NPS and NatureServe as a part of the U.S. Geological Survey (USGS)-NPS National Vegetation Mapping Program (Madden and Jordan, 2004; NPS, 2008). The geodatabase was

Figure 1.6. Location of GUCO in Greensboro, North Carolina.

created from manual interpretation of large-scale (i.e., fine-scale) CIR aerial photographs

combined with CRMS-NatureServe field observations and plot-level vegetation surveys

conducted by NatureServe. The manual interpretation was based on association (or community)-

level forest classes of the National Vegetation Classification System (NVCS) identified for the

park by NatureServe (2007). Table 1.3 summarizes association-level vegetation classes in the

GUCO National Park and the more general forest type class to which each association belongs.

In Table 1.3, NVCS Community Element Global (CEGL) codes are provided with related

association-level forests in the GUCO park.

According to NatureServe (2007), cold-deciduous forests are predominant in the park,

with oaks (*Quercus spp*) the dominant species among hardwoods, including White Oak (*Q. alba*),

Southern Red Oak (*Q. falcata*), Black Oak (*Q. velutina*), Chestnut Oak (*Q. prinus*), and Scarlet

Oak (*Q. coccinea*). The other hardwoods include various forest canopy species such as Shagbark

Hickory (*Carya ovata*) and Pignut Hickory (*Carya glabra*), Red Maple (*Acer rubrum*) and Sugar

Maple (*Acer saccharum*), Tuliptree (*Liriodendron tulipifera*), Sycamore (*Platanus occidentalis*),

and Sweetgum (*Liquidambar styraciflua*). Needle-leaved evergreen forests are dominated by

Shortleaf Pine (*Pinus echinata*), Loblolly Pine (*Pinus taeda*), or Virginia Pine (*Pinus virginiana*).

In addition, non-forest vegetation (herbaceous vegetation, shrubland and exotic species) and

man-made features (buildings, roads, cemeteries, trails and homesites) are found in the park. To

facilitate this research on OBIA techniques that required repeated iterations of image processing

procedures, association-level vegetation polygons of the CRMS-NPS vegetation geodatabase

were generalized to three forest type classes: deciduous forest, evergreen forest, and mixed

deciduous-evergreen forest, plus one non-forest class.

Table 1.3. Association-level forest vegetations in GUCO National Park.

Forest type	CEGL code	Association description
Needle-leaf Evergreen Forest	8462	Loblolly Pine/Sweetgum Successional
	2591	Virginia Pine Successional
	6327	Shortleaf Pine Successional
Submontane Cold-deciduous Forest	8475	White Oak (Red Oak, Scarlet Oak, Hickory)/ *Vaccinium pilidum* Piedmont Dry Mesic
	8465	American Beech – Northern Red Oak/ Flowering Dogwood/Christmas Fern-Virginia Heartleaf Acidic Piedmont Mesic
	7244	Southern Red Oak – White Oak – Mockernut Hickory/Sourwood/Deerberry Dry Mesic
	7221	Tuliptree – Red Maple – Oak Successional
	7216	Sweetgum Successional
Temporarily Flooded Cold-deciduous Forest	4418	Piedmont Small-stream Sweetgum (Tuliptree, Red Maple)/Northern Spicebush Bottomland

1.4.2 Data

This research employs IKONOS imagery to investigate objectives described in Section 1.4.1.[1]

The IKONOS satellite was launched as the world's first commercial VHR satellite on September

24, 1999, from Vandenberg Air Force Base, California (Tanaka and Sugimura, 2001). An

IKONOS image can be acquired by the sensor in either 1-m panchromatic or four 4-m

multispectral band mode. Table 1.4 describes the spectral resolution of each band of IKONOS

imagery.

Table 1.4. Spectral wavelength regions of IKONOS imagery.

		Spectral wavelength regions (µm)
Panchromatic band		0.450 - 0.900
Multispectral bands	Blue	0.445 - 0.516
	Green	0.506 - 0.595
	Red	0.632 - 0.698
	Near-infrared (NIR)	0.757 - 0.853

The IKONOS satellite revisits the same area every 3 to 5 days and collects an image of 11×11

km^2 with a radiometric resolution of 11 bits. The pixel size of the IKONOS panchromatic band is

the same as that of a USGS digital orthophoto quarter quadrangle (DOQQ), while 11-bit imagery

provides image contrast and quality superior to the DOQQ (Davis and Wang, 2003). An

IKONOS image for the GUCO park was conferred as a Space Imaging Award (now, GeoEye

Award) presented by the American Society of Photogramemtry and Remote Sensing (ASPRS)

---

[1] IKONOS means "image" in Greek.

and Space Imaging, Inc. (Figure 1.7).[2] The IKONOS image was provided as a Geo Bundle

Product, which has a nominal positional accuracy of 15 m with a circular error at 90 %

probability (CE90).
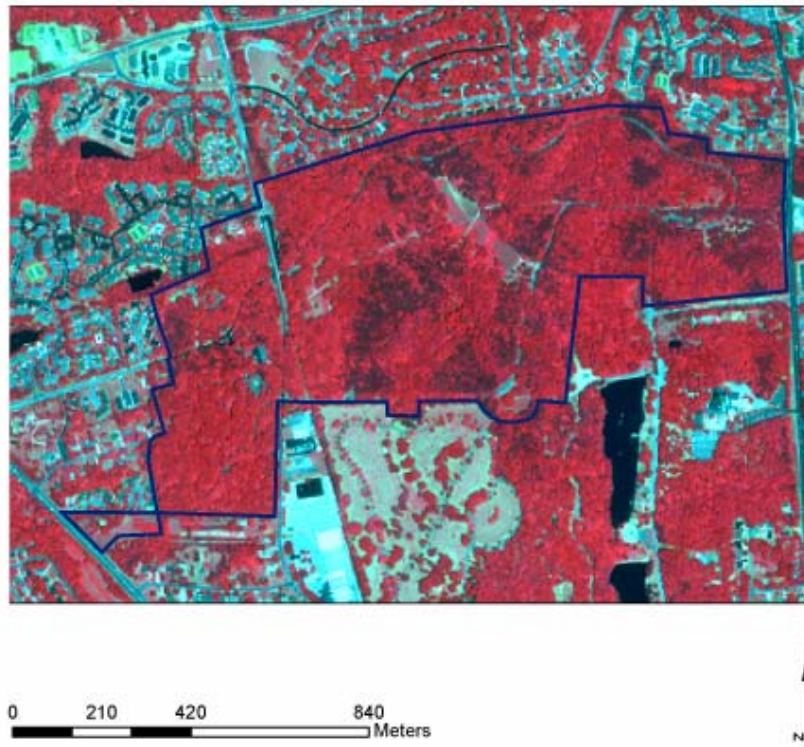
Figure 1.7. Multispectral IKONOS image of Guilford Courthouse National Military Park in false

color composite using NIR, red and green for RGB. The park boundary is outlined in blue.

---

[2] Space Imaging was merged with OrbImage and the name of the merged company has changed as GeoEye, Inc.

The CE90 denotes that 90 % of well-defined check points should fall within the specified

positional accuracy. Therefore, the IKONOS image must be rectified to guarantee positional

accuracy for further image analyses such as segmentations and classifications.

A large-scale CIR aerial photograph at 1:12,000 scale was orthorectified with a root-mean-

square error (RMSE) of ± 5 m (Jordan and Madden, 2008) and used as reference data with a

1999 USGS digital orthophoto quarter quadrangle (DOQQ) to correct the IKONOS imagery

geometrically to a RMSE of ± 3 m to ± 4m. The CIR air photo was also employed to derive

training samples that was used in object-based image classifications. The CIR air photo was

acquired on October 20, 2000, by the U.S. Forest Service and utilized in manual interpretation of

vegetation in the GUCO park by the CRMS (Welch *et al*., 2002). Figure 1.8 shows a CIR aerial

photo of the park. Besides the IKONOS image and the CIR air photos, a CRMS vegetation

geodatabase is employed to develop samples that will be utilized in accuracy assessment of

object-based classifications.
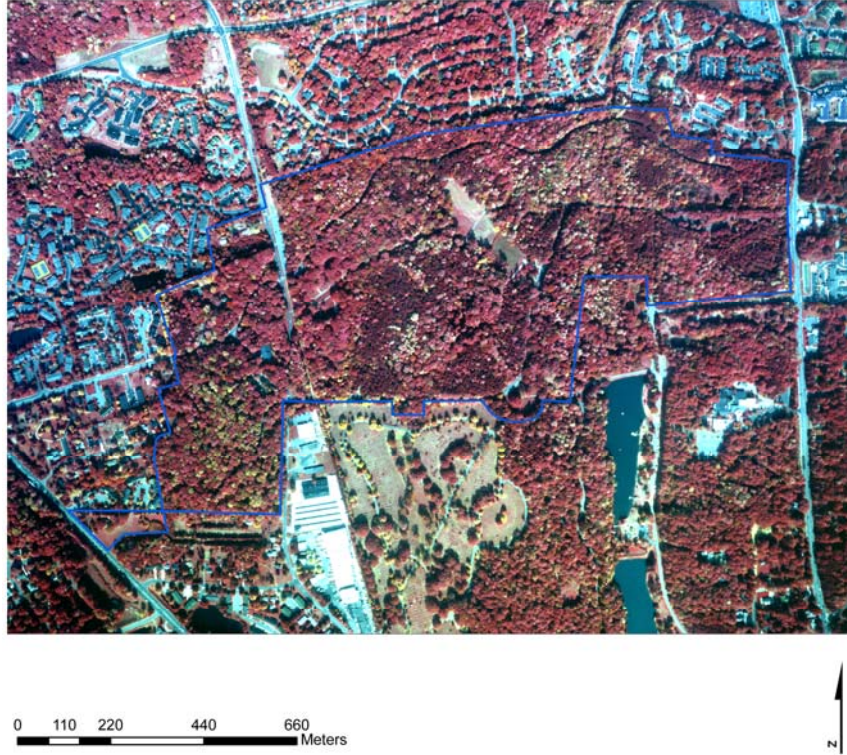
Figure 1.8. A false color composite of the 1:12,000 scale color infrared air photo with near

infrared, red and green for red, green and blue. The park boundary is shown in blue.

REFERENCES

Abkar, A., M.A. Sharifi, and N. J. Mulder. 2000. Likelihood-based image segmentation and classification: a framework for the integration of expert knowledge in image classification procedures. Journal of Applied Geophysics, 2(2):104-119.

Addink, E.A., S.M. de Jong, and E.J. Pebesma. 2007. The importance of scale in object-based mapping of vegetation parameters with hyperspectral imagery. Photogramemtric Engineering & Remote Sensing, 72(8):905-912.

Alpine, P., P.M. Atkinson, and P.J. Curran. 1999. Fine spatial resolution simulated satellite sensor imagery for land cover mapping in the United Kingdom. Remote Sensing of Environment, 68:206-216.

Asner, G.P. and A.S. Warner. 2003. Canopy shaodw in Ikonos satellite observations of tropical forests and savannas. Remote Sensing of Environment, 87:521-533.

Atkinson, P.M. and P. Aplin. 2004. Spatial variation in land cover and choice of spatial resolution for remote sensing. International Journal of Remote Sensing, 25(18):3687-3702.

Atkinson, P.M. and P.J. Curran. 1997. Choosing an appropriate spatial resolution for remote sensing investigations. Photogrammetric Engineering & Remote Sensing, 63(12):1345-1351.

Baskent, E.Z., R.A. Wightman, G.A. Jordan, and Y. Zhai. 2001. Object-oriented abstraction of contemporary forest management design. Ecological Modelling, 143:147-164.

Benz, U.C., P. Hofmann, G. Willhauck, I. Lingenfelder, and M. Heynen. 2004. Multi-resolution, object-oriented fuzzy analysis of remote sensing data for GIS-ready information. ISPRS Journal of Photogrammetry and Remote Sensing, 58:239-258.

Blaschke, T. 2003. Object-based contextual image classification built on image segmentation. Proceedings of the 2003 IEEE Workshop on Advances in Techniques for Analysis of Remotely Sensed Data, 27-28 October 2003, Washington DC, U.S., pp.113-119.

Blaschke, T. and J. Strobl. 2001. What's wrong with pixels? some recent developments interfacing remote Sensing and GIS. GIS-Zeitschrift für Geoinformationssysteme, 6:12-17.

Brandtberg T. and T. Warner. 2006. High resolution remote sensing, Computer Applications. Sustainable Forest Management (G. Shao and K. M. Reynolds, editors), Springer-Verlag, Dordrecht, Netherlands, pp.19-41.

Cao, C. and N.S. Lam. 1997. Understanding the scale and resolution effects in remote sensin. Scale in Remote Sensing and GIS (D.A. Quattrochi and M.F. Goodchild, editors), CRC Press Inc., U.S., pp.57-72.

Carleer, A.P., O. Debeir, and E. Wolff. 2005. Assessment of very high spatial resolution satellite image segmentations. Photogrammetric Engineering & Remote Sensing, 71(11):1285-1294.

Castilla, G. and G.J. Hay. 2008. Image objects and geographic objects. Object-Based Image Analysis - Spatial concepts for knowledge-driven remote sensing applications (T. Blaschke, S. Lang, and G.J. Hay, editors), Springer-Verlag, Berlin, pp.91-110.

Chan, J.C., N. Laporte, and R.S. Defries. 2003. Texture classification of logged forests in tropical Africa using machine-learning algorithms. International Journal of Remote Sensing, 24(6):1401-1407.

Coburn, C.A. and A.C.B. Roberts. 2004. A multiscale texture analysis procedure for improved forest stand classification. International Journal of Remote Sensing, 25(2):4287-4308.

Colwell, R.N. 1960. Some uses of infrared aerial photography in the management of wildland areas. Photogrammetric Engineering & Remote Sensing, 26(12):774-785.

Connors, K.F., T.W. Gardner, and G.W. Petersen. 1987. Classification of geomorphic features and landscape stability in Northwestern New Mexico using simulated SPOT imagery. Remote Sensing of Environment, 22(2):187-207.

Coops, N. and D. Culvenor. 2000. Utilizing local variance of simulated high spatial resolution imagery to predict spatial pattern of forest stands. Remote Sensing of Environment, 71:248-260.

Cufi, X., X. Munoz, J. Freixenet, and J. Marti. 2002. A review of image segmentation techniques integrating region and boundary information. Advances in Imaging and Electron Physics, 120:1-39.

Davis, C.H. and X. Wang. 2003. Planimetric accuracy of Ikonos 1m panchromatic orthoimage products and their utility for local government GIS basemap applications. Remote Sensing of Enviornment, 24(22):4267-4288.

Definiens. 2004. eCognition User Guide 4. Definiens AG, Germany.

Definiens. 2006. Definiens Professional 5 Reference Book. Definiens AG, Germany.

DigitalGlobe. 2006. QuickBird Imagery Products. URL: http://www.digitalglobe.com/index.php/130/Documents+%26+Tutorials (last accessed date: November 08, 2008).

Dorren, L.K.A., B. Maier, and A.C. Seijmonsbergen. 2003. Improved Landsat-based forest mapping in steep mountainous terrain using object-based classification. Forest Ecology and Management, 183:31-46.

Feitosa, C.U., G.A.O.P. Costa, and T.B. Cazes. 2006. A genetic approach for the automatic adaptation of segmentation parameters. Commission IV, WG IV/4 on Proceeding of 1_{st} OBIA Conference, 4-5 July, Salzburg, Austria (International Society for Photogrammetry and Remote Sensing), unpaginated CD-ROM.

Ferro, C.J.S. and T.A. Warner. 2002. Scale and texture in digital image classification. Photogrammetric Engineering & Remote Sensing, 68(1):51-63.

Fisher, P. 1997. The pixel: a snare and a delusion. International Journal of Remote Sensing, 18(3):679-685.

Franklin, S.E., R.J. Hall, L.M. Moskal, A.J. Maudie, and M.B. Lavigne. 2000. Incorporating texture into classification of forest species composition from airborne multispectral images. International Journal of Remote Sensing, 21(1):61-79.

Franklin, S.E., M.A. Wulder, and G.R. Gerylo. 2001a. Texture analysis of IKONOS panchromatic data for Douglas-fir forest age class separability in British Columbia. International Journal of Remote Sensing, 22(13):2627-2632.

Franklin, S.E., A.J. Maudie, and M.B. Lavigne. 2001b. Using spatial co-occurrence texture to increase forest structure and species composition classification accuracy. Photogrammetric Engineering & Remote Sensing, 67:849-855.

Frauman, E. and E. Wolff. 2005. Segmentation of very high spatial resolution satellite images in urban areas for segments-based classification. ISPRS WG VIII/1 on Proceedings of the ISPRS joint conference; 3rd International Symposium Remote Sensing and Data Fusion Over Urban Areas and 5th International Symposium Remote Sensing of Urban Areas, 14-16 March 2005, Tempe, Arizona, USA. URL: http://www.isprs.org/commission8/workshop_urban/frauman.pdf (last date accessed: September 26, 2008).

GeoEye. 2008. GeoEye IKONOS imagery products. URL: http://www.geoeye.com/CorpSite/assets/docs/brochures/IKONOSImagery_bifold2007_v2.pdf (last accessed date: November 08, 2008).

Gerard, F.F.G., B.K. Wyatt, A.C. Millington, and J. Wellens. 1998. The role of data from intensive sample plots in the development of a new method for mapping tropical forest types using satellite imagery. Forest Biodiversity Research, Monitoring and Modeling: Conceptual Background and Old World Case Studies (F. Dallmeier and J.H. Comiskey, editors), Man and the Biosphere, Volume 20, UNESCO, Paris, pp.141-158.

Guo, Q., M. Kelly, P. Gong, and D. Liu. 2007. An object-based classification approach in mapping tree mortality using high spatial resolution imagery. GIScience and Remote Sensing, 44(1):24-47.

Hall, O., G.J. Hay, A. Bouchard, and D.J. Marceau. 2004. Detecting dominant landscape objects through multiple scales: an integration of object-specific methods and watershed segmentation. Landscape Ecology, 19:59-76.

Haralick, R.M., K. Shanmugam, and I. Dinstein. 1973. Textural features for image classification. IEEE Transactions on Systems, Man and Cybernetics, SMC 3(6):610-620.

Haralick, R.M. and K.S. Shanmugam. 1974. Combined spectral and spatial processing of ERTS imagery data. Remote Sensing of Environment, 3:3-13.

Haralick, R.M. and L.G. Shapiro. 1985. Survey: Image Segmentation Techniques. Computer Vision, Graphics, and Image Processing, 29:100-132.

Hay, G.J., K.O. Nieman, and G.F. McLean. 1996. An object-specific image-texture analysis of H-resolution forest imagery. Remote Sensing of Environment, 55:108-122.

Hay, G.J., D.J. Marceau, P. Dube, and A. Bouchard. 2001. A multiscale framework for landscape analysis: object-specific analysis and upscaling. Landscape Ecology, 16:471-490.

Hay, G.J., T. Blaschke, and D.J. Marceau. 2008. GEOBIA 2008 - Pixels, Objects, Intelligence. Proceedings of the GEOgraphic Object Based Image Analysis for the 21st Century Conference. August 5-8, 2008, University of Calgary, Calgary, Alberta, Canada. ISPRS Archives, XXXVIII-4/C1, p.373

Heller, R.C. 1975. Evaluation of ERTS-1 data for forest and range-land survey. USDA Forest Service Research Paper PSW-112, Pacific S.W. Forest and Range Experiment Station, Berkeley, California.

Hiatt, J. 2003. Guilford Courthouse National Military Park: Cultural Landscape Report, National Park Service Web, Southeast Regional Office, Cultural Resources Division, URL: http://www.nps.gov/guco/pphtml/documents.html, National Park Service, Southeast Regional Office, Cultural Resources Division (last date accessed: September 29, 2007).

Jacobsen, K. 2003. Mapping with Ikonos images. Proceedings of 22nd EARSeL Symposium, Prague, p.7.

Jensen, J.R. 2000. Remote Sensing of the Environment: An Earth Resource Perspective, Prentice-Hall Series in Geographic Information Science, Prentice Hall, NJ, p.121.

Jordan, T. and M. Madden. 2008. Digital Vegetation Maps for National Park Service Cumberland-Piedmont Inventory and Monitoring Network. Final Report to the U.S. Department of Interior, National Park Service. Coorperative Agreement Number H5028-01-0651. Center for Remote Sensing and Mapping Science, The University of Georgia, Athens, GA, p.105.

Katrikeyan, B., A. Sarkar, and K.L. Majumder. 1998. A segmentation approach to classification of remote sensing imagery. International Journal of Remote Sensing, 19(9):1695-1709.

Kiema, J.B. 2002. Texture analysis and data fusion in the extraction of topographic objects from satellite imagery. International Journal of Remote Sensing, 23(4):767-776.

Kim, M. and M. Madden. 2006. Determination of optimal scale parameter for alliance-level forest classification of multispectral IKONOS image. Commission IV, WG IV/4 on Proceeding of 1_{st} OBIA Conference, 4-5 July, Salzburg, Austria (International Society for Photogrammetry and Remote Sensing), unpaginated CD-ROM.

Kim, M., M. Madden, and T.A. Warner. 2008. Estimation of optimal image object size for the segmentation of forest stands with multispectral IKONOS imagery. Object-Based Image Analysis - Spatial concepts for knowledge-driven remote sensing applications (T. Blaschke, S. Lang, and G.J. Hay, editors), Springer-Verlag, Berlin, pp.291-307.

Kim, M., M. Madden, and T. WARNER. in press. Forest type mapping using object-specific texture measures from multispectral IKONOS imagery: segmentation quality and image classification issues. Photogrammetric Engineering & Remote Sensing.

Kimes, D.S., R.F. Nelson, W.A. Salas, and D.L. Skole. 1999. Mapping secondary tropical forest and forest age from SPOT HRV data. International Journal of Remote Sensing, 20(18): 3625-3640.

Lachowski, H., P. Maus, and N. Roller. 2000. From pixels to decisions: digital remote sensing technologies for public land managers. Journal of Forestry, 98(6):13-15.

Laliberte, A., A. Rango, K.M. Havstad, J.F. Paris, R.F. Beck, R. Mcneely, and A.L. Gonzalez. 2004. Object-oriented image analysis for mapping shrub encroachment from1937 to 2003 in Southern New Mexico. Remote Sensing of Environment, 93:198-210.

Lloyd, C.D., S. Berberoglu, P.J. Curran, and P.M. Atkinson. 2004. A comparison of texture measures for the per-field classification of Mediterranean land cover. International Journal of Remote Sensing, 25(19):3943-3965.

Lobo, A. 1997. Image segmentation and discriminant analysis for the identification of land Cover units in ecology. IEEE Transactions on Geoscience and Remote Sensing, 35:1136-1145.

Lobo, A., K. Moloney, and N. Chiariello. 1998. Fine-scale mapping of a grassland from digitized aerial photography: an approach using image segmentation and discriminant analysis. International Journal of Remote Sensing, 19(1):65-84.

Lu, D. and Q. Weng. 2007. Survey of image classification methods and techniques for improving classification performance. International Journal of Remote Sensing, 28(5):823-870.

Madden, M. and T. Jordan. 2004. Database development and analysis for decision makers in National Parks of the Southeast. Proceedings of ASPRS Fall Conference, 12-16 September,Kansas City, Missouri (American Society for Photogrammetry and Remote Sensing, Bethesda, Maryland), unpaginated CR-ROM.

Maillard, P. 2003. Comparing texture analysis methods through classification. Photogrammetric Engineering & Remote Sensing, 69(4):357-367.

Marceau, D.J., P.J. Howarth, J.M. Dubois, and D.J. Gratton. 1990. Evaluation of the grey-level co-occurrence matrix method for land cover classification using SPOT imagery. IEEE Transactions on Geoscience and Remote Sensing, 28:513-519.

Marceau, D.J., P.J. Howarth, and D.J. Gratton. 1994. Remote sensing and the measurements of geographical entities in a forested environment. 1. The Scale and Spatial Aggregation Problem. Remote Sensing of Environment, 43:93-104.

Markham, B.L. and J.R.G. Townshend. 1981. Land cover classification accuracy as a function of sensor spatial resolution. Proceedings of 15_{th} International Symposium on Remote Sensing Environment, Ann Arbor, p.1075.

Meinel, G. and M. Neubert. 2004. A comparison of segmentation programs for high resolution remote sensing data. Commission VI in Proceeding of XX_{th} ISPRS Congress, 12-23 July, Istanbul, Turkey (International Society for Photogrammetry and Remote Sensing), unpaginated CD-ROM.

Metzler, J.W. and S.A. Sader. 2005. Model development and comparison to predict softwood and hardwood per cent cover using high and medium spatial resolution imagery. International Journal of Remote Sensing, 26(17):3749-3761.

Millington, A.C. and R.W. Alexander. 2000. Vegetation mapping in the last three decades of the twentieth century. Vegetation Mapping from Patch to Planet (R. Alexander and A.C. Millington, editors), John Wiley & Sons, Ltd., England, pp.321-331.

National Park Service (NPS). 2008. Vegetation Mapping Program, U.S. Geological Survey (USGS) Biological Resources Discipline (BRD) and National Park Service, URL: http://science.nature.nps.gov/im/inventory/veg/index.cfm (last date accessed: May 19, 2008).

NatureServe. 2007. Accuracy Assessment: Guilford Courthouse National Military Park. Final Report to the National Park Service Durham, North Carolina, p.5.

Nelson, J., D. Case, N. Horning, V. Anderson, and S. Pillai. 1987. Continental land cover assessment using Landsat MSS data. Remote Sensing of Environment, 21(1):61-81.

Neubert, M., H. Herold, and G. Meinel. 2006. Evaluation of remote sensing image segmentation quality - further results and concepts. Commission IV, WG IV/4 on Proceeding of 1_{st} OBIA Conference, 4-5 July, Salzburg, Austria (International Society for Photogrammetry and Remote Sensing), unpaginated CD-ROM.

Neubert, M., H. Herold, and G. Meinel. 2008. Assessing image segmentation quality - concepts, methods and application. Object-Based Image Analysis - Spatial concepts for knowledge-driven remote sensing applications (T. Blaschke, S. Lang, and G.J. Hay, editors), Springer-Verlag, Berlin, pp.769-784.

Oetter D.R., W.B. Cohen, M. Berterretche, T.K. Maiersperger, and R.E. Kennedy. 2000. Land cover mapping in an agricultural setting using multiseasonal Thematic Mapper data. Remote Sensing of Environment, 76(2):139-155.

Openshaw, S. 1984. The modifiable areal unit problem. CATMOG 38. GeoBooks, Norwich, England.

Pal, N.R. and S.K. Pal. 1993. A review on image segmentation techniques. Pattern Recognition, 26(9):1277-1294.

Puissant, A., J. Hirsch, and C. Weber. 2005. The utility of improve per-pixel classification for high to very high spatial resolution imagery. International Journal of Remote Sensing, 26(4):733-745.

Raptis, V.S., R.A. Vaughan, and G.G. Wright. 2003. The effect of scaling on land cover classification from satellite data. Computers and Geoscience, 29:705-714.

Read, J.M., D.B. Clark, E.M. Venticinque, and M.P. Moreira. 2003. Application of merged 1-m and 4-m resolution satellite data to research and management in tropical forest. Journal of Applied Ecology, 40:592-600.

Ryherd, S. and C. Woodcock. 1996. Combining spectral and texture data in the segmentation of remotely sensed images. Potogrammetric Engineering & Remote Sensing, 62(2):181-194.

Salovaara K.J., S. Thessler, R.N. Malik, and H. Tuomisto. 2005. Classification of Amazonian primary rain forest vegetation using Landsat ETM+ satellite imagery. Remote Sensing of Environment, 97(1):39-51.

Sande, C.J., S.M., de Jong, and A.P.J. de Roo. 2003. A segmentation and classification approach of IKONOS-2 imagery for land cover mapping to assist flood risk and flood damage assessment. International Journal of Applied Earth Observation, 4:217-229.

Shaban, M.A., and O. Dikshit. 2001. Improvement of classification in urban areas by the use of textural features: the case study of Lucknow city, Uttar Pradesh. International Journal of Remote Sensing, 22(4):565-593.

Shiewe, J., L. Tufte, and E. Ehlers. 2001. Potential and problems of multi-scale segmentation methods in remote sensing. GIS-Zeitschrift für Geoinformationssysteme, 6:34-39.

Souza, C.M. and D. Roberts. 2005. Mapping forest degradation in the Amazon region with Ikonos images. International Journal of Remote Sensing, 26(3):425-429.

Strahler, A.H., C.E.Woodcock, and J. Smith. 1986. On the nature of models in remote sensing. Remote Sensing of Environment, 20:121-139.

Stuchkens, J., P.R. Coppin, and M.E. Bauer. 2000. Integrating contextual information with per-pixel classification for improved land cover classification. Remote Sensing of Environment, 71:282-296.

Tanaka, S. and T. Sugimura. 2001. A new frontier remote sensing from Ikonos images. International Journal of Remote Sensing, 22(1):1-5.

Townshend, J.R.G, C. Huang, S.N.V. Kalluri, R.S. Defries, S. Liang, and K. Yang. 2000. Beware of per-pixel characterization of land cover. International Journal of Remote Sensing, 21(4):839-843.

Treitz, P. and P. Howarth. 2000. High spatial resolution remote sensing data for forest ecosystem classification: an Examination of spatial scale. Remote Sensing of Environment, 72:268-289.

Tuceryan, M. and A.K. Jain. 1998. Texture Analysis. Handbook of Pattern Recognition and Computer Vision (C.H. Chen, L.F. Pau, and P.S.P. Wang, editors.), World Scientific Publishing Co., pp.207-248.

Wallace, C.S.A., J.M. Watts, and S.R. Yool. 2000. Characterizing the spatial structure of vegetation communities in the Mojave desert using geostatistical techniques. Computers and Geosciences, 26:397-410.

Wang, L., W.P. Sousa, and P. Gong. 2004a. Integration of object-based and pixel-based classification for mapping mangroves with IKONOS imagery. International Journal of Remote Sensing, 25(24):5655-5668.

Wang, L., W.P., Sousa, P., Gong, and G.S., Biging. 2004b. Comparison of IKONOS and QuickBird images for mapping mangrove species on the Caribbean coast of Panama. Remote Sensing of Environment, 91:434-440.

Welch, R., M. Madden, and T. Jordan. 2002. Photogrammetric and GIS techniques for the development of vegetation databases of mountainous areas: Great Smoky Mountains National Park. ISPRS Journal of Photogrammetry and Remote Sensing, 57:53-68.

Woodcock, C.E. and A.H. Strahler. 1987. The factor of scale in remote sensing. Remote Sensing of Environment, 21:311-332.

Wulder, M.A. 1998. Optical remote-sensing techniques for the assessment of forest inventory and biophysical parameters. Progress in Physical Geography, 22(4):449-476.

Wulder, M.A., J.C. White, K.O. Niemann, and T. Nelson. 2004. Comparison of airborne and satellite high spatial resolution data for the identification of individual trees with local maxima filtering. International Journal of Remote Sensing, 25(11):2225-2232.

Wyatt, B.K. 2000. Vegetation mapping from ground, air and space - comparative or complementary techniques?. Vegetation Mapping from Patch to Planet (R. Alexander and A.C. Millington, editors), John Wiley & Sons, Ltd., England, pp.3-15.

Yu, Q., P. Gong, N. Clinton, G. Biging, M. Kelly, and D. Shirokauer. 2006. Object-based detailed vegetation classification with airborne high spatial resolution remote sensing imagery. Photogrammetric Engineering & Remote Sensing, 72(7):799-811.

Zawadzki, J., C.J. Cieszewski, M. Zasada, and R.C. Lowe. 2005. Applying geostatistics for investigations of forest ecosystems using remote sensing imagery. Silva Fennica, 39(4):599-617.

Zhang, Y. 1999. Optimization of building detection in satellite images by combining multispectral classification and texture filtering. International Journal of Remote Sensing, 54:50-60.

Zhang Q., J. Wang, P. Gong, and P. Shi. 2003. Study of urban spatial patterns from SPOTpanchromatic imagery using textural analysis. International Journal of Remote Sensing, 24(21):4137-4160.

Zhang, C., S.E. Franklin, and M.A. Wulder. 2004. Geostatistical and texture analysis of airborne-acquired images used in forest classification. International Journal of Remote Sensing, 25(4):859-865.

CHAPTER 2

ESTIMATION OF OPTIMAL IMAGE OBJECT SIZE FOR THE SEGMENTATION OF

FOREST STANDS WITH MULTISPECTRAL IKONOS IMAGERY[3]

ABSTRACT

The determination of segments, representing an optimal image object size, is very challenging in object-based image analysis (OBIA). This research employs local variance and spatial autocorrelation to estimate the optimal size of image objects for segmenting forest stands. Segmented images are visually compared to a manually interpreted forest stand database to examine the quality of forest stand segmentation in terms of the average size and number of image objects. Average local variances are then graphed against segmentation scale in an attempt to determine the appropriate scale for optimally derived segments. In addition, an analysis of spatial autocorrelation is performed to investigate how between-object correlation changes with segmentation scale in terms of over-, optimal, and under-segmentation.

INDEX WORDS: Image segmentation, Very high spatial resolution image, Over- and under-
                    segmentation, Object-based image analysis (OBIA), Forest stands, Local
                    variance, Spatial autocorrelation

2.1 INTRODUCTION

Conventional pixel-based classification approaches have limitations that should be considered when applied to very high spatial resolution (VHR) imagery (Fisher, 1997; Townshend *et al.*, 2000; Ehlers *et al.*, 2003; Brandtberg and Warner, 2006). The increased within-class spectral variation of VHR images decreases classification accuracy when used with the traditional pixel-based approaches (Shiewe *et al.*, 2001). Object-based image analysis (OBIA), which became an area of increasing research interest in the late 1990s, is a contextual segmentation and classification approach that may offer an effective method for overcoming some of the

limitations inherent to traditional pixel-based classification of VHR images. Particularly, the OBIA can overcome within-class spectral variation inherent to VHR imagery (Yu *et al.*, 2006). In addition, it can be used to emulate a human interpreter's ability in image interpretation (Blaschke and Strobl, 2001; Blaschke, 2003; Benz *et al.*, 2004; Meinel and Neubert 2004).

Although the OBIA scheme seems to hold promise for solving classification problems associated with VHR imagery, it also has an important related challenge, namely, the estimation of the desired size of image objects that should be obtained in an image segmentation procedure. Unfortunately, there is currently no objective method for deciding the optimal scale of segmentation, so the segmentation process is often highly dependent on trial-and-error methods (Meinel and Neubert, 2004). Yet, the size of image objects is one of the most important and critical issues which directly influences the quality of the segmentation, and thus the accuracy of the classification (Blaschke, 2003; Dorrren *et al.*, 2003; Meinel and Neubert, 2004).

In this paper, we employ a case study that builds on the results of Kim and Madden (2006) to investigate agreement between a manual interpretation and image segmentation at a variety of scales, and the pattern of segment variance and autocorrelation associated with those segmentation scales. Kim and Madden (2006) performed a research to examine the relationship between segmentation scale of general forest types (i.e., deciduous, evergreen, and mixed forests) and classification. For this follow-on study, we examine if an understanding of changes associated with segment variance and autocorrelation might provide image analysts with a method of determining optimal size of image objects in image segmentation for forest stand mapping.

2.2 LOCAL VARIANCE, SPATIAL AUTOCORRELATION AND IMAGE OBJECTS

ASSOCIATED WITH FOREST STAND MAP

A number of previous studies have investigated how image properties change with pixel

resolution (Cao and Lam 1997). One common method for understanding how image spatial

structure changes with pixel size is the graph of average local variance, used by Woodcock and

Strahler (1987). This approach has been used to determine the optimal spatial resolution for

identifying thematic information of interest in the context of pixel-based image classification. In

Woodcock and Strahler's (1987) approach, the image is degraded to a range of pixel size.

Variance in spectral reflectance or brightness is then computed a 3×3 moving window, and then

the average for the entire scene is graphed as a function of the associated pixel size. Woodcock

and Strahler (1987) found that the local variance was low if the spatial resolution was

considerably finer than objects on an image. When the pixel size was approximately one half to

three quarters of the size of the objects in the image, the local variance was found to reach a

maximum. On the other hand, if the pixel size was larger than the objects in the image, the local

variance decreases once again. Thus, the graph of local variance against pixel size is one method

that can be helpful for understanding spectral heterogeneity and the scale of the objects in the

image.

Building on this idea of linking variance and scale, we hypothesize that the average

variance of image objects, graphed as a function of image segment size, may provide insight as

to the optimal scale of image objects for image segmentation. We define the optimal scale as one

that is not over-segmented, with an excessive number of segments that are on average too small,

and also not under-segmented, with too few segments that are on average too large.

This definition of an optimal scale is useful for considering the relationship between image object variance and scale. As the segmentation becomes coarser, each segment will tend to incorporate a wider range of image brightness values. Therefore, a general trend of increasing average variance of the segments is expected with coarser scale (and decreasing number of segments). However, we hypothesize that with mixed forest stands, as the segments become too large (i.e., reach a stage of under-segmentation) each segment will tend to include more pixels from pure forest stands. This inclusion would lower the variance of image objects corresponding to mixed forest stands. Therefore, we suggest that the optimal segmentation actually would occur at the scale just before a flattening of the graph. Our second hypothesis is that the optimal scale generates the least positive, and potentially even negative, autocorrelation between the average brightness values of the segments. In other words, we assume that an optimal scale most clearly brings out contrasting average brightness values in the segmentation.

This autocorrelation hypothesis draws in part on the concept that ideal image enhancement should maximize autocorrelation at the pixel level (Warner, 1999). Likewise, image enhancements (Warner and Shank, 1997) and classifications (Warner *et al.*, 1999) can be ranked based on their information content as indicated by autocorrelation at the pixel level. However, for segmentation, we suggest that the optimal pattern is obtained when the adjacent segments are the least similar in brightness values. In an over-segmented image, we would expect that the adjacent segments are on average somewhat similar, and thus the segments will tend to be autocorrelated. On the other hand, in an under-segmented image, the segments are too large, and lose their spectral homogeneity. In this instance, the average brightness of the adjacent segment will tend to converge on relatively similar mixtures, and once again the autocorrelation of the segments is relatively high. Therefore, we suggest that in a graph of scale versus autocorrelation

of the segments, the optimal scale should be indicated by the scale associated with the least autocorrelation between segments.

2.3 STUDY AREA AND DATA SOURCES

The study area for the case research is the Guilford Courthouse National Military Park (GUCO) located in Greensboro, North Carolina, U.S.A. (Figure 2.1). The 1-km^2 park lies in one of the most rapidly developing portions of the city and provides increasingly important green space for recreational activities and wildlife refuge (Hiatt, 2003).
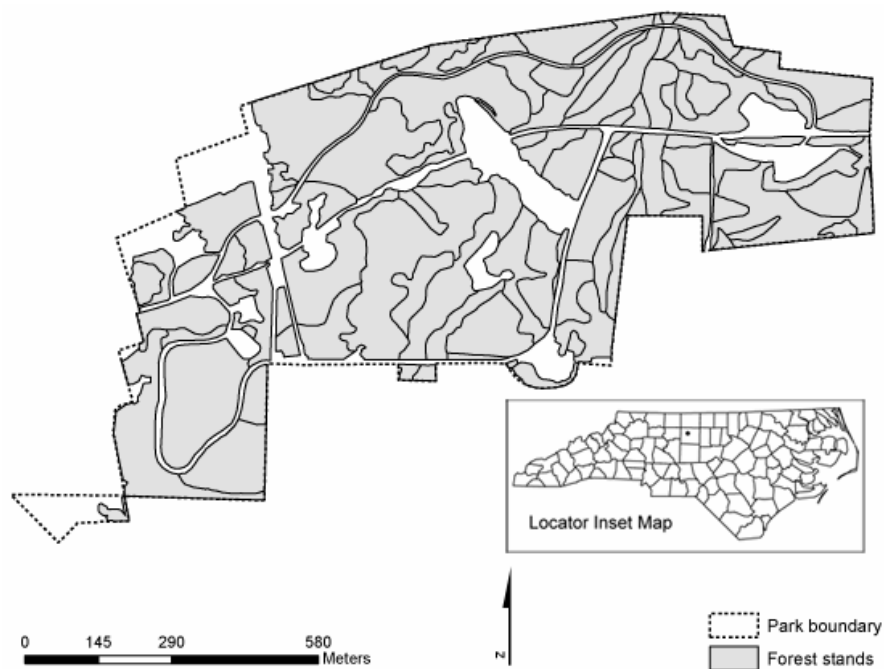
Figure 2.1. Forest stands of GUCO park from University of Georgia CRMS-NPS vegetation database produced by the manual interpretation of aerial photographs.

The park was initially mapped by the Center for Remote Sensing and Mapping Science (CRMS), Department of Geography at the University of Georgia, in conjunction with the National Park Service (NPS) and NatureServe, as part of the NPS/U.S. Geological Survey (USGS) National Vegetation Mapping Program (Welch *et al.*, 2002; Madden *et al.*, 2004). The mapping of the park was based on manual interpretation of 1:12,000-scale leaf-on color-infrared (CIR) aerial photographs using the National Vegetation Classification System (NVCS) (Grossmann *et al.*, 1998). Figure 2.1 illustrates the manually-interpreted association-level forest stands in GUCO.

In our study, we assume that the manually produced GUCO vegetation database/map can be used as a reference for determining the optimal scale of the segmentation. Although the manual map does not necessarily represent an objective optimal scale and classification of forest stands, it represents vegetation communities of the type, level of detail and scale that the resource managers require for management decisions. Furthermore, human interpreters bring to bear extensive local (i.e., field-based data) and expert knowledge of forest stands and associated remote sensing signatures. GUCO was visited several times throughout the course of the project by CRMS and NatureServe botanists to collect plot-level data of overstory and understory tree species, as well as numerous quick plots to identify the NVCS class of observation points geolocated with GPS (Madden et al. 2004). An independent accuracy assessment of the completed association-level vegetation and forest stand database conducted by NatureServe resulted in an overall accuracy of 83 % and a Kappa of 0.81 (NatureServe, 2007). Therefore, we can assume that the manually interpreted database represents the best approximation of the optimal scale and classification of GUCO forest stands.

A multispectral IKONOS image of 4-m pixel resolution acquired on July 6, 2002 by Space Imaging, Inc. (now GeoEye, Inc.) was used for this research with special attention to the near infrared band (NIR) that is crucial to vegetation studies. The image was georeferenced and co-registered to a scanned CIR aerial photograph that was acquired October 20, 2000 at 1:12,000 scale and rectified based on horizontal control from a 1998 USGS Digital Orthophoto Quarter Quadrangle (DOQQ). The study area has a very flat terrain, so the co-registration of the CIR aerial photograph and IKONOS image could be achieved to a root-mean-square-error of ±4 m with this process. The GUCO park includes non-forest areas such as open pasture, roads, cemeteries and homesites. These non-forest areas were masked out before image segmentation of forest stands.

2.4 METHODOLOGY

Multiresolution Segmentation, implemented in Definiens Professional Version 5.0 (formerly eCognition), was utilized for the OBIA. The segmentation is based on a region growing technique which places seed pixels over an entire image and groups surrounding pixels to the local seeds, if they meet specific criteria. The size and homogeneity of image objects are important parameters in the segmentation. The scale parameter, i.e. segmentation scale, controls the average size of the image objects (Definiens, 2004). The homogeneity criterion determines the importance or weight of three heterogeneity attributes: color, smoothness and compactness. The color criterion minimizes the standard deviation of spectral values within image objects and also considers the shape of image objects. The shape criterion itself is comprised of a smoothness criterion defined as how smooth the boundary of each image object is in a segmented image and a compactness criterion minimizing the deviation from the ideal compact form (Definiens, 2004).

For this study, a series of segmentations was conducted using the IKONOS image with the segmentation scale varying from 2 to 30 in steps of 1 to examine the segmentation quality of image objects representing more detailed (association-level) forest stands. These values were chosen so as to encompass a range of scales that were observed to extend from over-segmentation to under-segmentation. In addition, the scale step of 1 was made possible by the relatively small size of the park (1 km^2) and therefore minimal time for processing iterations. An additional analysis was conducted to assess the repeatability of segmentation processes. The entire range of segmentation scales from 2 to 30 was repeated 5 times each and the resulting segments were visually compared. This thorough analysis of this size range of segmentation scale was needed to determine the optimal object size for object-based forest stands segmentation.

The color and shape ratios are inversely proportional to each other in the homogeneity criterion. The shape of each image object approaches that of a circle as the shape value approaches a value of 1.0. Therefore, if the segmentation scale is consistent (e.g., 18) and the color to shape ratio decreases, forest segment boundaries became less complex and segment sizes became more uniform (see Figure 2.2) when compared to forest stands in the manually interpreted CRMS database (see Figure 2.1). Since a value of 0.9 for this ratio was found to produce a pattern most like that of the manual map, this value was used for the entire subsequent analysis. All segmentation procedures were performed using only brightness values of the four spectral bands.

Segmented images across entire segmentation scales were exported to polygon vector files of ArcView Shapefile format to compute average local variance and Moran's I indices. The standard deviations of image objects' spectral reflectance and an average for all the segments

49

were computed from the brightness values of NIR band. These average variances were then graphed as a function of segmentation scale. Moran's I indices were computed from the mean values of NIR band of the segmented images in order to examine between-object spatial autocorrelation at each scale. The contiguity matrix, used for computing the Moran's I, was calculated from the squared inverse Euclidean distance between segment centroids.
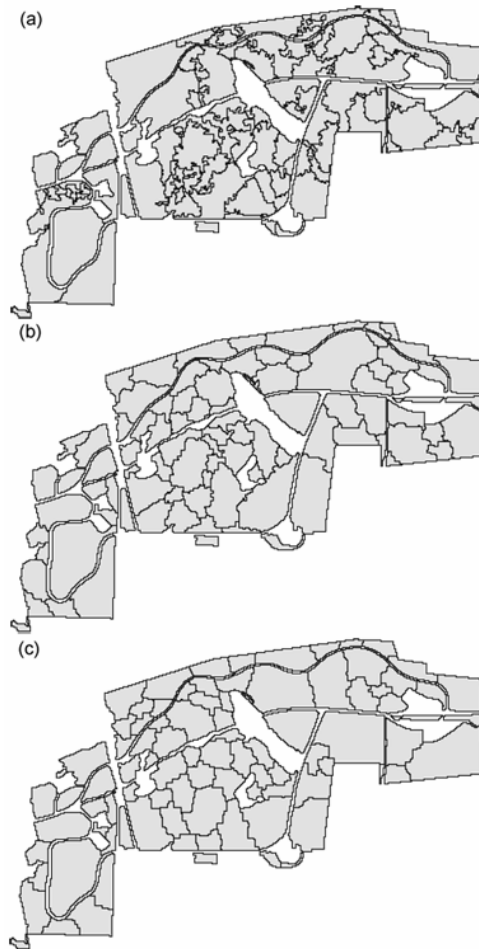
Figure 2.2. Different shapes of image objects with a constant segmentation scale of 18, but decreasing ratios of color to shape. Image objects derived from the color criterion of 0.9 (a), 0.5 (b) and 0.1 (c)

2.5 RESULTS AND DISCUSSION

The image segmentation was performed across the range of segmentation scales (2 to 30). This produced a range of sizes and numbers of image objects (Table 2.1). The segmentation across the entire range of scales (2 to 30) was repeated 5 times, with no discernable difference in the number and average size of segments, as well as the calculation of local variance and Moran's I autocorrelation.

Table 2.1. Average sizes and numbers of image object produced by the image segmentation.

Scale	Average size (m^2)	No. of image objects	Scale	Average size (m^2)	No. of image objects
2	50	13,182	17	6,207	107
3	125	5,321	18	6,991	96
4	228	2,907	19	8,407	79
5	378	1,756	20	9,488	70
6	565	1,175	21	9,767	68
7	829	801	22	11,451	58
8	1,094	607	23	12,299	55
9	1,466	453	24	13,023	51
10	1,965	339	25	13,283	50
11	2,424	274	26	13,283	50
12	2,913	228	27	15,095	45
13	3,477	191	28	15,445	43
14	3,907	170	29	16,199	41
15	4,677	142	30	16,604	40
16	5,535	120			

The average sizes of image objects across the range of scales were then compared to the average size of association-level forest stands derived from the manual interpretation to identify scales associated with under- and over-segmentation (Figure 2.3). Since the average size of the CRMS forest stands was 7,002 m^2 and the number of forest stands was 94, it can be inferred that the segmentation scale of 18 produced segmentation results most closely resembling manually interpreted forest stands in shape, size and location.
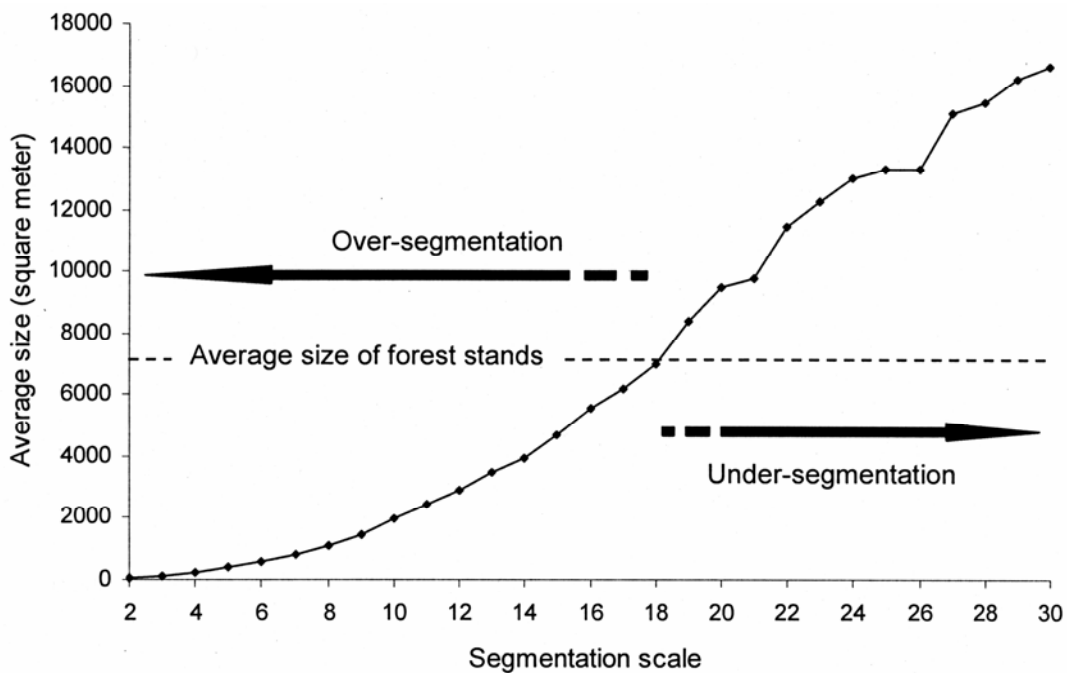
Figure 2.3. Average sized image objects resulting from a range of segmentation scales to determine under- and over-segmentation of image objects in comparison to the manually produced map (7,002 m^2).

We visually assessed segmentation quality associated with over-, optimal, and under-segmentation in comparison with manually interpreted forest stands. Figures 2.4a and 2.4b indicate over-segmentation of association-level forest stands compared with manual interpretation. At a scale of 6, the study area is clearly segmented to excess with over 5 times the desired number of segments. At the other extreme, small stands of pure evergreen forest, indicated by dashed circles on Figure 2.4a, do not appear in the under-segmented image as shown in Figure 2.4c. It is important to note, however, that even at the apparently optimal scale of 18 (Figure 2.4d), some small areas of disagreement do exist between the manual and automated segmentations. Forest stands, shown in the dashed-circle areas in Figure 2.4d, were divided into several image objects that do not match the manual forest stands.
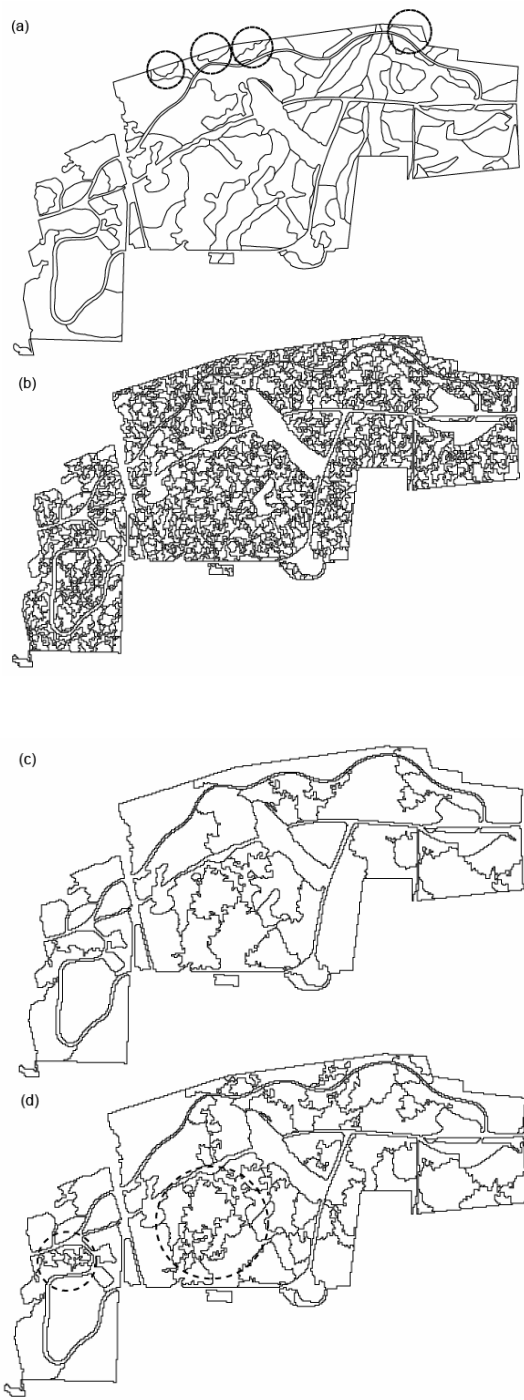
Figure 2.4. Segmentation quality compared with manual interpretation: (a) manually produced vegetation associations map of GUCO, (b) over-segmentation at the scale of 6, (c) under-segmentation at the scale of 25, (d) optimal segmentation at the scale of 18.

54

Two different analyses of object local variance and spatial autocorrelation provided evidence of 18 and 19 being strong candidates for the optimal segmentation scales in this study. The graph of average local variance of image objects over the range of segmentation scale is shown in Figure 2.5.
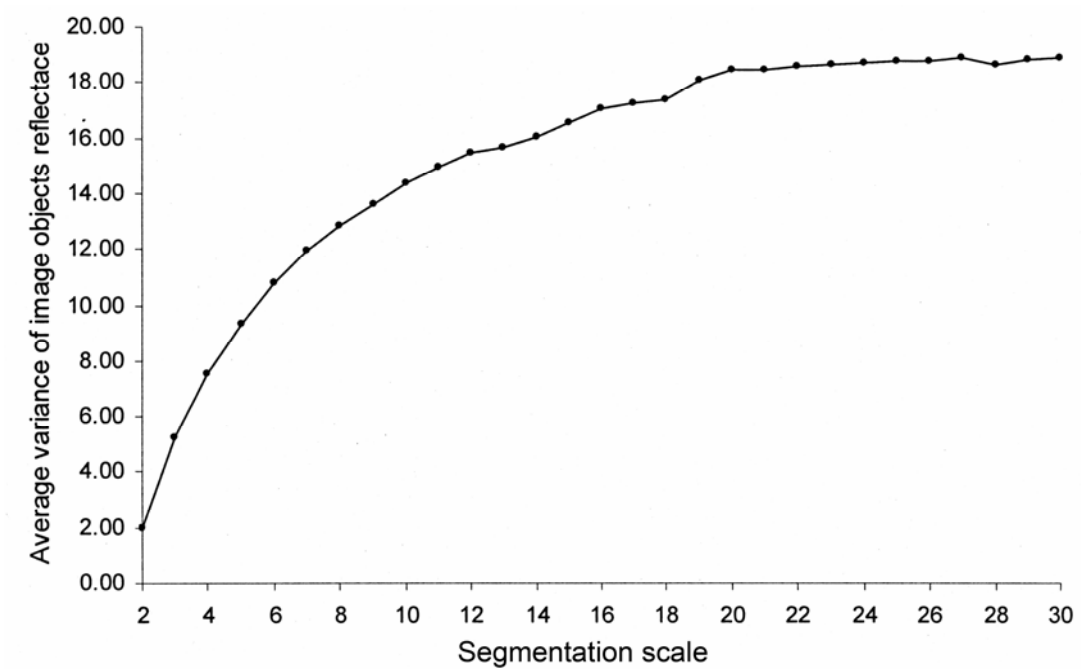
Figure 2.5. Graph of local variance as a function of segmentation scale.

Average local variance increases from a low value of 2.0 at the minimum scale of 2, and levels off at the scale of 20. As discussed earlier, we anticipated that the under-segmentation would occur at the scale where the graph of local variance began to level off and the optimal scale would actually come just before this point. Therefore, Figure 2.5 supports a scale of 19 being optimal for forest objects. Additional support for determining the optimal segmentation scale

55

comes from Table 2.1. This table indicates the number and average size of image objects is most similar to those of the manually produced forest stands map at the segmentation scale of 18. The graph of spatial autocorrelation, as calculated by Moran's I, versus segmentation scale also shows a distinct overall bowl shape with minima at scale of 14 and 18 (Figure 2.6). The lowest minimum at scale 18 coincides with the scale that produced the segmentation most similar to the manually produced map. It should also be noted that between the scale of 14 and 21, the autocorrelation is negative, indicating dissimilarity between adjacent values. The graph confirms the expectation that excessive over- and under-segmentation is associated with positive autocorrelation, while an optimal segmentation should be associated with the lowest autocorrelation.
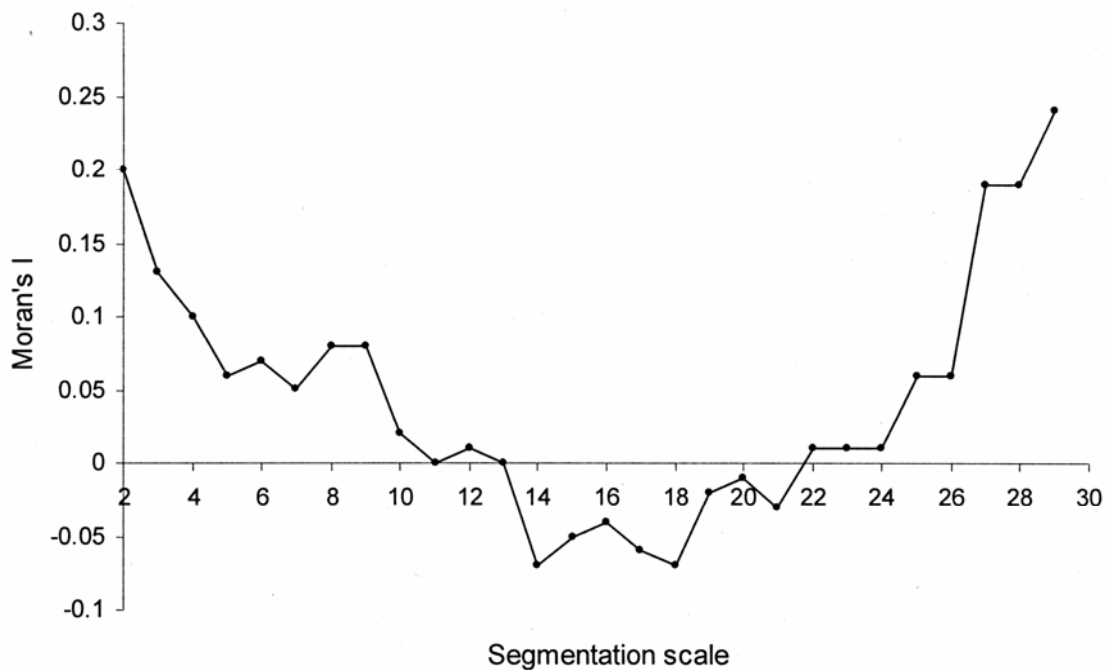
Figure 2.6. Moran's I indices as a function of segmentation scale.

2.6 SUMMARY AND CONCLUSION

In summary, object-based forest stand segmentation was performed using a 4-m multispectral IKONOS image. Visual comparison was made between a vegetation database compiled by manual interpretation and segmented images to examine segmentation quality associated with over-, optimal, and under- segmentation. Local variance and spatial autocorrelation were utilized in an attempt to estimate the optimal scales related to sizes of image objects for forest stand segmentation.

Average local variance was graphed as a function of segmentation scales. The average variance was found to increase with the magnitude of the segmentation scale, leveling off at the scale of 20 and therefore, indicating an optimal scale of 19. We also expected that the optimal segmentation scale would result in image objects similar in number and size to those of the manual forest stands before the scale where the graph leveled off. This expectation was validated at a scale of 18 which produced the number/size of image objects closet to those of the manual interpretation. The average size and number of image objects at the scale of 18 (6,991 m^2 and 96, respectively) were very close to those of manually interpreted association-level forest stands in the park (7,002 m^2 and 94, respectively).

The analysis of spatial autocorrelation indicated that there was high positive correlation between segmentation scales and Moran's I indices calculated for image objects with excessive over- and under-segmentation. In contrast, between-object autocorrelation was lowest, and indeed negative, when the scale was 18. This supports the scale at which the average size and number of segmented image objects were similar to those of manually interpreted forest stands.

In conclusion, three types of analyses (i.e., number/average size of objects, local variance, and spatial autocorrelation) all confirmed that segmentation scales of 18 to 19 are optimal for

obtaining segmented image objects that most closely resemble those of manual interpretation of forest stands by vegetation experts. Although the analyses did not agree on the exact same optimal segmentation scale, they narrowed the wide range of possible segmentation scales to 18 or 19. Indeed, users often do not know the order of magnitude to begin for the determination of segmentation scale (e.g., 10 or 100). By 1) comparing segmentation results to objects in a dataset of known accuracy completeness, and 2) analyzing measures of image variance heterogeneity and spatial autocorrelation vs. segmentation scale, it is now possible to propose an image analysis methodology that may be useful for identifying optimal segmentation scales. Researchers, for example, could perform a rough cut of segmentation at a few scales between a wide range of (e.g., 5, 10, 15, 20) and then graph local variance and Moran's I. The shapes of these graphs will reveal scale ranges most likely to be associated with optimal image object sizes. The local variance graph will level off and Moran's I will dip to negative values. OBIA researchers can then target specific scales (e.g., 10-15) and avoid wasting time for segmentation at non-optimal scales. It is hoped that these results will lead to more automated procedures of segmentation for the extraction of high quality features from very high resolution digital images.

ACKNOWLEDGEMENTS

REFEERENCES

Benz, U.C., P. Hofmann, G. Willhauck, I. Lingenfelder, and M. Heynen. 2004. Multi-resolution, object-oriented fuzzy analysis of remote sensing data for GIS-ready information. ISPRS Journal of Photogrammetry and Remote Sensing, 58:239-258.

Blaschke, T. 2003. Object-based contextual image classification built on image segmentation. Advances in Techniques for Analysis of Remotely Sensed Data 2003 IEEE Workshop, pp.113-119.

Blaschke, T. and J. Strobl. 2001. What's wrong with pixels? Some recent developments interfacing remote sensing and GIS. GIS-Zeitschrift für Geoinformationssysteme, 6:12-17.

Brandtberg, T. and T. Warner. 2006. High resolution remote sensing. Computer Applications and Sustainable Forest Management (G. Shao and K.M. Reynolds, editors), Springer-Verlag, Dordrecht, Netherlands, pp.19-41.

Cao, C. and N.S. Lam. 1997. Understanding the scale and resolution effects in remote sensing and GIS. Scale in Remote Sensing and GIS (D.A. Quattroachi and M.F. Goodchild, editors), CRC Press Inc., U.S., pp.57-72.

Definiens. 2004. eCognition User Guide 4, Definiens AG, Germany

Dorren, L.K.A., B. Maier, and A.C. Seijmonsbergen. 2003. Improved Landsat-based forest mapping in steep mountainous areas using object-based classification. Forest Ecology and Management, 183:31-46.

Ehlers, M., M. Gähler, and R. Janowsky. 2003. Automated analysis of ultra high resolution remote sensing data for biotope type mapping: new possibilities and challenges. ISPRS Journal of Photogrammetry and Remote Sensing, 57:315-326.

Fisher, P. 1997. The pixel: a snare and a delusion. International Journal of Remote Sensing, 18(3):679-685.

Grossman, D.H., D. Faber-Langendoen, A.S. Weakley, M. Anderson, P. Bourgeron, R. Crawford, K. Goodin, S. Landaal, K. Metzler, K.D. Patterson, M. Payne, M. Reid, and S. Sneddon. 1998. International Classification of Ecological Communities: Terrestrial Vegetation of the United States. Vol I. The National Vegetation Classification System: Development, Status and Applications. The Nature Conservancy, Arlington, Virginia, p.126.

Hiatt, J. 2003. Guilford Courthouse National Military Park: Cultural Landscape Report. National Park Service, Southeast Regional Office, Cultural Resources Division, URL: http://www.nps.gov/guco/pphtml/documents.html (last date accessed: March 22, 2006).

Kim, M. and M. Madden. 2006. Determination of optimal scale parameter for alliance-level forest classification of multispectral IKONOS image. Commission IV, WG IV/4 on Proceeding of 1st OBIA Conference, Salzburg, Austria, unpaginated CD-ROM.

Madden, M., R. Welch, T. Jordan, P. Jackson, R. Seavey, and J. Seavey. 2004. Digital Vegetation Maps for the Great Smoky Mountains National Park. Final Report to the U.S. Dept. of Interior, National Park Service, Cooperative Agreement Number 1443-CA-5460-98-019, Center for Remote Sensing and Mapping Science, The University of Georgia, Athens, Georgia, p.112.

Meinel, G. and M. Neubert. 2004. A comparison of segmentation programs for high resolution remote sensing data. Commission VI on Proceeding of 20th ISPRS Congress in Istanbul, URL: http://www.isprs.org/istanbul2004/comm4/papers/506.pdf (last date accessed: October 16, 2005).

NatureServe. 2007. Accuracy Assessment: Guilford Courthouse National Military Park. Final Report to the National Park Service, Durham, North Carolina.

Shiewe, J., L. Tufte, and E. Ehlers. 2001. Potential and problems of multi-scale segmentation methods in remote sensing. GIS-Zeitschrift für Geoinformationssysteme 6:34-39.

Townshend, J.R.G., C. Huang, S.N.V. Kalluri, R.S. Defries, S. Liang, and K. Yang. 2000. Beware of per-pixel characterization of land cover. International Journal of Remote Sensing 21(4):839-843.

Warner, T. 1999. Analysis of spatial pattern in remotely sensed data using multivariate spatial autocorrelation. Geocarto International 14(1):59-65.

Warner, T. and M. Shank. 1997. Spatial autocorrelation analysis of hyperspectral imagery for feature selection. Remote Sensing of Environment 60:58-70.

Warner, T., K. Steinmaus, and H. Foote. 1999. An evaluation of spatial autocorrelation-based feature selection. International Journal of Remote Sensing 20(8):1601-1616.

Welch, R., M. Madden, and T. Jordan. 2002. Photogrammetric and GIS techniques for the development of vegetation databases of mountainous areas: Great Smoky Mountains National Park. ISPRS Journal of Photogrammetry and Remote Sensing 57(1-2): 53-68.

Woodcock, C.E. and A.H. Strahler. 1987. The factor of scale in remote sensing. Remote Sensing of Environment 21:311-332.

Yu, Q.P., P. Gong, G. Clinton, M.K. Biging, and D. Shirokauer. 2006. Object-based detailed vegetation classification with airborne high spatial resolution remote sensing imagery. Photogrammetic Engineering & Remote Sensing 72(7):799-811.

CHAPTER 3

FOREST TYPE MAPPING USING OBJECT-SPECIFIC TEXTURE MEASURES FROM

MULTISPECTRAL IKONOS IMAGERY: SEGMENTAITON QUALITY AND IMAGE

CLASSIFICATION ISSUES[4]

ABSTRACT

This study investigated the use of an object-based image analysis (OBIA) approach with the incorporation of object-specific grey-level co-occurrence matrix (GLCM) texture measures from a multispectral IKONOS image for delineation of deciduous, evergreen and mixed forest types in Guilford Courthouse National Military Park, North Carolina. A series of automated segmentations was produced at a range of scales, each resulting in an associated range of number and size of objects (or segments). Prior to classification, the spatial autocorrelation of each segmentation was evaluated by calculating Moran's I using the average image digital numbers (DNs) per segment. An initial assumption was made that the optimal segmentation scales would have the lowest spatial autocorrelation, and conversely, that over- and under-segmentation would result in higher autocorrelation between segments. At these optimal segmentation scales, the automated segmentation was found to yield information comparable to manually interpreted stand-level forest maps in terms of the size and number of segments. A series of object-based classifications was carried out on the image at the entire range of segmentation scales. The results demonstrated that the scale of segmentation directly influenced the object-based forest type classification results. The accuracies were higher for classification of images identified from a spatial autocorrelation analysis to have an optimal segmentation, compared to those determined to have over- and under-segmentation. An overall accuracy of 79 % with a Kappa of 0.65 was obtained at the optimal segmentation scale of 19. The addition of object-specific GLCM multiple texture analysis improved classification accuracies up to a value of 83 % overall accuracy and a Kappa of 0.71 by reducing the confusion between evergreen and mixed forest types. Although some misclassification still remained because of local segmentation quality, a visual assessment

63

of the texture-enhanced OBIA classification was generally agreeable with manually interpreted forest types.

INDEX WORDS: Object-based image analysis, Segmentation quality, Grey-level co-occurrence matrix, Forest type classification

3.1 INTRODUCTION

Natural resources managers have relied on the manual interpretation of aerial photographs since the 1940s and automated classification of medium resolution satellite image data since the 1970s (Colwell, 1960; Heller, 1975; Hoffer and Staff, 1975; Jensen, 1979; Lachowski *et al.*, 2000). Large-scale color infrared (CIR) aerial photographs have been manually interpreted to develop detailed forest databases and manage resources in state and federal conservation lands (Welch *et al.*, 1995; Lund *et al.*, 1997; Welch *et al.*, 1999). Manual interpretation to identify forest stands from aerial photographs is typically performed by human interpreters using basic image interpretation elements of tone, texture, shape, size, pattern, and associations (Avery, 1962; Teng *et al.*, 1997). Although this technique provides a high level of detail, it is a labor intensive classification of forest types from digital imagery (Welch *et al.*, 2002; Read *et al.*, 2003).

Very high spatial resolution (VHR) satellite imagery with spatial resolutions of similar magnitude to those of aerial photographs (1-4 m pixels) became available for resource inventory and monitoring with the successful launch of commercial imaging satellites in the late 1990s (Ehlers *et al.*, 2003; Ehlers, 2004). The VHR imagery is anticipated to be an alternative to aerial photos for characterization of forest structure and dynamics using automatic image classification techniques. In recent years, for example, IKONOS imagery has been frequently utilized for

forest/vegetation mapping purpose using pixel-based image classification methods (Franklin *et al*., 2001a; Asner and Warner, 2003; Read *et al*., 2003; Wang *et al*., 2004a; Wulder *et al*., 2004; Metzler and Sader, 2005; Souza and Roberts, 2005).

Pixel-based approaches, however, have limitations for use with VHR image classification because high spectral variability within classes decreases classification accuracy (Woodcock and Strahler, 1987; Marceau *et al*., 1990; Shiewe *et al*., 2001; Yu *et al*., 2006; Lu and Weng, 2007). Pixel-based approaches also ignore the context and the spectral values of adjacent pixels (Fisher, 1997; Townshend *et al*., 2000; Brandtberg and Warner, 2006). Various image classification techniques have been developed in remote sensing research, including object-based, textural, and contextual image classifications, in order to reduce the limitations associated with VHR images (Guo *et al*., 2007; Lu and Weng, 2007). In this study, we employ an object-based image classification approach with the incorporation of texture for automatically interpreting forest types from VHR satellite imagery.

3.1.1 Object-based image analysis and object-specific texture

The object-based image analysis (OBIA) approach has the potential to overcome inherent problems of high spectral variability within the same land cover classes in VHR imagery (Yu *et al*., 2006). The OBIA approach has been recognized as an important research area since the late 1990s, partly in the hope that this approach will emulate the human interpreters' ability to identify and delineate features of interest (Blaschke and Strobl, 2001; Schiewe *et al*., 2001; Blaschke, 2003; Benz *et al*., 2004; Meinel and Neubert, 2004).

Two steps typically involved in OBIA are: 1) image segmentation to produce image objects (or segments) that are relatively homogeneous groups of pixels; and 2) image

classification based on these image objects. The quality of segmentation is known to influence the accuracy of image classification (Dorren *et al.*, 2003; Meinel and Neubert, 2004; Addink *et al.*, 2007). Blaschke (2003) suggests estimation of the appropriate size of image objects (i.e., optimal segmentation scale) is a critical, but challenging, issue in OBIA. In addition, Dorren *et al.* (2003) and Ryherd and Woodcock (1996) emphasize the importance of image object size in forest mapping. However, there have been few studies to investigate the relationship between segmentation quality and forest type classification using VHR satellite imagery compared to a reliable reference data set. For example, with a manually interpreted and field verified data set for comparison, it is possible to examine how accurately object-based image classification can delineate the boundaries of forest types, and to investigate optimal segmentations for forest type mapping.

Even though there have been a number of attempts to determine optimal segmentation (Wang *et al.*, 2004a; Kim and Madden, 2006; Feitosa *et al.*, 2006; Kim *et al.*, 2008), there are no specific guidelines on this issue and the selection procedure remains highly dependent on trial-and-error methods which subjectively influence segmentation quality (Definiens, 2004; Meinel and Neubert, 2004). For this reason, defining an optimal segmentation for the object-based classifications of various landscape units on the ground and developing methodologies for estimating the optimal segmentation can be regarded as urgent research issues. An example of a methodology to determine the appropriate segmentation for forest stands delineation is the spatial autocorrelation analysis employed by Kim *et al.* (2008). They performed a series of image segmentations and found three levels of segmentation in terms of spatial autocorrelation: over-segmentation, optimal segmentation, and under-segmentation. *Optimal segmentation* is considered a segmentation that produces desired image objects of the lowest autocorrelation in

terms of spectral reflectance. On the contrary, *over- and under-segmentations* result in image objects of higher autocorrelation than optimal segmentation. Kim *et al.* (2008) computed and graphed Moran's I values across various segmentation scales to find these three levels of segmentation quality for forest stands.

In addition, the problem of within-class spectral variation of VHR imagery can potentially be addressed by an OBIA approach that uses a combination of spectral and texture information (Lu and Weng, 2007). The incorporation of texture in pixel-based classification approaches is a recurrent theme in remote sensing literature and has been successfully used to improve the accuracy of pixel-based forest/vegetation mapping with VHR satellite imagery (Zhang, 1999; Ferro and Warner, 2002). For example, Wang *et al.* (2004b) utilized first- and second-order texture measures to map mangrove species from VHR satellite images such as IKONOS and QuickBird.

The grey-level co-occurrence matrix (GLCM) (Haralick *et al.*, 1973; Haralick and Shanmugam, 1974) is one of the most common algorithms for computing texture measures (Coburn and Roberts, 2004; Franklin *et al.*, 2000, 2001a, 2001b; Zhang *et al.*, 2004). Common pixel-based texture is dependent on the size of the moving window (also called the kernel), specified by a particular number of columns and rows, used in the texture calculation. In OBIA, texture is essentially computed for non-overlapping irregularly-shaped "windows" that correspond to individual image objects (Benz *et al.*, 2004). We term such texture *object-specific texture* to distinguish it from texture computed with overlapping, moving kernels. When using kernel-based texture, it has been reported that between-class texture tends to degrade the overall performance of kernel-based texture classification (Ferro and Warner, 2002). However, between-class texture is potentially excluded by computing texture based only on pixels from within the

boundary of an image object, as long as the quality of the segmentation is reliable. In addition, because image objects can potentially vary in size, object-specific texture is not inherently limited to a single scale to the extent that a single fixed-kernel size texture is limited. Hay *et al.* (1996) conducted a study utilizing object-specific texture measures which were computed within individual triangulated areas, the vertices of which were derived from the centers of tree crowns. Although they did not adopt an image segmentation procedure, their calculation of texture is similar to that of the object-specific texture adopted in this study and they found forest stand classification could be improved by adding texture information computed from triangulated areas of tree crowns.

3.1.2 Research objectives

The overall research objective was to investigate object-based classification with GLCM texture measures, using a case study of forest type mapping in the Eastern U.S., 4-m multispectral IKONOS imagery, and a comparison with a reliable manually interpreted forest data set.

The overall research objective was addressed through three research questions:

1) Does segmentation quality, associated with segmentation scale, directly influence the classification results of forest types from VHR satellite imagery? If so, which segmentation is optimal for forest type mapping?

2) Can we determine optimal segmentation scale(s) prior to actual object-based forest type classification?

3) Will classification accuracies be improved by adding texture measures in object-based image classifications? If so, for what forest types?

The first question is closely associated with finding optimal segmentation of meaningful image objects for forest type classification related to shape, size, and placement. Although segmentation can be conducted across all possible scales, there is no guideline to determine what scale will produce optimal segmentation or to estimate the scale before actual image classification. In this study, a series of object-based forest type classifications was performed to: 1) examine the effect of segmentation quality on classification results; 2) evaluate optimal segmentation scales for forest type mapping; 3) confirm the validation of spatial autocorrelation analysis for estimating optimal segmentation; and 4) compare the effects of object-specific texture measures on forest type classification with a benchmark of a manually interpreted and field verified forest stands database. In addition, the boundary delineation of forest types from object-based classification was compared to the boundaries of a forest stands database derived from manual interpretation.

3.2 STUDY AREA AND DATA

The study site is the National Park Service (NPS) Guilford Courthouse National Military Park (GUCO) which is located in Greensboro, North Carolina (Figure 3.1). The geographic coordinates of the site are 36° 07'39" - 36°08'11" N, and 79°49'56" - 79°50'58" W. The National Military Park is about 1 km^2 in area, and it is located in a region experiencing rapid urban sprawl (Hiatt, 2003). This remaining green space is heavily used for recreation by the surrounding residents, placing increasing pressure on park managers to protect its natural and cultural resources. The park is managed to preserve the vegetation and landscape of the battlefield in a state as similar as possible to that of the time of the American Revolution.

69
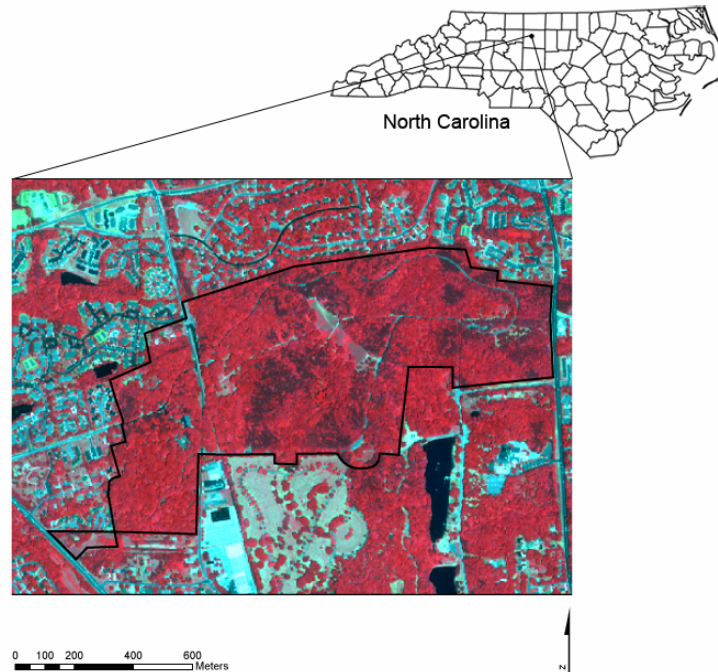
Figure 3.1. The Guilford Courthouse National Military Park study area depicted in a false color

multispectral IKONOS image (bands 4, 3, and 2 as RGB).

The vegetation of the GUCO park was mapped by the UGA-CRMS in conjunction with

NPS and NatureServe, as a part of the USGS-NPS National Vegetation Mapping Program

(Madden and Jordan, 2004; NPS, 2008). CIR aerial photographs, acquired on 20 October 2000,

at 1:12,000 scale, were utilized for manual interpretation of vegetation based on the National

Vegetation Classification System (NVCS) with 19 association (community)-level forest classes

for the GUCO park. An independent field-based assessment performed by NatureServe, a non-

profit conservation organization, indicated that the overall classification accuracy of the GUCO

vegetation geodatabase was 83 %, with a Kappa of 0.81 (NatureServe, 2007). In this study, we

collapsed the 19 floristic forest associations into 3 physiognomic formations (Figure 3.2):

deciduous broad-leaved forest (DF), evergreen needle-leaved forest (EF), mixed evergreen-

deciduous forest (MF). These classes approximate the upper L3-Formation Hierarchy Level of the Federal Geographic Data Committee (FGDC) National Vegetation Classification Standard Version 2 (Draft) and will hereafter be referred to as forest types (FGDC, 2007).
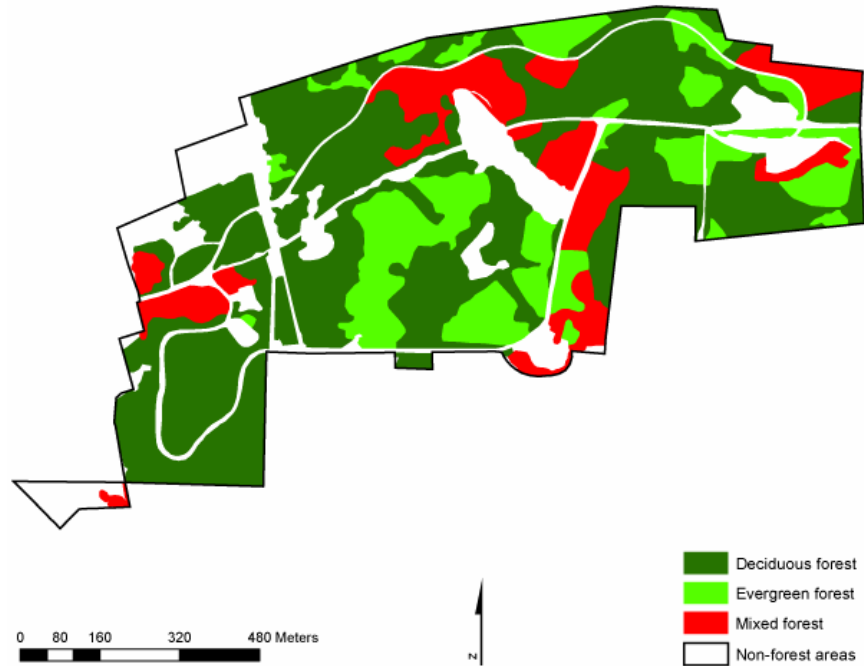
Figure 3.2. Forest types of GUCO park from the CIR manual interpretation.

A multispectral IKONOS image with 8-bit radiometric resolution and 4-m spatial resolution was used for object-based forest type classifications of the park. The IKONOS image was acquired on 6 July 2002 (see Figure 3.1) and rectified to a 1999 USGS digital orthophoto quarter quadrangle (DOQQ) with a root-mean-square-error of ±4 m. The CRMS vegetation geodatabase was employed to obtain training data sets for individual forest types and samples for

71

evaluating classification accuracy. The sample points were obtained by stratified random sampling method and verified using the DOQQ and CIR air photos.

3.3 METHODS

In order to compare the different OBIA classification strategies, a systematic series of classifications was undertaken. Before image segmentation and classification, we masked out non-forest areas such as pastures, home-sites, cemeteries and roads since the main concern of our study focused on forest types.

A series of segmentations was conducted using Definiens Developer Version 7.0 software. All spectral bands of the masked IKONOS image were used in the segmentations. Segmentations were produced using Definiens scale parameters (hereafter referred to as "scales") varying from 2 to 29, in steps of 1, producing a total of 28 segmentations. We chose 29 as a maximum scale because at this scale the largest image object was 45,920 m^2, which is similar to the maximum size of forest stands produced by the manual interpretation (46,286 m^2). The values of 0.1 and 0.9 were chosen for the ratios of shape and color, respectively. Each segmentation, produced from the entire range of segmentation scales, was separately processed using object-based forest type classification.

Spectral signatures of individual forest types were extracted from the four bands of the masked IKONOS image by using training data sets identified from the CRMS geodatabase, and then supervised object-based image classifications were performed by standard nearest neighbor classifier implemented in Definiens Developer. For these initial classifications, we utilized only the spectral values of the image to find the effect of segmentation quality and optimal segmentation for object-based forest type classification.

For the classifications involving object-specific texture classification, eight GLCM texture measures were employed: angular second moment (ASM), contrast (CON), correlation (COR), dissimilarity (DIS), entropy (ENT), homogeneity (HOM), mean (MEAN), and variance (VAR). The object-specific texture measures were computed using Definiens Developer from the near infrared (NIR) band of a segmentation which resulted in the highest overall classification accuracy when using spectral information alone. The NIR band was chosen for this segmentation because it contained the greatest range in spectral brightness values, and also carries important information for differentiating deciduous and coniferous species. A directionally invariant texture measure was obtained by calculating the mean of the texture results in all four directions (0°, 45°, 90°, and 135°), which was then assigned to the associated image object. These object-specific texture measures were entered into forest type classifications as additional bands.

3.4 ACCUARCY ASSESSMENT

Based on the assumption that the manual map represented an optimal classification, overall accuracy and Kappa coefficient were employed to provide summary measures, and conditional Kappa coefficients to quantify accuracies of individual forest types based on agreement with the manual interpretation of forest types. A conditional Kappa coefficient indicates the classification accuracy of each individual class (Gong *et al*., 1992), and it can be used to compare individual class differences between distinct classifications (Coburn and Roberts, 2004).

In addition, error maps were generated to explore the spatial distribution of differences between the classifications. The CRMS forest type Shapefile was rasterized with 4-m pixel size and overlaid on the classified images in order to generate error maps which displayed the spatial distribution of differences between the automated OBIA classifications and the manual mapping, and to compute the percentages of classification confusions among three forest types.

73

3.5 RESULTS AND DISCUSSION

3.5.1 Segmentation quality for forest stands and spatial autocorrelation

Figure 3.3 illustrates a visual comparison of how the segmentation scale influences the quality of image segmentations. Figure 3.3a shows the manually interpreted community-level forest stands considered as the smallest unit on the GUCO park. Vegetation mapping for National Parks is normally carried out with a minimum mapping unit (MMU) of 0.5 ha (5,000 m^2), however for GUCO Park, a much smaller MMU was realized because photointerpreters included smaller mappable units of discernable forest communities. Thus, the smallest forest stand mapped was 240 m^2, with an average size of 4,025 m^2. The other parts of Figure 3.3 illustrate three levels of segmentation at four scales.

The results at smaller segmentation scales were highly over-segmented, and the size of image objects was much smaller than the manually-interpreted forest stands, as shown in Figure 3.3b. As the scale increases, the segmentation results start to resemble the forest stands of the manual interpretation. In particular, the scales of 18 and 19 produced image segmentations most similar to the manually interpreted forest stands. Even at a scale of 18, the dashed-circle areas in Figure 3.3c indicate manually-interpreted forest stands that were divided into several image objects on the segmented image. Conversely, some forest stands on the manually interpreted database corresponded to merged image objects as indicated by arrows in Figure 3.3c. The other segmentation at scale of 19 showed several image objects produced with the scale of 18 were merged further and formed larger image objects illustrated by arrows in Figure 3.3 d. Nevertheless, the segmentation from the scale of 19 was relatively similar to that of scale 18. At a scale of 26, the image was under-segmented, particularly in areas indicated by arrows (Figure 3.3e). These areas were composed of several image objects at scales of 18 and 19, but at the

Figure 3.3. Over- and under-segmentation compared to manual interpretation: (a) manually-interpreted map, (b) over-segmentation at the scale of 4, (c) optimal segmentation at the scale of 18, and (d) optimal segmentation at the scale of 19, and (e) under-segmentation at the scale of 25.

scale of 26, each area was represented as a single image object where more than two forest types were included.

In a previous evaluation of segmentation quality for GUCO park, Kim *et al.* (2008) found that optimal segmentations occurred at scales that were close to manually-interpreted forest

stands in terms of number and average size (Figure 3.4). The average sizes of image objects at the scales were 4,432 and 6,608 m^2, respectively. These object sizes are comparable to the average size of manually interpreted forest stands (4,025 m^2) indicating automatic segmentation can potentially delineate forest stands at least similar to that obtained from a manual interpretation.

In addition to image object size, quality of segmentation can be assessed by using spatial autocorrelation. Kim *et al*. (2008) assumed that with over-segmentation, as in Figure 3.3b, neighboring image objects would be spatially autocorrelated due to their similar mean spectral values. Similarly, the spatial autocorrelation of neighboring objects would be high with under-segmentation (as in Figure 3.3e) as the segments would tend to comprise mixtures of spectral values.
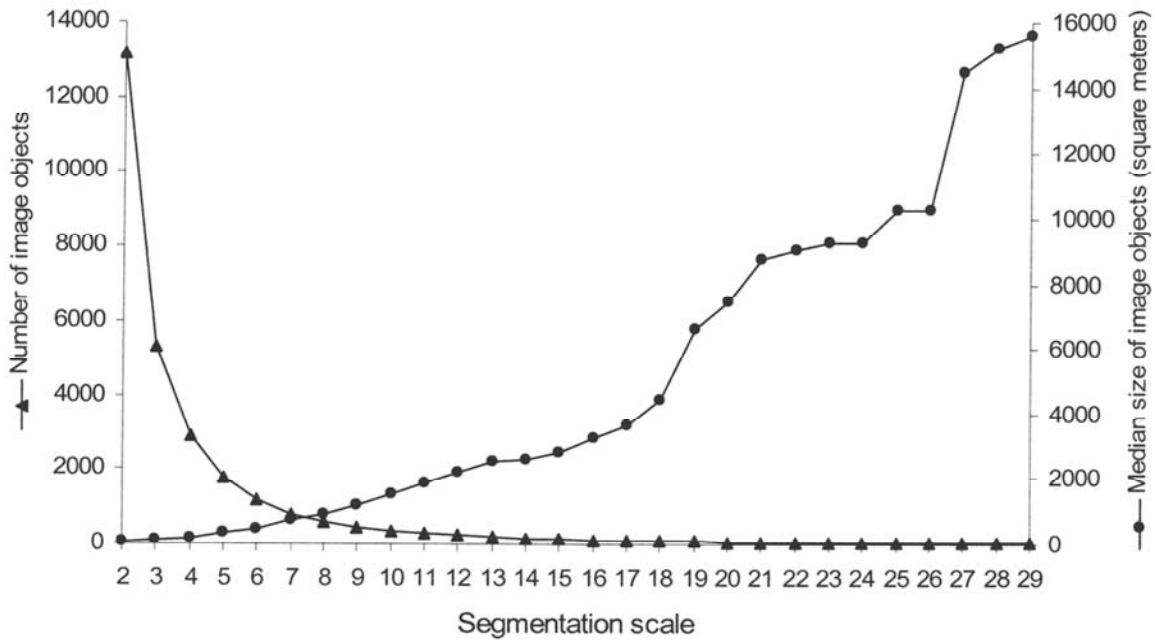
Figure 3.4. Median size and number of image objects produced at each segmentation scale.

On the other hand, they suggested that the least similarity in spectral values of adjacent segments would indicate optimal segmentation. Kim *et al.* (2008) found that over- and under-segmentations occurred when Moran's I index values were positive, while optimal segmentation was associated with lowest, even negative, index values (Figure 3.5).
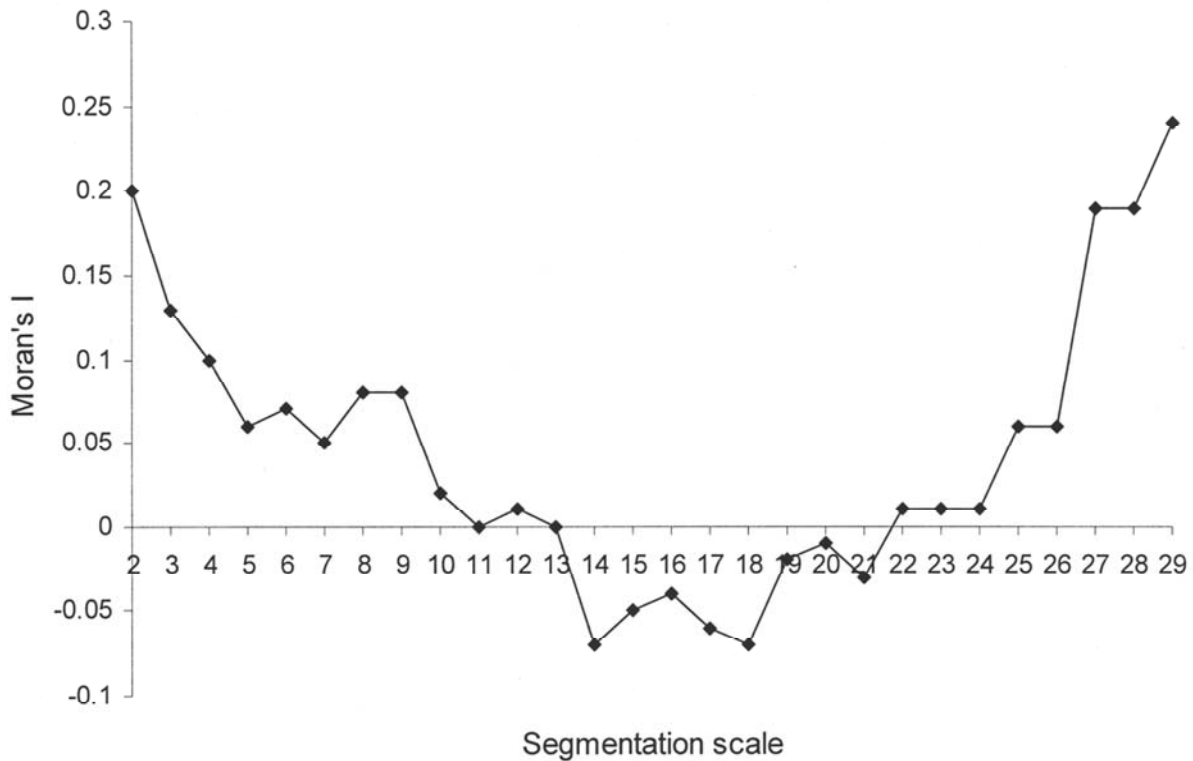
Figure 3.5. Moran's I graphed as a function of segmentation scale. The figure was reprinted with permission of Springer Science and Business Media.

3.5.2 Object-based Spectral Classification

The relationship between classification accuracy and segmentation scale is shown in Figure 3.6.

Generally, the accuracy rises from the smallest scale of 2, with a peak accuracy at the scale of 19 (overall accuracy 79 % and Kappa 0.65). By comparison, the scale of 18, which was determined to be the optimal scale based on image object size, has an overall accuracy of 76 % with a Kappa of 0.57.
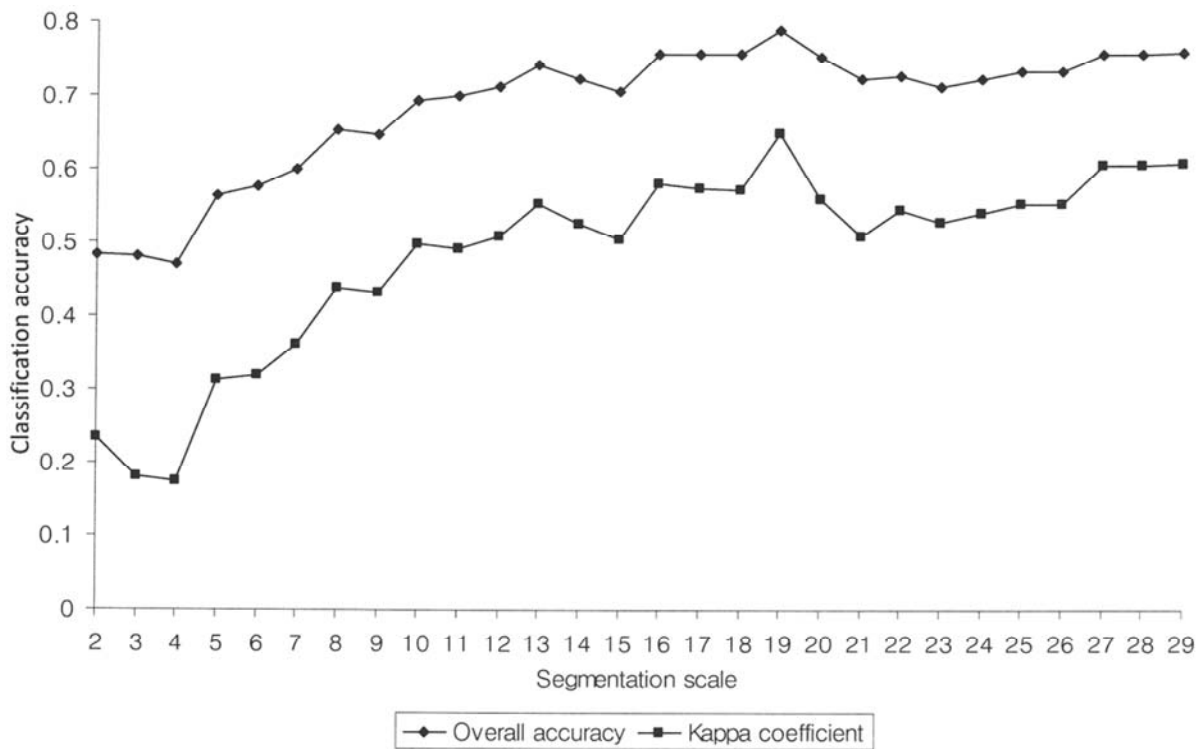
Figure 3.6. Object-based classification accuracies graphed against segmentation scales.

In general, Figure 3.6 shows lower overall classification accuracies for the scales that produced over- and under-segmentations, and higher accuracies for those that produced more optimal segmentations. The accuracies of forest type classification were directly influenced by the quality of segmentation related to the average size of image objects (see Figure 3.4). Higher

classification accuracies were obtained at segmentations that resemble the average size of forest stands from the manual interpretation. This result supports our hypothesis that optimal segmentation scales for forest type mapping can create a meaningful segmentation that resembles stand-level forest polygons on manual interpretation, and the appropriate scale can be estimated by computing Moran's I values, and graphing them against segmentation scales. As shown in Table 3.1, at the scale of 19, individual classification accuracies of deciduous forest based on spectral information alone were 85 % and 90 % for producer's and user's accuracies, respectively, with a Kappa of 0.76. However, the producer's accuracy of evergreen forest and the user's accuracy of mixed forest were 62 % and 61 % with Kappa of 0.64 and 0.52, respectively. Figure 3.7a illustrates a classification result that was derived at a scale of 19 with only spectral bands.

Table 3.1. Error matrix of an object-based classification at the scale of 19 using spectral bands.

		Reference			User's accuracy (%)
		DF	EF	MF	
Classification	DF	144	13	3	90
	EF	11	46	6	73
	MF	15	15	47	61
	Producer's accuracy (%)	85	62	84	

Overall accuracy: 79 %, Kappa coefficient: 0.65
DF Kappa coefficient: 0.76
EF Kappa coefficient: 0.64
MF Kappa coefficient: 0.52

In order to compare the edge boundaries and placement of image segments from the optimal scale of 19 vs. manually interpreted forest stands, the two data sets were overlaid to produce an "error" map as shown in Figure 3.7b. The classification error map depicts misclassifications visually and quantitatively between the automatic classification and the manual interpretation with differences generally being less than 10 %. The percentage of misclassification between deciduous and evergreen forest types was 8 % and that between deciduous and mixed forest was 6 % when compared with manual interpretation. The confusion between evergreen and mixed forest types was 6 %. The spectral information alone in object-based forest type classification produced higher confusion between pure and mixed forest types than between pure forest types. Therefore, object-specific texture classifications were adopted to reduce this classification confusion.
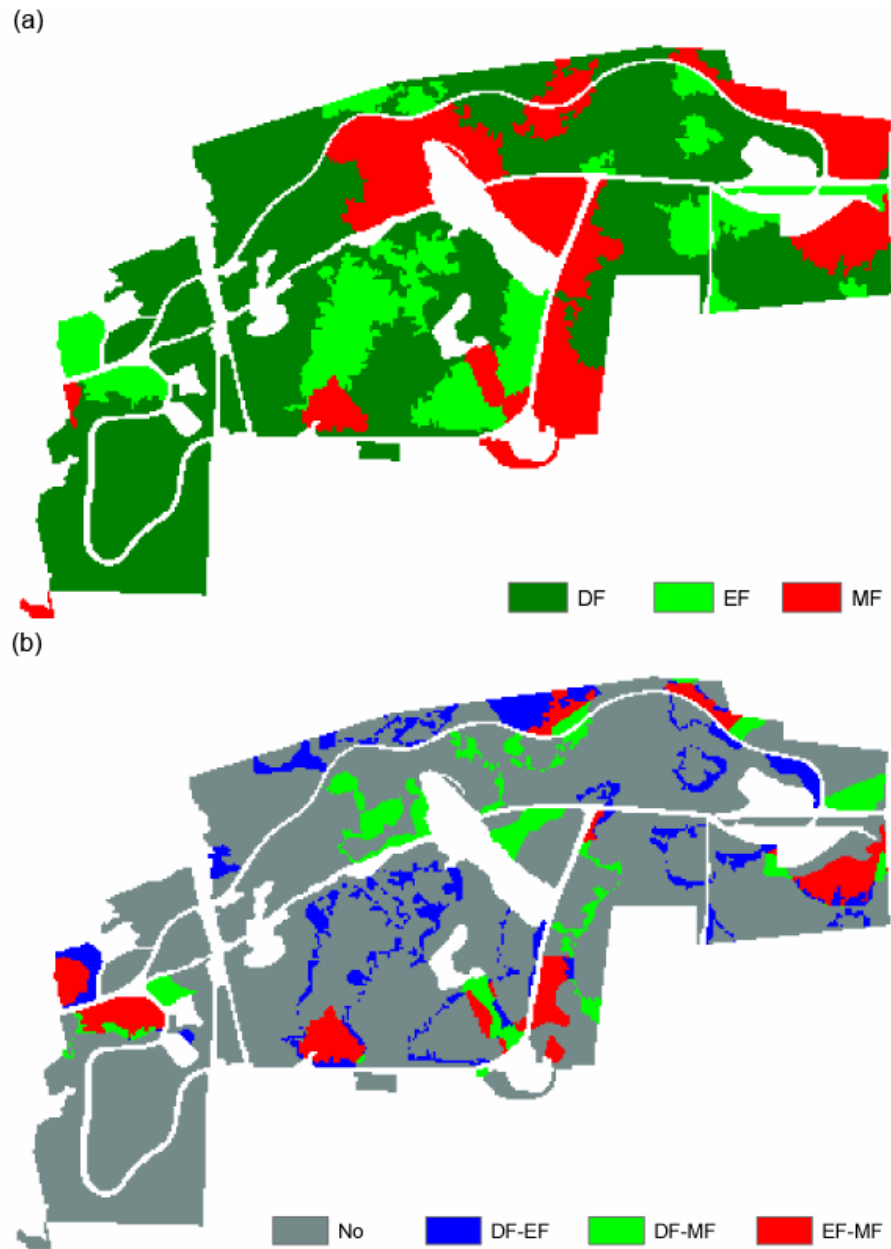
Figure 3.7. Object-based classification of spectral data at a scale of 19 (a) and differences between the object-based classification and the manually interpreted map (b).

3.5.3 Object-specific Texture Classification

A total of eight object-specific GLCM texture measures were computed based on the
segmentation that resulted in the best overall classification accuracies, i.e., at the scale of 19.
Texture measures for the segmented objects were individually combined with the spectral bands
of mean brightness values, and then entered into each object-based texture classification. Object-
specific texture classification accuracy results using a single texture measure ranged from 60 %
(Kappa of 0.37) for GLCM homogeneity, to 79.3 % (Kappa of 0.65) for GLCM mean (Figure
3.8). Compared to the 79 % accuracy (Kappa of 0.65) of object-based classification using
spectral bands alone, the addition of the GLCM correlation texture measure enhanced overall
accuracy by just 0.3 %, and the incorporation of the remaining texture measures, except angular
second moment and contrast, decreased classification accuracy.

As another way of using texture measures, the multiple texture analyses, which
incorporated multiple texture measures simultaneously for object-specific texture classifications,
were employed using the same segmentation scale (i.e., 19). Seven combinations of GLCM
texture measures were investigated: all combinations of two, three, four, five, six, seven and
eight texture measures. Figure 3.9 illustrates the minimum, median, maximum, first quartile and
third quartile of overall classification accuracies for texture combinations with 2 to 7 measures.
The incorporation of all 8 texture measures resulted in an overall accuracy of 78 %, with a Kappa
of 0.64. The highest overall classification accuracies, with relatively uniform values of
approximately 83 % and Kappa values of 0.71, were obtained with selected combinations from
two to five texture measures.
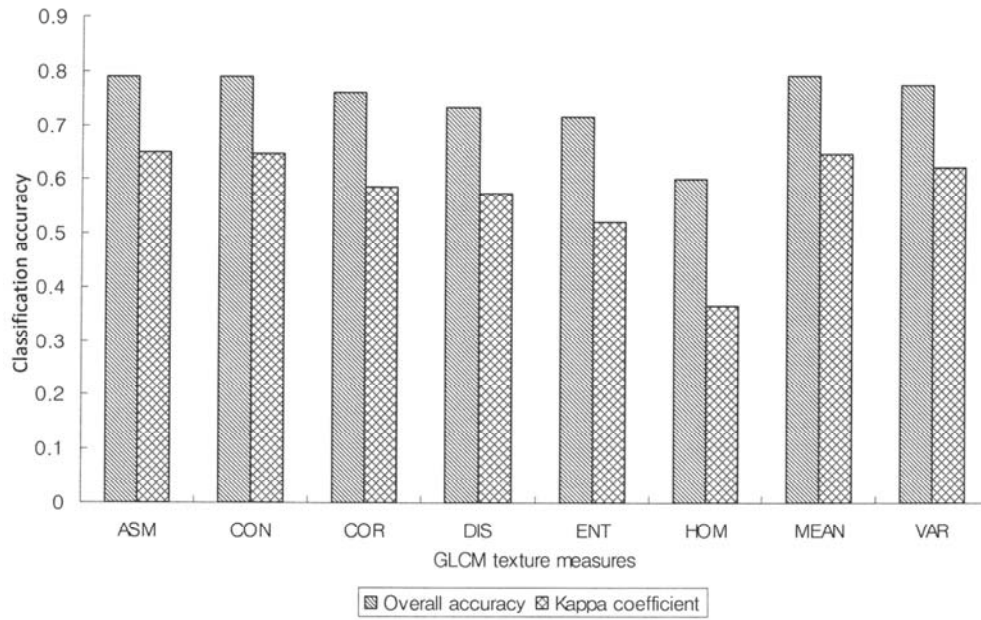
Figure 3.8. Classification accuracies using individual GLCM texture measures.
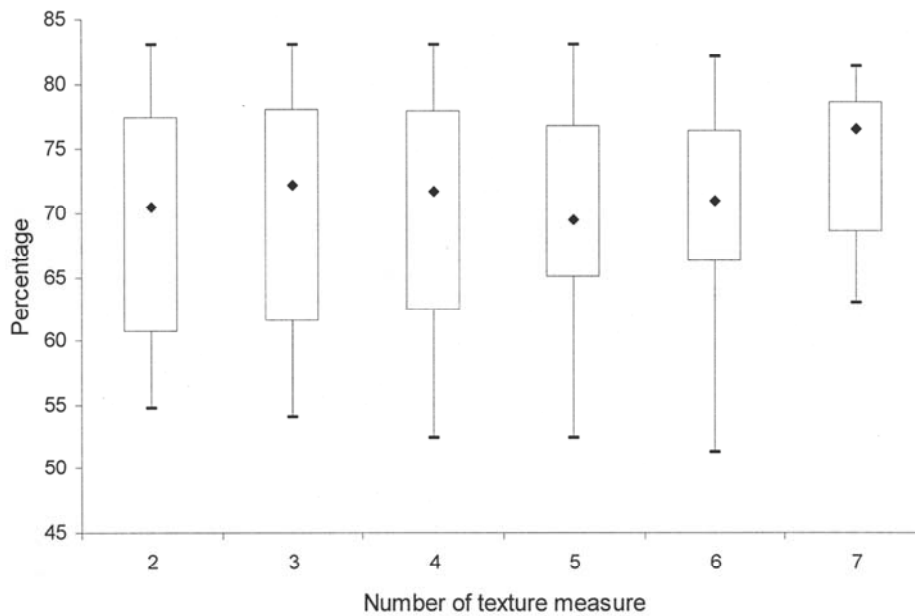

Figure 3.9. Box plot illustrating classification accuracies across possible combinations of GLCM texture measures. Each marker within individual boxes represents median values and the number on the abscissa represents the number of texture measures entered into classification.

For example, for just two texture measures, the combination that produced the highest accuracy was GLCM correlation and variance. The highest accuracy for three texture measures was obtained with GLCM correlation, variance, and dissimilarity. The highest accuracy for four texture measures was acquired with two different groups: GLCM contrast, correlation, dissimilarity and variance, and GLCM correlation, dissimilarity, mean and variance. The highest accuracy that was obtained with five texture measures was GLCM contrast, correlation, dissimilarity, mean and variance. A notable feature of this multiple texture analysis is that the incorporation of GLCM homogeneity texture measure generally degraded classification accuracies of the object-based texture classifications.

Besides these enhanced overall classification accuracies and Kappa coefficients using combined spectral and texture information, there also was notable improvement of individual classification accuracies for evergreen and mixed forest types. For example, as shown in Table 3.2, classification accuracies of evergreen and mixed forest types were generally improved (ranging from 72 % to 88 % correct) by incorporating multiple texture measures in terms of producers' accuracy, user's accuracy and conditional Kappa coefficient. By adding GLCM contrast, correlation, dissimilarity and variance, the producer's and user's accuracies of evergreen forest type were improved by 16 % and 9 %, respectively, when compared with those accuracies from spectral information alone. In addition, the user's accuracy of mixed forest type was enhanced by 11 % with four object-specific GLCM texture measures. Gains of 0.12 and 0.13 in conditional Kappa coefficients for mixed and evergreen forest types, respectively, were observed, although there was a slight decrease (i.e., 0.04) in the conditional Kappa coefficient of deciduous forest type.

Table 3.2. Error matrix of an object-based classification at the scale of 19 using spectral bands and texture measures of GLCM contrast, correlation, dissimilarity and variance.

		Reference			User's accuracy (%)
		DF	EF	MF	
Classification	DF	145	13	7	88
	EF	10	58	3	82
	MF	15	3	46	72
	Producer's accuracy (%)	85	78	82	

Overall accuracy: 83 %, Kappa coefficient: 0.71
DF Kappa coefficient: 0.72
EF Kappa coefficient: 0.76
MF Kappa coefficient: 0.65

The other GLCM texture combinations, mentioned above, also enhanced classification accuracies by reducing the classification confusion between evergreen and mixed forest types. Overall, the accuracy of object-based classification could be improved through the incorporation of multiple GLCM texture measures, although not in all cases as shown in Figure 3.9 by the variation between the minimum and maximum accuracy achieved. Figure 3.10a illustrates an OBIA forest type classification result produced by using spectral information and GLCM texture measures of contrast, correlation, dissimilarity and variance.
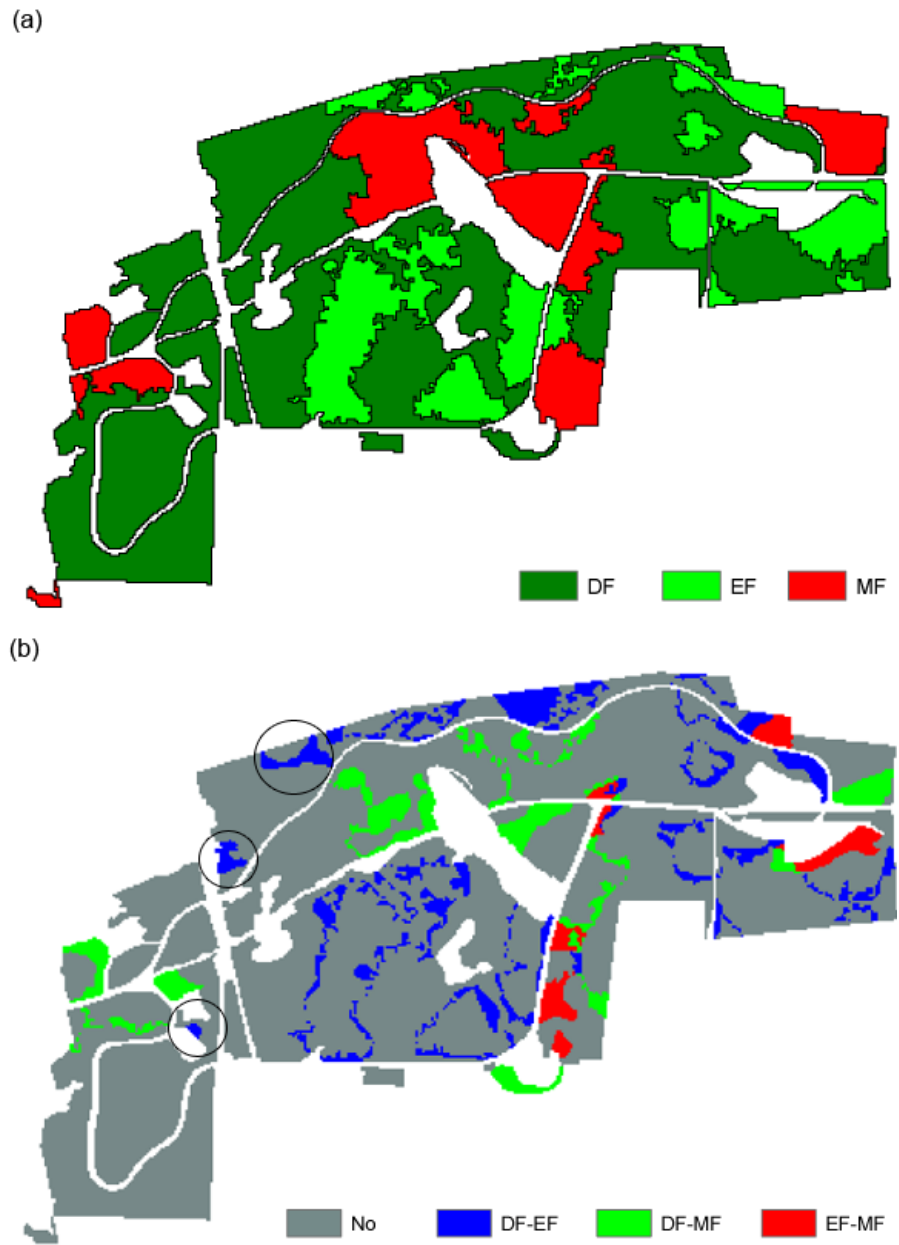
Figure 3.10. Forest type classification result (a) and misclassifications on object-specific texture

classification using GLCM contrast, correlation, dissimilarity and variance (b).

This object-specific GLCM multiple texture analysis raises the question of why overall classification results were not enhanced beyond 83 %. To answer this question, we produced a classification error map using an automatic classification result from a texture combination of GLCM contrast, correlation, dissimilarity and variance and the manually-interpreted forest stands, as shown in Figure 3.10b. In addition, we calculated the percentages of confused classification among the three forest types. The confusion percentages of DF-EF and DF-MF were the same as those from the spectral classification (i.e., 8 % and 6 %, respectively) even though the classification confusion between evergreen and mixed forest types was lowered to 2 %. As illustrated in Figure 3.10b, the confusion between deciduous and evergreen forest types came from transition areas between the two types and local segmentation result that did not produce smaller evergreen stands designated by circles in Figure 3.10b. In addition, the confusion between deciduous and mixed forest types resulted from local segmentation quality even at the optimal scale of 19. The classification confusion between evergreen and mixed forest types also occurred because of local segmentation quality even after adding object-specific GLCM multiple texture measures. The confusion percentages and error map of this study revealed that the object-based forest type classification result could not perfectly resemble the manual interpretation possibly because of poor segmentation quality even at the optimal scale of 19 or due to the subjective nature of manual interpretation. At any rate, the quality of segmentation has a critical effect on forest type classifications when using object-based classification and VHR satellite imagery.

Overall, the object-based classification combined with object-specific GLCM texture produced a map of forest types that most closely resembled the manually interpreted forest type map (see Figure 3.10a). In addition, the best object-based classification could be converted to a

vector polygon format representing forest type stands. This vector file of forest type stands can be used for further GIS analysis, e.g., vegetation modeling or forest fire fuels analysis.

3.6 CONCLUSIONS

Forest type mapping for a National Park unit was performed using an object-based approach applied to a 4-m multispectral IKONOS image acquired during the summer. The classification of forest types, including deciduous broadleaf, evergreen coniferous and mixed forests, was achieved through exploration of the effects of combining spectral and contextual texture information. A manually interpreted forest stands geodatabase was employed as a benchmark to investigate the extent to which object-based segmentation and classification can emulate a field-verified manual interpretation of forest types.

Important findings associated with object-based forest type classification on the IKONOS image include:

1) The level of segmentation directly influenced forest type mapping when adopting an object-based approach. In general, classification accuracies were lower for data sets resulting from over- and under-segmentation than optimal segmentation. Overall classification accuracy for OBIA results with extreme over-segmentation, i.e., at the scale of 2, was improved by 31 % (0.42 Kappa) when optimal segmentation (i.e., 19) was used. At the optimal segmentation scale of 19, an overall classification accuracy of 79 % with a Kappa 0.65 was realized using only with spectral information. Our previous study (Kim *et al*., 2008) showed the number and average sizes of image objects obtained at segmentation scales of 18 and 19 were comparable to the number and size of forest stands contained in a manually interpreted and field verified forest type data set.

2) Given the importance of segmentation quality on object-based classification accuracy, an objective method of determining the optimal segmentation level was desired. A series of object-based classification results demonstrated that a spatial autocorrelation analysis, based on Moran's I index values, could discriminate segmentation levels. The analysis yielded lowest, even negative, Moran's I values at optimal segmentations compared with over- and under-segmentations. This analysis is anticipated to reduce processing time and labor of selecting appropriate segmentation scales for object-based forest type mapping with VHR satellite imagery in comparison with a trial-and-error method.

3) Object-specific GLCM texture measures did not produce a notable increase in classification accuracies (ranging from 60 % to 79 % for overall accuracy) when they were employed individually with spectral information in classification procedures. However, forest type classification results were enhanced by adopting multiple texture measures. By employing selected multiple texture analysis, classification accuracies were enhanced to 83 % for overall accuracy with Kappa of 0.71 at the optimal segmentation of scale 19. These improved results were attributed to reducing classification confusion between evergreen and mixed forest types up to 2 %. An error map, produced from an OBIA classified image and manual interpretation, showed that the placement of image objects only differed by 8 % or less. Some misclassification occurred because of local over-segmentation, and other misclassification occurred at transition areas between two different forest types.

4) It is possible to produce GIS-ready vector polygons of forest type stands from object-based classification of a VHR satellite image for further GIS analysis, thus enhancing the potential for a close coupling between remote sensing and GIS analyses.

Overall, this study resulted in a forest type map that was similar to that of a manual interpretation by adopting object-based image classification with the addition of multiple object-specific GLCM texture measures. The best classification meets accuracy standards that are required for National Park vegetation mapping (over 80 % in overall accuracy).

With increasing availability of VHR imagery and high demand for mapping natural and cultural resources, the OBIA approach offers great potential for automated classification techniques that emulate the delineation and classification of manual interpretation. However, it is important to develop methodologies that estimate optimal segmentations across various landscape units and that enhance the quality of segmentation. In addition, although a single segmentation scale was utilized in this study, future research needs to consider multi-scale segmentation analyses when employing hierarchical classification scheme. That is because a single segmentation scale may not be appropriate for object-based land use and land cover classifications.

In future work, we plan to evaluate optimal segmentation quality by using a spatial autocorrelation analysis for other landscapes, e.g., urban or suburban land use and land cover, and investigate the relationship between segmentation quality and classification results. Keeping the need for future updating of databases within the National Vegetation Mapping Program in mind, we plan to perform stand-level forest/vegetation OBIA classification for a large National Park like Great Smoky Mountains National Park. In addition, we intend to investigate whether it

is possible to find a method to assist researchers in identifying the optimal combination of GLCM texture measures for inclusion in OBIA classification.

ACKNOWLEDGEMENTS

REFERENCES

Addink, E.A., S.M. de Jong, and E.J. Pebesma. 2007. The importance of scale in object-based mapping of vegetation parameters with hyperspectral imagery. Photogramemtric Engineering & Remote Sensing, 72(8):905-912.

Asner, G.P. and A.S. Warner. 2003. Canopy shadow in Ikonos satellite observations of tropical forests and savannas. Remote Sensing of Environment, 87:521-533.

Avery, T.E. 1962. Interpretation of Aerial Photograph, 2_{nd} edition, Burgess Publishing Co., 324 p.

Benz, U.C., P. Hofmann, G. Willhauck, I. Lingenfelder, and M. Heynen. 2004. Multi-resolution, object-oriented fuzzy analysis of remote sensing data for GIS-ready information. ISPRS Journal of Photogrammetry and Remote Sensing, 58:239-258.

Blaschke, T. 2003. Object-based contextual image classification built on image segmentation. Proceedings of the 2003 IEEE Workshop on Advances in Techniques for Analysis of Remotely Sensed Data, 27-28 October 2003, Washington DC, U.S., pp.113-119.

Blaschke, T. and J. Strobl. 2001. What's wrong with pixels? Some recent developments interfacing remote sensing and GIS. GIS-Zeitschrift für Geoinformationssysteme, 6:12-17.

Brandtberg T. and T. Warner. 2006. High resolution remote sensing. Computer Applications in Sustainable Forest Management (G. Shao and K. M. Reynolds, editors), Springer-Verlag, Dordrecht, Netherlands, pp.19-41.

Coburn, C.A. and A.C.B. Roberts. 2004. A multiscale texture analysis procedure for improved forest stand classification. International Journal of Remote Sensing, 25(2):4287-4308.

Colwell, R.N. 1960. Some uses of infrared aerial photography in the management of wildland areas. Photogrammetric Engineering & Remote Sensing, 26(12):774-785.

Definiens. 2004. eCognition User Guide 4, Definiens AG, Germany.

Dorren, L.K.A., B. Maier, and A.C. Seijmonsbergen. 2003. Improved Landsat-based forest mapping in steep mountainous terrain using object-based classification. Forest Ecology and Management, 183:31-46.

Ehlers, M., M. Gaehler, and R. Janowsky. 2003. Automated analysis of ultra high resolution remote sensing data for biotope type mapping: new possibilities and challenges. ISPRS Journal of Photogrammetry and Remote Sensing, 57:315-326.

Ehlers, M. 2004. Remote sensing for GIS applications: new sensors and analysis methods. Remote Sensing for Environmental Monitoring, GIS Applications, and Geology III (M. Ehlers, J.J. Kaufmann, and U. Michel, editors), Proceedings of SPIE, Bellingham, WA, 5239:1-13.

Federal Geographic Data Committee (FGDC). 2007. National Vegetation Classification Standard Version 2. Submitted Draft, November 30, 2006, Edited October 2007, FGDC-STD-005 (Version 2), URL: http://www.fgdc.gov/standards/projects/FGDC-standards-projects/vegetation/Draft_FGDC_Std_FINAL_Oct2007.doc (last date accessed: May 19, 2008).

Feitosa, C.U., G.A.O.P. Costa, and T.B. Cazes. 2006. A genetic approach for the automatic adaptation of segmentation parameters. Commission IV, WG IV/4 on Proceeding of 1_{st} OBIA Conference, 4-5 July, Salzburg, Austria (International Society for Photogrammetry and Remote Sensing), unpaginated CD-ROM.

Ferro, C.J.S. and T.A. Warner. 2002. Scale and texture in digital image classification. Photogrammetric Engineering & Remote Sensing, 68(1):51-63.

Fisher, P. 1997. The pixel: a snare and a delusion. International Journal of Remote Sensing, 18(3):679-685.

Franklin, S.E., R.J. Hall, L.M. Moskal, A.J. Maudie, and M.B. Lavigne. 2000. Incorporating texture into classification of forest species composition from airborne multispectral images. International Journal of Remote Sensing, 21(1):61-79.

Franklin, S.E., M.A. Wulder, and G.R. Gerylo. 2001a. Texture analysis of IKONOS panchromatic data for Douglas-fir forest age class separability in British Columbia. International Journal of Remote Sensing, 22(13):2627-2632.

Franklin, S.E., A.J. Maudie, and M.B. Lavigne. 2001b. Using spatial co-occurrence texture to increase forest structure and species composition classification accuracy. Photogrammetric Engineering & Remote Sensing, 67:849-855.

Gong, P., D.J. Marceau, and P.J. Howarth. 1992. A comparison of spatial feature extraction algorithms for land-use classification with SPOT HRV data. Remote Sensing of Environment, 40:137-151.

Guo, Q., M. Kelly, P. Gong and D. Liu. 2007. An object-based classification approach in mapping tree mortality using high spatial resolution imagery. GIScience and Remote Sensing, 44(1):24-47.

Haralick, R.M., K. Shanmugam, and I. Dinstein. 1973. Textural features for image classification. IEEE Transactions on Systems, Man and Cybernetics, SMC, 3(6):610-620.

Haralick, R.M. and K.S. Shanmugam. 1974. Combined spectral and spatial processing of ERTS imagery data. Remote Sensing of Environment, 3:3-13.

Hay, G.J., K.O. Niemann, and G.F. McLean. 1996. An object-specific image-texture analysis of H-resolution forest imagery. Remote Sensing of Environment, 55:108-122.

Heller, R.C. 1975. Evaluation of ERTS-1 data for forest and range-land survey. USDA Forest Service Research Paper PSW-112, Pacific S.W. Forest and Range Experiment Station, Berkeley, California.

Hiatt, J. 2003. Guilford Courthouse National Military Park: Cultural Landscape Report, National Park Service Web, Southeast Regional Office, Cultural Resources Division, URL: http://www.nps.gov/guco/pphtml/documents.html, National Park Service, Southeast Regional Office, Cultural Resources Division (last date accessed: September 29, 2007).

Hoffer, R.M. and Staff. 1975. Natural resource mapping in mountainous terrain by computer analysis of ERTS-1 satellite data; Agricultural Experiment Station Research Bulletin 919, Purdue University, W. Lafayette, Indiana.

Jensen, J.R. 1979. Computer graphic feature analysis and selection. Photogrammetric Engineering & Remote Sensing, 45(11):1507-1512.

Kim, M. and M. Madden. 2006. Determination of optimal scale parameter for alliance-level forest classification of multispectral IKONOS image. Commission IV, WG IV/4 on Proceeding of 1_{st} OBIA Conference, 4-5 July, Salzburg, Austria (International Society for Photogrammetry and Remote Sensing), unpaginated CD-ROM.

Kim, M., M. Madden, and T.A. Warner. 2008. Estimation of optimal image object size for the segmentation of forest stands with multispectral IKONOS imagery. Object-Based Image Analysis - Spatial concepts for knowledge-driven remote sensing applications (T. Blaschke, S. Lang, and G.J. Hay, editors), Springer-Verlag, Berlin, pp.291-307.

Lachowski, H., P. Maus, and N. Roller. 2000. From pixels to decisions: digital remote sensing technologies for public land managers. Journal of Forestry, 98(6):13-15.

Lu, D. and Q. Weng. 2007. Survey of image classification methods and techniques for improving classification performance. International Journal of Remote Sensing, 28(5):823-870.

Lund, H.G., W.A. Befort, J.E. Brickell, W.M. Ciesla, E.C. Collins, R.L. Czaplewski, A.A. Disperati, R.W. Douglass, C.W. Dull, J.D. Greer, R.R. Hershey, V.J. LaBau, H. Lachowski, P.A. Murtha, D.J. Nowak, M.A. Roberts, P. Schram, M.D. Shedha, A. Singh, and K.C. Winterberger. 1997. Forestry. Manual of Photographic Interpretation: 2_{nd} edition (W.R. Philipson, editor), American Society of Photogrammetry and Remote Sensing, pp.399-433.

Madden, M. and T. Jordan. 2004. Database development and analysis for decision makers in National Parks of the Southeast. Proceedings of ASPRS Fall Conference, 12-16 September, Kansas City, Missouri (American Society for Photogrammetry and Remote Sensing, Bethesda, Maryland), unpaginated CR-ROM.

Marceau, D.J., P.J. Howarth, J.M.M. Dubois, and D.J. Gratton. 1990. Evaluation of grey-level co-occurrence matrix method for land-cover classification using SPOT imagery. IEEE Transactions on Geoscience and Remote Sensing, 28(4):513-519.

Meinel, G. and M. Neubert. 2004. A comparison of segmentation programs for high resolution remote sensing data. Commission VI in Proceeding of XX_{th} ISPRS Congress, 12-23 July, Istanbul, Turkey (International Society for Photogrammetry and Remote Sensing), unpaginated CD-ROM.

Metzler, J.W. and S.A. Sader. 2005. Model development and comparison to predict softwood and hardwood per cent cover using high and medium spatial resolution imagery. International Journal of Remote Sensing, 26(17):3749-3761.

National Park Service (NPS). 2008. Vegetation Mapping Program, U.S. Geological Survey (USGS) Biological Resources Discipline (BRD) and National Park Service, URL: http://science.nature.nps.gov/im/inventory/veg/index.cfm (last date accessed: May 19, 2008).

NatureServe. 2007. Accuracy Assessment: Guilford Courthouse National Military Park. Final Report to the National Park Service Durham, North Carolina, p.5.

Read, J.M., D.B. Clark, E.M. Venticinque, and M.P. Moreira. 2003. Application of merged 1-m and 4-m resolution satellite data to research and management in tropical forest. Journal of Applied Ecology, 40:592-600.

Ryherd, S. and C. Woodcock. 1996. Combining spectral and texture data in the segmentation of remotely sensed images. Photogrammetric Engineering & Remote Sensing, 62(2):181-194.

Shiewe, J., L. Tufte, and E. Ehlers. 2001. Potential and problems of multi-scale segmentation methods in remote sensing. GIS-Zeitschrift für Geoinformationssysteme, 6:34-39.

Souza, C.M. and D. Roberts. 2005. Mapping forest degradation in the Amazon region with Ikonos images. International Journal of Remote Sensing, 26(3):425-429.

Teng, W.T., E.R. Loew, D.I. Ross, V.G. Zsilinsky, C.P. Lo, W.R. Philipson, W.D. Philpot, and S.A. Morain. 1997. Fundamentals of photographic interpretation. Manual of Photographic Interpretation (W.R. Philipson, editor), American Society of Photogrammetry and Remote Sensing, pp.49-110.

Townshend, J.R.G, C. Huang, S.N.V. Kalluri, R.S. Defries, S. Liang, and K. Yang. 2000. Beware of per-pixel characterization of land cover. International Journal of Remote Sensing, 21(4):839-843.

Wang, L., W.P. Sousa, and P. Gong. 2004a. Integration of object-based and pixel-based classification for mapping mangroves with IKONOS imagery. International Journal of Remote Sensing, 25(24):5655-5668.

Wang, L., W.P. Sousa, P. Gong, and G.S. Biging. 2004b. Comparison of IKONOS and QuickBird images for mapping mangrove species on the Caribbean coast of Panama. Remote Sensing of Environment, 91(3-4):434-440.

Welch, R., M. Remillard, and R. Doren. 1995. GIS database development for South Florida's National Parks and Preserves. Photogrammetric Engineering & Remote Sensing, 61(11):1371-1381.

Welch, R., M. Madden, and R. Doren. 1999. Mapping the Everglades. Photogrammetric Engineering & Remote Sensing, 65(2):163-170.

Welch, R., M. Madden, and T. Jordan. 2002. Photogrammetric and GIS techniques for the development of vegetation databases of mountainous areas: Great Smoky Mountains National Park. ISPRS Journal of Photogrammetry and Remote Sensing, 57:53-68.

Woodcock, C.E. and A.H. Strahler. 1987. The factor of scale in remote sensing. Remote Sensing of Environment, 25:349-379.

Wulder, M.A., J.C. White, K.O. Niemann, and T. Nelson. 2004. Comparison of airborne and satellite high spatial resolution data for the identification of individual trees with local maxima filtering. International Journal of Remote Sensing, 25(11):2225-2232.

Yu, Q., P. Gong, N. Clinton, G. Biging, M. Kelly, and D. Shirokauer. 2006. Object-based detailed vegetation classification with airborne high spatial resolution remote sensing imagery. Photogrammetric Engineering & Remote Sensing, 72(7):799-811.

Zhang, Y. 1999. Optimization of building detection in satellite images by combining multispectral classification and texture filtering. International Journal of Remote Sensing, 54:50-60.

Zhang, C., S.E. Franklin, and M.A. Wulder. 2004. Geostatistical and texture analysis of airborne-acquired images used in forest classification. International Journal of Remote Sensing, 25(4):859-865.

CHAPTER 4

SUMMARY AND CONCLUSIONS

4.1 OVERVIEW

Object-based image analysis (OBIA) has been considered as an alternative methodology to

traditional pixel-based approaches in the hope that it resolves the limitations of pixel-based

classifications with VHR imagery. Image segmentation, a primary step of OBIA, produces image

objects that are groups of similar individual pixels. The segmentation makes it possible to gather

spectral, spatial and contextual information of each image segment for use in classification

procedures. In this sense, OBIA is considered a similar methodology to manual interpretation in

association with VHR imagery.

The OBIA approach, however, has an important aspect to be considered in the thematic

classification of VHR imagery, i.e., segmentation quality. As addressed in the Introduction, the

estimation of segmentation quality is critical since it has been reported to have a direct effect on

classification results. For this reason, it is an urgent issue in OBIA to determine the optimal

segmentation that is assumed to produce the best classification results. In addition, the effect of

spatial information, i.e., texture, is also an important research issue in automated techniques of

classification since it has traditionally been a critical element for manual interpretation. This

research investigated the potential of utilizing OBIA in delineating forest stands mainly in terms

of the levels of segmentation quality: over-segmentation, optimal segmentation and under-

segmentation. The estimation of optimal segmentation also was examined by using local variance and spatial autocorrelation analysis for stand-level forest delineation. Lastly, the effect of GLCM texture measures on forest type classifications was inspected in this research. For the research objectives, 4-m multispectral IKONOS imagery was utilized to produce stand-level forest segmentation and classify forest types, i.e., deciduous, evergreen and mixed forests, in Guilford Courthouse National Military National Park located in Greensboro, North Carolina. A 1:12,000-scale CIR aerial photograph and the vegetation geodatabase of the CRMS were also employed to rectify the IKONOS imagery, determine training samples and derive sample points for accuracy assessment.

4.2 SUMMARY

4.2.1 Estimation of optimal segmentation quality

A series of segmentations was conducted with a range of scales from 2 to 30, and the numbers and average sizes of image objects (i.e., association-level forest stands) at all scales were computed and compared with those of the vegetation geodatabase of the CRMS that was created by manual interpretation. Then, each segmentation result was visually assessed with the forest stands of the vegetation geodatabase in terms of segmentation quality. Lastly, average local variances and Moran's I indices were graphed as a function of segmentation scales as indicators of segmentation quality associated with forest stands.

The visual evaluation of forest stands segmentation discovered that there were different levels of segmentation quality associated with scales. It was found that the average size of forest stands was 7,002 m^2 with 94 for the number of forest stands based on the manual interpretation. According to Table 2.1 and Figures 2.3 and 3.4, optimal segmentation results occurred around a

scale 18 in terms of the number/size of image objects related to forest stands. The scale produced a segmentation with 6,991 m^2 and 96 for the average size and number of segments, respectively. The segmentation scales, smaller than the potential optimal scale of 18, generated over-segmentations. For instance, the scale 6 yielded a segmentation that showed excessive number/average size of image objects (over 12 times) when compared with the manual interpretation. The scale 6 generated a segmentation with average size of 565 m^2 and 1,175 image objects in relation to the number and average size of manually mapped forest stands. At an extremely large scale of 30, under-segmentation occurred with the image object number of 40 and the average size of 16,604 m^2.

The visual assessment of segmentation results confirmed the levels of segmentation quality recognized by the number/size (see Figures 2.4 and 3.3). Segmentation results with scales 18 and 19 were very similar to forest stands of manual interpretation in general shape, size and location. However, it was very apparent that smaller scales generated highly detailed over-segmented results (see Figure 2.4b and Figure 3.4b). On the contrary, under-segmentations of mixed classes were acquired with larger scales compared to forest stands from the manual interpretation.

The graph of average local variance leveled off at the scale of 20, which indicated that under-segmentation occurred before optimal segmentations came (see Figure 2.6). The occurrence of under segmentation was supported by the number/size of image objects and visual assessment of segmentation quality. In addition, the graph of Moran's I indices associated with segmentation scales revealed that optimal segmentations occurred at minimum, even negative, spatial autocorrelation indicating spectral dissimilarity between adjacent image segments (see

Figure 2.6). On the other hand, between-segment correlation resulted in high positive Moran's I values in over- and under- segmentation.

4.2.2 Image segmentation quality and its effect on classification results

Object-based forest type classifications were performed to examine the relationship between segmentation quality, particularly focusing on spatial autocorrelation analysis, and classification with a range of segmentation scales of 2 to 29. Forest types included pure deciduous, pure evergreen and mixed forests. In addition, this research investigated the effect of GLCM texture on forest type classifications of the multispectral IKONOS imagery.

This research found that the graph of classification accuracies, in general, had a tendency to produce lower overall accuracies in over- and under-segmentations and higher accuracies with optimal segmentations (see Figure 3.6). Based on the results of Chapter 2, the scales of 18 and 19 produced optimal segmentations that resembled forest stands of manual interpretation in terms of size, shape and location. In fact, the highest overall accuracy of 79 % with a Kappa of 0.65 was acquired at the scale of 19, which was improved by 3 % and 0.08 for overall accuracy and Kappa, respectively, compared with those from the scale of 18. This result confirmed that the best classification of forest types can be obtained from optimal segmentations very similar to the stand-level forests of the manual interpretation. In addition, the optimal scale of segmentation can be potentially determined by graphing Moran's I values that are computed with a range of scales.

An error map was created to visually and quantitatively assess misclassifications between an automatic classification and a manual interpretation in terms of the edge boundaries and placement (see Figure 3.7). According to the error map, the percentage of misclassifications

101

between deciduous and evergreen forests was 8 %, which was less than the 12 %

misclassifications between pure and mixed forests. This result was also confirmed in an error

matrix, described in Table 3.1. Deciduous forest was more accurately classified with 85 % and

90 % of producer's and user's accuracies, respectively. On the contrary, evergreen and mixed

forests were less accurately classified in comparison with deciduous forest (see Table 3.1).

This research discovered that overall accuracy was improved by 0.3 % with the addition of

GLCM correlation when a single texture measure was incorporated with spectral bands in forest

type classification. The additions of other single GLCM textures, including dissimilarity, entropy,

homogeneity, mean and variance, actually decreased the overall accuracies of classifications

compared with spectral-only classification (see Figure 3.8). However, classification results were

found to be enhanced with the addition of multiple GLCM texture measures (see Figure 3.9).

The use of two to five texture measures produced the relatively highest overall classification

accuracy of 83 % and Kappa of 0.71. Nevertheless, the addition of multiple GLCM texture

measures did not always improve classification accuracies as shown in Figure 3.9.

When it comes to individual classification accuracies, notable gains were achieved for

evergreen and mixed forest types with the utilization of GLCM contrast, correlation,

dissimilarity and variance (see Tables 3.1 and 3.2). The accuracy of evergreen forest

classification was improved by 16 % and 9 % for producer's and user's accuracies, respectively,

and mixed forest type also obtained a gain of 11 % in user's accuracy. In addition, the gains of

12 % and 13 % in conditional Kappa coefficients were acquired for evergreen and mixed forest

types, respectively. The addition of four GLCM texture measures was found to lower

classification by 8 % confusion between pure and mixed forests with the aid of an error map (see

Figure 3.10), derived from the difference between an object-based classification with the texture measures and spectral bands at the scale of 19 and the manual interpretation.

4.3 CONCLUSIONS

This research performed object-based forest stand delineation and forest type classification of Guilford Courthouse National Military Park, North Carolina, U.S., with a 4-m multispectral IKONOS image. The quality of segmentation was evaluated particularly in terms of scale, i.e., the size of image objects, with a benchmark of the CRMS vegetation geodatabase produced for the National Park Service. This research also explored a potential to anticipate optimal segmentation in a quantitative manner by using average local variance and spatial autocorrelation analysis with Moran's I. In addition, this research explored the relationship between the quality of segmentation and the accuracies of classification for deciduous broadleaf, evergreen coniferous and mixed forests. Finally, the effects of incorporating spectral and texture information on forest type classification results were investigated.

The quality of segmentation was found to be directly associated with segmentation scale. In comparison with a manually-interpreted forest stand geodatabase, three distinct levels of segmentation quality were produced: 1) over-segmentation, 2) optimal segmentation and 3) under-segmentation. Small scales produced over-segmented images, where a large number and small size of image segments were found to compose a single forest stand on the manual interpretation. On the contrary, under-segmented images were generated with large scales in a way that the average size of image segments became larger and the number of mixed class image objects fewer. Thus, there would be a possibility that a single image object contained different types of forest. This inclusion of different landscape features decreases the performance of OBIA

classification in under-segmentation. An optimal segmentation with an appropriate scale, e.g., 18 or 19, resembled the forest stands of the manual interpretation in terms of shape, size and location. Nevertheless, it was difficult to directly relate the appropriate scale to the average size of segments, although it is reported that the average size of image objects is closely related to segmentation scale, i.e., scale parameter (Definiens, 2004) (see Table 2.1). In association with the difficulty, Blaschke (2003) reported that this importance of determining optimal segmentation would be a challenging issue in the OBIA.

In this research, average local variance anticipated the approximate starting scale of under-segmentation. The graph of local variance had a tendency to rise from the smallest scale, i.e., 2, and leveled off at a scale of 20. The leveling-off scale occurred after optimal scales that generated segmentations resembling the manually-interpreted forest stands in terms of qualitative (or visual) and quantitative (number/size of segments) assessments was reached. When it comes to spatial autocorrelation analysis, this study produced a bowl-shaped graph of Moran's I values across segmentation scales. In the graph, negative autocorrelation, representing dissimilarity between adjacent image objects in spectral values, occurred within a range of segmentation scales including the candidates of optimal scale, i.e., 18 and 19. According to the graph of Moran's I values, excessive over- and under-segmentations were associated with positive autocorrelation. Taking into account the qualitative and quantitative assessments of segmentation quality, the use of average local variance and spatial autocorrelation analysis is anticipated to aid OBIA researchers in selecting a range of segmentation scales that will potentially produce optimal segmentations. In addition, this approach will play a critical role in reducing the degree of selection and processing time related to object-based image classification, particularly with VHR imagery encompassing a large area.

104

Object-based forest type classification results based only on spectral information showed that the highest overall accuracies occurred in coincidence with optimal segmentation scales of forest stand delineation. The results also confirmed an important finding by Dorren *et al.* (2003). In their study, the highest forest type classification result was obtained with a segmentation that was very close to real-world forest stands in average size. Frauman and Wolff (2006) found that an over-segmented image produced better classification results related urban area mapping. This research, however, discovered that excessive over- segmentations resulted in the lowest classification accuracies. A possible reason, related to this disagreement, would be assumed that an excessive over-segmentation may not reduce spectral variation of the same forest type (i.e., within-class spectral variation). Another potential reason would be associated with between-class spectral variation, considered to decrease the performance of image classifications, since spectral similarity would occur among landscape features in over-segmentation. In association with spectral variations, optimal segmentation should have little over-segmentation and no under-segmentation (Castilla and Hay, 2008), which may also indicate increased between-class spectral variation and reduced within-class spectral variation.

This research here demonstrated that object-specific texture measures aided in improving forest type classification results. In particular, the incorporation of multiple GLCM texture measures with spectral bands enhanced the overall accuracies of three forest type classifications by 4 % of overall accuracy with 0.06 for Kappa. Nevertheless, the accuracy of object-based forest type classification was not always improved from the combination of single or multiple GLCM texture measures with spectral bands. In addition, the individual accuracies of forest types increased with the multiple GLCM texture analysis. This research confirmed a previous texture analysis study conducted by Coburn and Roberts (2004). Most studies have attempted to

105

utilize individual texture measures combined with spectral bands in pixel-based image classification. Coburn and Roberts (2004), however, incorporated multiple texture, derived from a variety of window sizes, with spectral bands of 4-m airborne imagery, into a pixel-based classification of pure and mixed forest stands. According to their study, the addition of multi-scale and multiple texture measures into pixel-based forest type classification gained 13 % of overall accuracy compared with spectral-only classification.

4.4 RESEARCH ISSUES IN OBIA

Object-based image analysis has received increasing attention in remote sensing with VHR imagery as a means to tackle the limitations associated with conventional pixel-based classification approaches. With the increased availability of VHR remote sensing data, the OBIA approach sheds a promising light on feature extraction/thematic classification, and may lead to a paradigm shift in remote sensing fields. However, there are some challenging issues to be answered in association with OBIA.

The fundamental levels of the OBIA include segmentation as well as attribution and classification (Hay and Castilla, 2008). The attribution of image objects is greatly affected by segmentation quality as assessed by classification accuracy when a reference data set is available for comparison with OBIA results, as this research utilized the CRMS-NPS vegetation geodatabases. In this sense, the quality of segmentation is considered a critical factor in the OBIA. This research mainly focused on exploring the relationship between segmentation scale and its effect on segmentation quality, particularly in terms of image segmentation with only spectral bands. The type of input data, however, also plays an important role in determining the quality of segmentation (Blaschke, 2003). Texture, as a spatial information carrier, has

previously been entered into image segmentation procedures with spectral information (Hay *et al.*, 1996; Ryherd and Woodcock, 1996; Lucieer and Stein, 2005; Kim *et al.*, submitted(a)). Besides texture measures, topographic variables such as elevation, aspect and slope also are considered as important data sources to decide the locations and types of vegetations under interest and enhance classification results (Parker, 1982; Florinsky and Kurakova, 1996; Florinsky, 1998; Treitz and Howarth, 2000; Madden, 2004; Boyd and Danson, 2005). In OBIA, topographic information has been incorporated with spectral information for vegetation mapping and landform unit classification (Domaç *et al.*, 2006; Dragut and Blaschke, 2006; Xu, 2008; Chastain *et al.*, 2008; Kim *et al.*, submitted(b)). In addition to spatial and topographic information, the OBIA approach has been conducted with the addition of existing GIS layers, e.g., transportation and hydrography, and the results of GIS analysis related to proximity derivation (Debeir *et al.*, 2002; Burrough *et al.*, 2001; Kim *et al.*, 2008; Kim *et al.*, submitted(b)). The inclusion of auxiliary data sets aids in disentangling between-class spectral variations with VHR imagery and enhance classification results of landscape features, as described by Kim *et al.* (in press(b)).

This research has mainly focused on a single-scale segmentation and classification approach to automatically interpret forest stands and forest types with VHR imagery. In the real world, however, a single scale may not be appropriate to resolve multiple-sized ground features taking it into account that the landscape is typically composed of a large number of complex and heterogeneous components in size (Hay *et al.*, 2003). In this sense, multi-scale approaches will be required to perform feature extraction and thematic classification from image segmentations based on multiple spatial dimensions (Hay *et al.*, 2005). Many attempts have been made to embody the multi-scale concept in the OBIA literature (Hay *et al.*, 2003; Hay *et al.*, 2005; Hall *et*

al., 2004; Tian and Chen, 2007; Corbane *et al.*, 2008; Kim *et al.*, submitted(a); Kim *et al.*, in press(b)). Nevertheless, researchers need to develop a robust methodology to decide optimal segmentation scales inherent in multi-scale OBIA approaches.

A major advantage of the OBIA approach is a potential to utilize spatial information related to each image object and contextual information between image segments as human interpreters employ image interpretation elements. The spatial and contextual characteristics of image objects are critical factors to extract and classify landscape features with spectral information in OBIA (Blaschke, 2003). Theoretically, there are a large number of possibilities to create and utilize class-separation criteria in the OBIA. Researchers can compute and employ distinct types associated with spatial information such as texture and shape for feature extraction and thematic classification when using Definiens. It allows researchers to compute GLCM texture measures of angular second moment, contrast, correlation, dissimilarity, entropy, homogeneity, mean and standard deviation and shape-related criteria of area, asymmetry, border index, compactness, elliptic fit, length, main direction, rectangular fit, shape index, width and so on. Since users often find the large number of options overwhelming, especially when first using OBIA techniques, an attempt should be made to reduce the flood of potential separation criteria, and also reduce processing time in object-based analysis research. In addition, the acquisition of remote sensing imagery with very high resolution provides researchers with a high level of detail for landscape features, which occurs at the expense of data volume and associated image processing time for large study areas. Although this is expected to be solved to some extent by increased computing power with a parallel processing method, guidance for remote sensing practioners is needed to assist in the best selection of input parameters and highest quality of segmented image objects. The results of this research contribute to conceptual aspects of

automated object-based image processing by providing evidence of methodologies that improve

classification accuracies and demonstrate best practices for optimal parameters input to OBIA

REFERENCES

Blaschke, T. 2003. Object-based contextual image classification built on image segmentation, Proceedings of the 2003 IEEE Workshop on Advances in Techniques for Analysis of Remotely Sensed Data, 27-28 October 2003, Washington DC, U.S., pp.113-119.

Boyd, D.S. and F.M. Danson. 2005. Satellite remote sensing for forest resources: three decades of research development. Progress in Physical Geography, 29(1):1-26.

Burrough, P.A., J.P. Wilson, P.F.M. Gaans and A.J. Hansen. 2001. Fuzzy k-means classification of topo-climatic data as an aid to forest mapping in the Greater Yellowstone area, USA. Landscape Ecology, 36:523-546.

Castilla, G. and G.J. Hay. 2008. Image objects and geographic objects. Object-Based Image Analysis - Spatial concepts for knowledge-driven remote sensing applications (T. Blaschke, S. Lang, and G.J. Hay, editors), Springer-Verlag, Berlin, pp.91-110.

Chastain, R.A., A.S. Matthew, H.S. He, and D.R. Larsen. 2008. Mapping vegetation communities using statistical data fusion in the Ozark National Scenic Riverways, Missouri, USA. Photogrammetric Engineering & Remote Sensing, 74(2): 247-264.

Coburn, C.A. and A.C.B. Roberts. 2004. A multiscale texture analysis procedure for improved forest stand classification. International Journal of Remote Sensing, 25(2):4287-4308.

Corbane, C., D. Raclot, F. Jacob, J. Albergel and P. Andrieux. 2008. Remote sensing of soil surface characteristics from a multiscale classification approach. Catena, 75(3):308-318.

Debeir, O., I.V. den Steen, P. Latinne, P.V. Ham, and E. Wolff. 2002. Textural and contextual land-cover classification using single and multiple classifier systems. Photogrammetric Engineering & Remote Sensing, 68(6):597-605.

Definiens. 2004. eCognition user guide 4, Definienes Imaging Co., Germany.

Dorren, L.K.A., B. Maier, and A.C. Seijmonsbergen. 2003. Improved Landsat-based forest mapping in steep mountainous terrain using object-based classification. Forest Ecology and Management, 183:31-46.

Domac, A., M.L. Suzen, and C. Bilgin. 2006. Integration of environmental variables with satellite images in regional scale vegetation classification. International Journal of Remote Sensing, 27(1):1329-1350.

Dragut, L. and T. Blaschke. 2006. Automated classification of landform elements using object-based image analysis. Geomorphology, 81:330-344.

Florinsky, I.V. and G.A. Kurakova. 1996. Influence of topography on some vegetation cover properties. Catena, 27:123-141.

Florinsky, I.V. 1998. Combined analysis of digital terrain models and remotely sensed data in landscape investigations. Progress in Physical Geography, 22(1):33-60.

Fraumann, E. and E. Wolff. 2006. Segmentation of very high spatial resolution satellite images in urban areas for segments-based classification. In ISPRS WG VIII/1 on Proceedings of the ISPRS joint conference; 3rd International Symposium Remote Sensing and Data Fusion Over Urban Areas and 5th International Symposium Remote Sensing of Urban Areas, 14-16 March 2005, Tempe, Arizona, USA. Available online at: http://www.isprs.org/commission8/workshop_urban/frauman.pdf (accessed 26 September 2008).

Hall, O., G.J. Hay, A. Bouchard, and D.J. Marceau. 2004. Detecting dominant landscape objects through multiple scales: an integration of object-specific methods and watershed segmentation. Landscape Ecology, 19:59-76.

Hay, G.J., K.O. Nieman, and G.F. McLean. 1996. An object-specific image-texture analysis of H-resolution forest imagery. Remote Sensing of Environment, 55:108-122.

Hay, G.J., T. Blaschke, D.J. Marceau and A. Bouchard. 2003. A comparison of three image-object methods for the multiscale analysis of landscape structure. ISPRS Journal of Photogrammetry & Remote Sensing, 57:327-345.

Hay, G.J. and G. Castilla. 2008. Geographic object-based image analysis (GEOBIA): a new name for a new discipline. Object-Based Image Analysis - Spatial concepts for knowledge-driven remote sensing applications (T. Blaschke, S. Lang, and G.J. Hay, editors), Springer-Verlag, Berlin, pp.75-89.

Hay, G.J., G. Castilla, M.A. Wulder and J.R. Ruiz. 2005. An automated object-based approach for the multiscale image segmentation of forest scenes. International Journal of Applied Earth Observation and Geoinformation, 7:339-359.

Kim, M. T.A. Warner, M. Madden, and D.S. Atkinson. submitted(a). Multi-scale GEOBIA with VHR digital imagery: feature, scale and spectral variation. International Journal of Remote Sensing, in review.

Kim, M., M. Madden and B. Xu. submitted (b). GEOBIA forest mapping in Great Smoky Mountains National Park. Photogrammetric Engineering & Remote Sensing, in review.

Kim, M., J.B. Holt, C.Y. Ku, and M. Madden. in press. GEOBIA building extraction of Mae La refugee camp, Thailand: step-wise multi-scale feature classification approach. Landscape Analysis using Geospatial Tools: Community to the Globe (M. Madden and Allen, E., editors), Springer-Verlag, New York, U.S.

Kim, M., M. Madden, and T.A. Warner. 2008. Estimation of optimal image object size for the segmentation of forest stands with multispectral IKONOS imagery. Object-Based Image Analysis - Spatial concepts for knowledge-driven remote sensing applications (T. Blaschke, S. Lang, and G.J. Hay, editors), Springer-Verlag, Berlin, pp.291-307.

Lucieer, A. and A. Stein. 2005. Texture-based landform segmentation of LiDAR imagery. International Journal of Applied Earth Observation and Geoinformation, 6:261-270.

Madden, M. 2004. Visualization and analysis of vegetation patterns in National Parks of the Southeastern United States. Proceedings of challenges in geospatial analysis, integration and visualization II (International Society for Photogrammetry and Remote Sensing), Commission IV joint workshop, Stuttgardt, Germany, pp.143-146.

Parker, A.J. 1982. The topographic relative moisture index: an approach to soil-moisture assessment in mountain terrain. Physical Geography, 3(2):160-168.

Ryherd, S. and C. Woodcock. 1996. Combining spectral and texture data in the segmentation of remotely sensed images. Photogrammetric Engineering & Remote Sensing, 62(2):181-194.

Tian, J. and D.M. Chen. 2007. Optimization in multi-scale segmentation of high-resolution satellite images for artificial feature recognition. International Journal of Remote Sensing, 28(20):4625-4644.

Treitz, P. and P. Howarth. 2000. Integrating spectral, spatial, and terrain variables for forest ecosystem classification. Photogrammetric Engineering & Remote Sensing, 66(3):305-317.

Xu, B. 2008. Vegetation mapping using object-based image analysis in Great Smoky Mountains National Park. Masters of Science Thesis. Department of Geography, The University of Georgia, p.110.

APPENDIX I

KAPPA COEFFICIENT

The accuracy of classification is, in general, evaluated with overall accuracy (OA) and Kappa coefficient. The two overall indices of classification accuracy are computed from an error matrix (also called contingency table), which are composed of correctly- and incorrectly-classified units for individual classes of interest. An overall accuracy means the percent of correctly classified classification units to total units, defined as

$$OA = (S_d / n) \times 100$$

where S_d means the sum of diagonal entries in an error matrix and n denotes the total number of classified units.

Overall accuracy, however, overestimates classification accuracy if the area of a class is much larger than those of the other classes. In addition, it does not consider change agreements that might occur between sample and reference data. Therefore, Kappa coefficient is employed to control the overestimation tendency of overall accuracy by adding all the off-diagonal entries of an error matrix during accuracy computation. A Kappa coefficient is also calculated from an error matrix, defined as

$$K = \frac{P_o - P_c}{1 - P_c}$$

where P_o is computed with dividing the number of entries along diagonal in an error matrix by the total number of samples and P_c is calculated with marginal distribution of classification and reference data in an error matrix. Further detailed description of P_o and P_c is available in Lo and Yeung (2002)[5]. Kappa coefficient ranges from 0 to 1, where 0 means random (by-chance) agreement and 1 denotes perfect agreement between classification and reference data. According to Congalton (1991)[6], A Kappa coefficient greater than 0.8 indicates strong agreement between a classification result and a reference data set. A Kappa coefficient between 0.4 and 0.8 represents moderate agreement, and a coefficient less than 0.4 poor agreement.

---

[5] Lo, C.P. and A.K.W. Yeung, 2002. Concepts and techniques of geographic information systems, Prentice-Hall, Inc., NJ, p. 116.
[6] Congalton, R.G., 1991. A review of assessing the accuracy of classifications of remotely sensed data. Remote Sensing of Environment, 37(1):35-46.

APPENDIX II

MORAN'S I

Spatial autocorrelation indicates the relationship of spatial distribution between objects and their neighbors and is described as positive, random and negative autocorrelations. Positive autocorrelation occurs when spatial features with same attributes cluster in a geographic space. On the contrary, even distribution of the features, which have the same attributes, results in negative autocorrelation. Random autocorrelation, however, does not have any clustering pattern of spatial features with same attributes.

Moran's I is a measure to describe spatial distribution pattern of interested spatial objects in a geographic area and is computed with a formula:

$$I = \frac{N}{\sum_{i=1}^{N}\sum_{j=1}^{N} w_{ij}} \times \frac{\sum_{i=1}^{N}\sum_{j=1}^{N} w_{ij}(X_i - \overline{X})(X_j - \overline{X})}{\sum_{i=1}^{N}(X_i - \overline{X})^2}$$

where N is the total number of spatial features, w_{ij} is the spatial weight between feature i and j, X is an attribute value of a spatial feature and $\overline{X}$ is the mean attribute value of all spatial features of interest. Moran's I index ranges from -1 to +1, where -1 means perfect negative

116

autocorrelation and +1 perfect positive autocorrelation. A Moran's I value of 0 indicates random distribution, i.e. no-clustering pattern.

In this research, the quality of segmentation was estimated with spatial autocorrelation analysis using Moran's I indices. The definition of optimal segmentation, particularly related to forest types, needs to be made before explaining the result of spatial autocorrelation. A mixed forest, literally, is composed of pure deciduous and evergreen trees. A mixed forest area will be delineated with several image objects of pure deciduous and evergreen forests in its boundary in an over-segmentation with a small scale. Figure A-1 illustrates forest types from manual interpretation and automatic object-based classifications. When compared with manual interpretation (Figure A-1a), an extreme small scale did not produce appropriate image segments to encompass deciduous and evergreen trees in their boundary, and individual pure forests were classified as they were in a classification result, shown in Figure A-1b. On the contrary, pure forests were well classified particularly for evergreen forests at a scale of 10, and mixed forests also produced as forest patches (Figure A-1c).

The estimation of optimal segmentation for forest stands was made with a spatial autocorrelation analysis using Moran's I in this research. Segmentation results from a range of scales were converted to shapefiles that have the mean spectral values of near-infrared band for individual image objects. Then, individual shapefile were entered into ArcGIS (version 9.3) to compute Moran's I values with inversely-squared Euclidean distances. According to the graph of Moran's I values (see Figure 2.6), over-segmentations resulted in higher values than optimal segmentations. As illustrated in Figure 3-3(b), an over-segmentation produced many image objects for each forest stand, which would indicate that they are clustered with similar spectral reflectance in relation to a near-infrared band of IKONOS imagery. Under-segmentations

117

resulted in larger image segments that included different forest types and would generate similar spectral mixture. Therefore, image objects in under-segmentations would also be clustered with similar spectral reflectance, which generated relatively higher Moran's I values than optimal segmentations. In this spatial autocorrelation analysis, optimal segmentations were hypothesized to produce relatively less correlated image objects with spectral values. Figure A-2 illustrates choropleth maps that were generated with the equal interval between minimum and maximum values using 3 classes. As shown in the figure, over- and under-segmentations at scales of 5 and 27, respectively, show a spatial pattern where neighboring image objects with similar spectral values are clustered than an optimal segmentation at scale 18.

Taking into consideration optimal segmentation, a spatial autocorrelation analysis needs to be performed with the pre-defined size of minimum mapping unit (MMU) particularly for object-based classification of deciduous, evergreen and mixed forests. It is essential particularly to produce appropriate boundaries of mixed forest stands and is anticipated to improve classification result as well as segmentation quality.
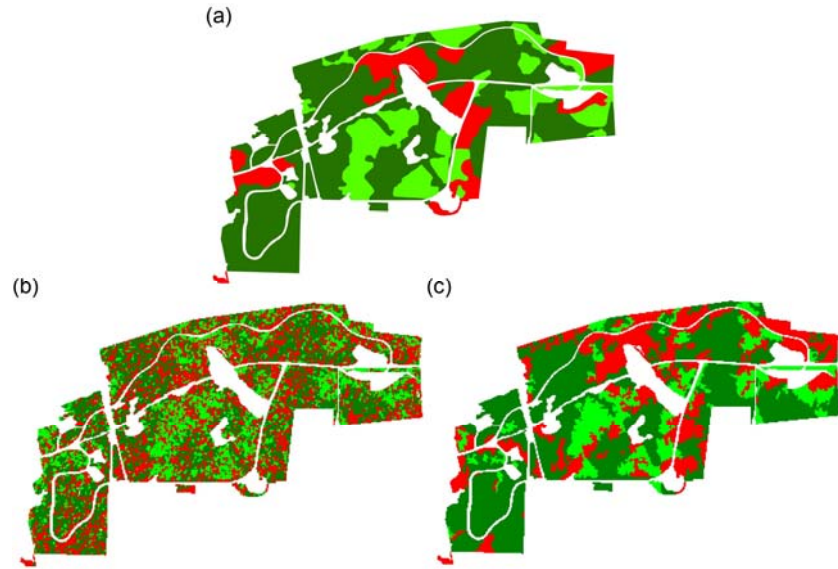
Figure A.1. Manual interpretation (a), GEOBIA classification at a scale 2 with only spectral bands (b) and GEOBIA classification at scale 10 with only spectral bands (c). Dark green represents deciduous forests, light green evergreen forest and red mixed forests.
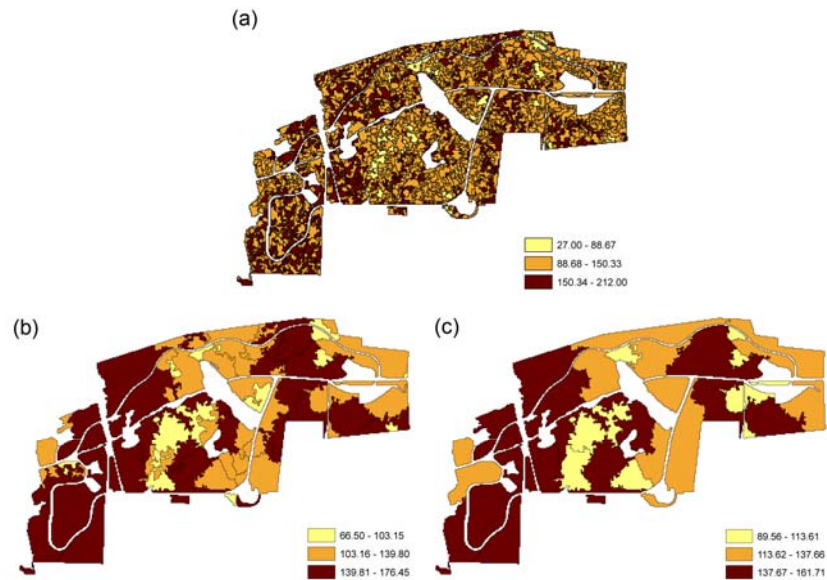

Figure A.2. An over-segmentation at scale of 5 (a), an optimal segmentation at scale of 18 (b) and an under-segmentation at scale of 27 (c).

APPENDIX III

LIST OF ACRONYMS

Acronym	Full description
A	
ASM	Angular Second Moment
ASPRS	American Society of Photogrammetry and Remote Sensing
B	
BD	Bhattacharya Distance
C	
CE	Circular Error
CEGL	Community Element Global
CIR	Color Infrared
CON	Contrast
COR	Correlation
CRMS	Center for Remote Sensing and Mapping Science
D	
DF	Deciduous Forest
DIS	Dissimilarity
DN	Digital Number
DOQQ	Digital Orthophoto Quarter Quadrangle
E	
EF	Evergreen Forest
ENT	Entropy
ETM+	Enhanced Thematic Mapper Plus
F	
FGDC	Federal Geographic Data Committee
G	
GIS	Geographic Information System

	GLCM	Grey-level Co-occurrence Matrix
	GPS	Global Positioning System
	GUCO	Guilford Courthouse
H		
	HOM	Homogeneity
L		
	LULC	Land Use and Land Cover
M		
	MAUP	Modifiable Areal Unit Problem
	MEAN	Mean
	MF	Mixed Forest
	MMU	Minimum Mapping Unit
	MSS	Multispectral Scanner
N		
	NIR	Near Infrared
	NPS	National Park Service
	NVCS	National Vegetation Classification System
O		
	OBIA	Object-based Image Analysis
R		
	RGB	Red, Green, and Blue
	RMSE	Root Mean Square Error
S		
	SPOT	Satellite Pour l'Observation de la Terra
T		
	TM	Thematic Mapper
U		
	USGS	United States Geological Survey
V		
	VAR	Variance
	VHR	Very High Resolution